A NEW METHOD TO INCREASE EFFECTIVENESS OF BASE ISOLATION ON TORSIONALLY UNRESTRAINED STRUCTURES

A THESIS SUBMITTED TO
THE GRADUATE SCHOOL OF NATURAL AND APPLIED SCIENCES
OF
MIDDLE EAST TECHNICAL UNIVERSITY

BY

EMREN CAN ALEMDAĞ

IN PARTIAL FULFILLMENT OF THE REQUIREMENTS
FOR
THE DEGREE OF MASTER OF SCIENCE
IN
CIVIL ENGINEERING

OCTOBER 2016

Approval of the thesis:

A NEW METHOD TO INCREASE EFFECTIVENESS OF BASE ISOLATION ON TORSIONALLY UNRESTRAINED STRUCTURES

Submitted by **EMREN CAN ALEMDAĞ** in partial fulfillment of the requirements for the degree of **Master of Science in Civil Engineering Department, Middle East Technical University** by,

Prof. Dr. Gülbin Dural Ünver
Dean, Graduate School of **Natural and Applied Sciences** _____

Prof. Dr. İsmail Özgür Yaman
Head of Department, **Civil Engineering** _____

Prof. Dr. Uğurhan Akyüz
Supervisor**, Civil Engineering Dept., METU** _____

Examining Committee Members:

Prof. Dr. Ahmet Yakut
Civil Engineering Dept., METU _____

Prof. Dr. Uğurhan Akyüz
Civil Engineering Dept., METU _____

Assoc. Prof. Dr. Gökhan Özdemir
Civil Engineering Dept., Anadolu University _____

Prof. Dr. Murat Altuğ Erberik
Civil Engineering Dept., METU _____

Assoc. Prof. Dr. Özgür Kurç
Civil Engineering Dept., METU _____

Date: 17.10.2016

I hereby declare that all information in this document has been obtained and presented in accordance with academic rules and ethical conduct. I also declare that, as required by these rules and conduct, I have fully cited and referenced all material and results that are not original to this work.

Name, Last name: Emren Can Alemdağ

Signature:

ABSTRACT

A NEW METHOD TO INCREASE EFFECTIVENESS OF BASE ISOLATION ON TORSIONALLY UNRESTRAINED STRUCTURES

Alemdağ, Emren Can

M. Sc., Department of Civil Engineering

Supervisor: Prof. Dr. Uğurhan Akyüz

October 2016, 143 pages

The torsional behavior of the seismically isolated structures is one of the subjects that has been studied least. Especially, in the structures with first mode as torsional mode, i.e., torsionally coupled. In these type of structures, using conventional design method does not increase the torsional stiffness of the system and makes system weak in torsion when compared to other directions. This is not a desired situation in designing. Solving seismic isolation systems with lead-rubber bearings using the conventional design method can not solve the issue. To get system more torsionally rigid, isolators standing at the outer axes must be strengthened, relatively. However, while doing this operation, targeted period of the structure decreases because the total lateral stiffness of the system is increased. Hence, floor accelerations and shear forces can be increased, as well. Besides, in torsionally unrestrained systems, because displacement differences between the isolators and torsional amplifications are high, effectiveness of isolators decreases under different mass eccentricities. To overcome this issue,

instead of conventional method, an other design method developed in this study can be used.

In developed design method, instead of designing isolators for the seismic weights on them which is conventional method, system is separated as inner and outer groups and then, isolators are designed with a stiffness ratio. To calculate the stiffness ratio, a formulation was improved including basic parameters related to system. Isolation system designed according to the stiffness ratio calculated from the formulation, provides system to get translational modes in first two modes by increasing the torsional rigidity.

Same building was investigated with two design methods, comparatively. After that these systems were examined under different mass eccentricity cases. In all cases, systems were solved using conventional and method developed in the study, with SAP2000. Results were examined in different seismic records and loading methods. According to results, developed method gives more effective systems when looked to the uniformity of displacements and shear forces of isolators.

Keywords: Torsional Response of Seismically Isolated Structures, Seismically Isolated Structures, Torsionally Unrestrained Structures, Seismic Isolation Methods, Response of Lead-Rubber Bearings

ÖZ

BURULMASI ÖNLENMEMİŞ YAPILARDA SİSMİK İZOLASYON VERİMLİLİĞİNİ ARTIRACAK YENİ BİR YÖNTEM

Alemdağ, Emren Can

Yüksek Lisans, İnşaat Mühendisliği Bölümü

Tez Yöneticisi: Prof. Dr. Uğurhan Akyüz

Ekim 2016, 143 sayfa

Sismik olarak izole edilmiş yapıların burulma davranışı, sismik izolasyon hakkında en az çalışılan konulardan biridir. Özellikle birinci modu burulma yönünde olan, yani burulma ve ötelenme birlikte olan yapılarda. Bu tarz yapılarda geleneksel dizayn yöntemi kullanmak yapının burulma rijitliğini yeteri kadar artırmayıp, yapının yine burulma yönünde diğer yönlere göre zayıf kalmasına sebep olmaktadır. Bu yapı dizaynında istenmeyen bir durumdur. Sorunu aşmak kurşun çekirdekli elastomer mesnetler kullanılarak tasarlanan sismik izolasyon sistemlerinin geleneksel yöntemle çözülmesiyle mümkün olmamaktadır. Yapıya burulma rijitliği kazandırmak için ise sistemin en dış akslarındaki izolatörlerin görece güçlendirilmesi gerekmektedir. Ancak bu yapılırken sistemin genel olarak rijitliği artırıldığından sistemin hedeflenen periyodu azalmaktadır. Dolayısıyla, sistemden beklenen kat ivmeleri ve kesme kuvveti daha yüksek çıkabilir. Ayrıca, burulması önlenmemiş, burulma yönünde zayıf olan sistemlerde, değişen kütle eksantrisitelerinde izolatörler arasındaki deplasman farkı ve burulma artışları da çok olacağından, izolatör verimliliği de düşmektedir. Sorunu

aşmak için geleneksel yöntem yerine bu çalışmada geliştirilen bir dizayn yöntemi kullanılabilir.

Geliştirilen yöntemde, geleneksel sistemin ön gördüğü, izolatörler üzerlerindeki sismik ağırlığa göre tasarlanmak yerine, sistem iç ve dış izolatörler olarak ikiye ayrılıp, bu izolatörler belirli bir rijitlik oranında tasarlanmaktadır. Rijitlik oranını hesap etmek içinse, içerisinde sisteme ait belirli parametreler barındıran bir formül geliştirilmiştir. Bu formülden elde edilen rijitlik oranına göre tasarlanan izolatör sistemi, yapının burulma rijitliğini artırarak, ilk iki modu ötelenme yönlerine çekmektedir.

Aynı yapı iki dizayn yöntemine göre çözülmüştür. Daha sonra farklı eksantrisite durumlarında bu sistemler incelenmiştir. Bütün durumlarda sistem hem geleneksel yöntemle hem de bu çalışmada geliştirilen yöntemle SAP2000 programında çözülmüştür. Sonuçlar, değişik deprem kayıtları ve yöntemleri altında incelenmiştir. İzolatörlerin deplasmanları ve kesme kuvvetlerindeki eşit dağılıma bakıldığında, geliştirilen metodun daha verimli sonuçlar verdiği görülmektedir.

Anahtar kelimeler: Sismik İzolasyonlu Yapıların Burulma Davranışı, Sismik Olarak İzole Edilmiş Yapılar, Burulma Önlemi Alınmamış Yapılar, Sismik İzolasyon Yöntemleri, Kurşun Çekirdekli Mesnetlerin Davranışı

To My Parents…

ACKNOWLEDGEMENTS

First of all, I would like to thank to my supervisor Prof. Dr. Uğurhan Akyüz for his helps and encouragements through my research. I could not overcome the problems I experienced in my studies without his teachings.

I would further like to thank to Dr. Özgür Kurç for his helps about my structural modelling in the research.

I have to admit that my family had always positive energy on me. They provided every materially and morally contributions to me. Although we were far away from each other, they were like just behind me to handle what I faced. In my last year in this program, I had a chance to live in this city with my sister. I was pleased to see her near to me during this rough period.

I must thank to my friends of course. My housemate Mustafa Ulutaş and my close friend Erkan Durmuş really helped me by providing me extra computers through the long time history analyses cases. I saved extra days thanks to them. Moreover, I must thank especially to Seda Özdemir because she teached me some modelling techniques and concepts related to my topic.

When I needed to relax and have some fun during my studies, my best friends Mahyar Azizi, Onur Dursun, Çağan Dizdar, Serdar Ateşal, Erkan Durmuş and Murat Aydınoğlu were always near to me. Also, I was very happy thanks to my football team frieds that we played once a week since they helped me to reduce my stress.

Finally, I would like to thank to my cats Kenks and Tolcay for their little contributions to me. Although they waked me up some nights and disarranged my room sometimes, I really love them and can not forget their kind supports for me.

TABLE OF CONTENTS

ABSTRACT v

ÖZ vii

ACKNOWLEDGEMENTS x

TABLE OF CONTENTS xi

LIST OF TABLES xiv

LIST OF FIGURES xx

CHAPTERS

1. INTRODUCTION 1

1.1 LITERATURE SURVEY 1

1.2 AIM OF THE THESIS 10

2. THEORY 13

2.1 SEISMIC BASE ISOLATION 13

2.2 BACKGROUND OF SEISMIC BASE ISOLATION 15

2.3 TYPES OF SEISMIC BASE ISOLATION SYSTEMS 17

2.3.1 Elastomeric Based Systems 18

2.3.2 Sliding Based Systems 19

2.4 FORMULATION OF SEISMIC BASE ISOLATION SYSTEM 21

2.4.1 Linear Theory of Seismic Isolation Systems 21

2.4.2 Mechanical Formulations of Seismic Isolation 24

2.5 DESIGN OF SEISMIC BASE ISOLATION 29

2.5.1 Preliminary Design of Seismic Isolators 30
2.5.2 Final Design of Seismic Isolators 32
3. CASE STUDIES 37
3.1 DEFINITION OF THE STRUCTURE 37
3.1.1 Load Combinations 40
3.1.2 Response Spectrum Function 41
3.1.3 3D Model of the Structure 42
3.2 FIXED-BASE CASE 43
3.3 DESIGN METHODS 45
3.3.1 Conventional Method 45
3.3.2 Proposed Method 46
3.4 ISOLATED CASES 80
3.4.1 Symmetric Systems 81
3.4.2 Asymmetric Systems 89
3.5 DYNAMIC ANALYSES 91
3.5.1 Response spectrums 91
3.5.2 Time Histories 92
4. RESULTS AND DISCUSSIONS 95
4.1 RESULTS 95
4.1.1 Symmetric Systems 96
4.1.2 Asymmetric Systems 101
4.2 DISCUSSIONS 111
5. CONCLUSIONS 115
REFERENCES 119
APPENDICES 123

APPENDIX A 123

BILINEAR MODELS OF THE LEAD-RUBBER BEARINGS DEFINED IN SAP2000 FOR EACH SYSTEM 123

APPENDIX B 127

DESIGN CALCULATION DETAILS OF ISOLATORS 127

APPENDIX C 141

CHECKS OF ISOLATORS UNDER GROUND MOTION HISTORIES 141

LIST OF TABLES

TABLES

Table 1. First and second periods of coupled modes [4] 7

Table 2. Modal analysis results of fixed-base case 43

Table 3. Floor accelerations of symmetric case 43

Table 4. Base reactions of fixed-base case 44

Table 5. Weight and stiffness parameters of the formula when shear wall thicknesses were changed 50

Table 6. Period parameter of formula when shear wall thicknesses were changed ... 50

Table 7. Distance parameters of formula at rigidity case 51

Table 8. Parametric ratios of the formula at rigidity case 52

Table 9. Related parameters of formula when outer axes were displaced 25 cm 52

Table 10. Outer distance of formula when outer axes were displaced 25 cm 53

Table 11. Related parameters of formula when outer axes were displaced 50 cm 53

Table 12. Outer distance of formula when outer axes were displaced 50 cm 54

Table 13. Related parameters of formula when outer axes were displaced 75 cm 54

Table 14. Outer distance of formula when outer axes were displaced 75 cm 54

Table 15. Related parameters of formula when outer axes were displaced 100 cm .. 55

Table 16. Outer distance of formula when outer axes were displaced 100 cm 55

Table 17. Related parameters of formula when outer axes were displaced 125 cm .. 56

Table 18. Outer distance of formula when outer axes were displaced 125 cm 56

Table 19. Related parameters of formula when outer axes were displaced 150 cm .. 56

Table 20. Outer distance of formula when outer axes were displaced 150 cm..... 57

Table 21. Related parameters of formula when outer axes were displaced 50 cm in X direction 57

Table 22. Outer distance of formula when outer axes were displaced 50 cm in X direction 57

Table 23. Related parameters of formula when outer axes were displaced 100 cm in X direction 58

Table 24. Outer distance of formula when outer axes were displaced 100 cm in X direction 58

Table 25. Related parameters of formula when outer axes were displaced 150 cm in X direction 59

Table 26. Outer distance of formula when outer axes were displaced 150 cm in X direction 59

Table 27. Related parameters of formula when outer axes were displaced 50 cm in Y direction 59

Table 28. Outer distance of formula when outer axes were displaced 50 cm in Y direction 60

Table 29. Related parameters of formula when outer axes were displaced 100 cm in Y direction 60

Table 30. Outer distance of formula when outer axes were displaced 100 cm in Y direction 60

Table 31. Related parameters of formula when outer axes were displaced 150 cm in Y direction 61

Table 32. Outer distance of formula when outer axes were displaced 150 cm in Y direction 61

Table 33. Parametric ratios of the formula at distance case..... 62

Table 34. Weight and stiffness parameters of formula when slabs loaded 0.3 to 0.5 ton/m^2 62

Table 35. Period parameter of formula when slabs loaded 0.3 to 0.5 ton/m^2 63

Table 36. Parametric ratios of the formula at weight case 63

Table 37. Weight and stiffness parameters when the heights of the stories were changed..... 64

Table 38. Period parameter when the heights of the stories were changed 64

Table 39. Parametric ratios of the formula at height case 65

Table 40. Weight and stiffness parameters when the system was arranged for different stories 65

Table 41. Period parameter when the system was arranged for different stories..... 66

Table 42. Parametric ratios of the formula at story case 66

Table 43. Weight and stiffness parameters when the stories and heights of the system were changed..... 67

Table 44. Period parameter when the stories and heights of the system were changed 67

Table 45. Parametric ratios of the formula at story - height case..... 67

Table 46. Related parameters of random case 1..... 68

Table 47. Distance parameter of random case 1 68

Table 48. Related parameters of random case 2..... 69

Table 49. Distance parameter of random case 2 69

Table 50. Related parameters of random case 3..... 70

Table 51. Distance parameter of random case 3 70

Table 52. Parametric ratios of the formula at randomly change cases..... 70

Table 53. Weight and stiffness parameters when elasticity was changed..... 71

Table 54. Period parameter when elasticity was changed..... 71

Table 55. Weight and stiffness parameters when assumed period was changed 72

Table 56. Period parameter when assumed period was changed 73

Table 57. Parametric ratios of the formula at period case 73
Table 58. Parametric ratios of the formula at period case 74
Table 59. Outer stiffness check when the formulation is used 78
Table 60. Seismic weights on isolators in symmetric case 81
Table 61. Effective lateral stiffnesses of isolators at first iteration in symmetric case 83
Table 62. Analysis results in symmetric case for conventional method 84
Table 63. Design results of the isolators designed with conventional method 84
Table 64. Final results of isolators at DBE in symmetric case 85
Table 65. Final effective damping of the system at DBE in symmetric case 85
Table 66. Final effective damping of the system at MCE in symmetric case 85
Table 67. Design results of isolators designed with conventional method (Q/W = 0.1) 86
Table 68. Analysis results in symmetric case for proposed method 87
Table 69. Design results of the isolators designed with proposed method 88
Table 70. Final results of isolators at DBE in symmetric case 88
Table 71. Final effective damping of the system at DBE in symmetric case 89
Table 72. Final effective damping of the system at MCE in symmetric case 89
Table 73. Updated values of isolators under different mass eccentricities 90
Table 74. Updated values of isolators under different mass eccentricities 90
Table 75. Effective damping levels of each system with different mass eccentricities 92
Table 76. Modal results for symmetric system with conventional design method 96
Table 77. Modal results for symmetric system with proposed design method 96
Table 78. Floor accelerations of symmetric systems in MCE 98
Table 79. Floor accelerations of symmetric systems in DBE 98

Table 80. Results of isolator types for symmetric system with each design method. 99

Table 81. Maximum axial loads (tons) on isolators in symmetric systems 100

Table 82. Modal results for asymmetric systems for each design method 101

Table 83. Displacements and shear forces of isolators analyzed with response spectrum 102

Table 84. Corner isolator displacements at two design methods 102

Table 85. Displacement differences of corner isolators at two design methods 103

Table 86. Base reactions for 4 mass eccentricities at response spectrum analyses.. 103

Table 87. Results of isolator types for 5% asymmetric systems for each design method 104

Table 88. Displacement differences of corner isolators at two design methods 108

Table 89. Displacements and shear forces of isolators analyzed with response spectrum 108

Table 90. Corner isolator displacements of two design methods 109

Table 91. Modal results for asymmetric systems (stiffness eccentricity) for each design method 109

Table 92. Displacements and shear forces of isolators on stiffness eccentricity cases 110

Table 93. Corner isolator displacement of two design methods at stiffness eccentricity cases 110

Table 94. Displacement differences of isolators at stiffness eccentricity cases 111

Table 95. Design calculations of SC1 in symmetric case 127

Table 96. Design calculations of SC1 in symmetric case 128

Table 97. Design calculations of SC1 in symmetric case 128

Table 98. Design calculations of SC1 in symmetric case 129

Table 99. Design checks of SC1 in symmetric case 129

Table 100. Design calculations of SC2 in symmetric case 130
Table 101. Design calculations of SC2 in symmetric case 130
Table 102. Design calculations of SC2 in symmetric case 131
Table 103. Design checks of SC2 in symmetric case 131
Table 104. Design calculations of SC2 in symmetric case 132
Table 105. Design calculations of SC3 in symmetric case 132
Table 106. Design calculations of SC3 in symmetric case 133
Table 107. Design calculations of SC3 in symmetric case 133
Table 108. Design calculations of SC3 in symmetric case 134
Table 109. Design checks of SC3 in symmetric case 134
Table 110. Design calculations of STI in symmetric case 135
Table 111. Design calculations of STI in symmetric case 135
Table 112. Design calculations of STI in symmetric case 136
Table 113. Design checks of STI in symmetric case 136
Table 114. Design calculations of STI in symmetric case 137
Table 115. Design calculations of STO in symmetric case 137
Table 116. Design calculations of STO in symmetric case 138
Table 117. Design calculations of STO in symmetric case 138
Table 118. Design calculations of STO in symmetric case 139
Table 119. Design checks of STO in symmetric case 139
Table 120. Design checks of SC1 141
Table 121. Design checks of SC2 142
Table 122. Design checks of SC3 142
Table 123. Design checks of STI 143
Table 124. Design checks of STO 143

LIST OF FIGURES

FIGURES

Figure 1. Plan view of the system [1] 2

Figure 2. Response ratio vs eccentricity [1] 3

Figure 3. Static eccentricity definitions [2] 4

Figure 4. Ratio between peak isolator displacement for asymmetric and symmetric systems for different isolators [2] 4

Figure 5. Definition of static eccentricities [3] 5

Figure 6. Displacements and rotations of the plan [4] 7

Figure 7. Floor plan displacements [4] 8

Figure 8. Amplification ratio vs velocity (mm/s) [5] 10

Figure 9. Deformations of conventional vs isolated structures [9] 14

Figure 10. Effects of increasing period and damping on the demands of acceleration and displacement [10] 14

Figure 11. Fire Command and Control Facility, Los Angeles, California [12] 15

Figure 12. Los Angeles City Hall [13] 16

Figure 13. High-Damping Natural Rubber Bearing [16] 18

Figure 14. Lead-Rubber Bearing [17] 19

Figure 15. Resilient-Friction Base Isolation System [11] 20

Figure 16. Friction Pendulum System [19] 20

Figure 17. Friction Pendulum System 27

Figure 18. Damping Coefficients [6] 31

Figure 19. Ground floor formwork plan [27] 38
Figure 20. Upper floors formwork plan [27] 39
Figure 21. Response spectrum of fixed-base case [24] 41
Figure 22. 3D view of the fixed-base model of the structure 42
Figure 23. Isolator distributions under the shear walls 45
Figure 24. Isolator distributions under the shear walls 47
Figure 25. Distance ratio vs Stiffness ratio 74
Figure 26. Distance ratio vs Stiffness ratio, only in X direction 75
Figure 27. Distance ratio vs Stiffness ratio, only in Y direction 75
Figure 28. Weight ratio vs Stiffness ratio 76
Figure 29. Period ratio vs Stiffness ratio 77
Figure 30. Isolator types in symmetric case 82
Figure 31. Isolated response spectrum in symmetric case 83
Figure 32. Stiffness eccentricity 89
Figure 33. Isolated response spectrums in symmetric system 92
Figure 34. Ground motion history of Chi Chi 93
Figure 35. Ground motion history of Kocaeli 93
Figure 36. Ground motion history of Northridge 94
Figure 37. Labeled isolators for whole systems 96
Figure 38. Modes calculated for conventional and proposed methods 97
Figure 39. Labeled isolator displacements for symmetric systems 100
Figure 40. Labeled isolator displacements for asymmetric systems 105
Figure 41. Displacements of corner isolators at conventional method 106
Figure 42. Displacements of corner isolators at proposed method 106
Figure 43. Displacement differences between the isolators for each seismic input. 107

Figure 44. Lateral bilinear model of SC1 123
Figure 45. Lateral bilinear model of SC2 124
Figure 46. Lateral bilinear model of SC3 124
Figure 47. Lateral bilinear model of SC1 124
Figure 48. Lateral bilinear model of SC2 125
Figure 49. Lateral bilinear model of SC3 125
Figure 50. Lateral bilinear model of STI 125
Figure 51. Lateral bilinear model of STO 126

CHAPTER 1

INTRODUCTION

Base isolation is a seismic application that separates the superstructure from the ground. Then, movement of the ground is turned into displacements of isolators so that superstructure is protected by the damaging effects of earthquakes. In addition to superstructure, nonstructural components of the building are protected, as well.

Principles in base isolation are the shifting the effective period of the structure to get lower accelerations and increasing the effective damping of the structure to reduce the displacements isolation system.

1.1 LITERATURE SURVEY

The researches about the torsional response of base isolated structures are not much when compared to other researches about seismic base isolation. Moreover, design comparison of torsionally restrained and unrestrained structures does not exist. Generally, researches were done on idealized simple structures and relationships between the displacements of the specific isolators, time histories and mass or stiffness eccentricities were considered and examined. Nevertheless, studies about torsional behavior of the base isolation systems and the articles that shed light on about the aim of this study are briefly described here.

Jangid studied the seismic response of an asymmetric base isolated structure [1]. In that study, a sliding system is examined as the seismic isolation system of the model.

A simple framing system was considered which is symmetric about one axis and asymmetric about other axis and has mass eccentricity levels. Figure 1 shows the plan of the system. Parameters were indicated in the test are; R (ratio of mean peak response of the sliding system to mean peak response of fixed-base system), eccentricity, frequency ratios of rotational and translational modes, mass ratio of base and superstructure and friction coefficient.

Eccentricity effect can be explained as considering the uncoupled direction, if the eccentricity increases peak response of sliding system increases thus, R value increases, as well. Figure 2 that was illustrated in the article is showing this relation.

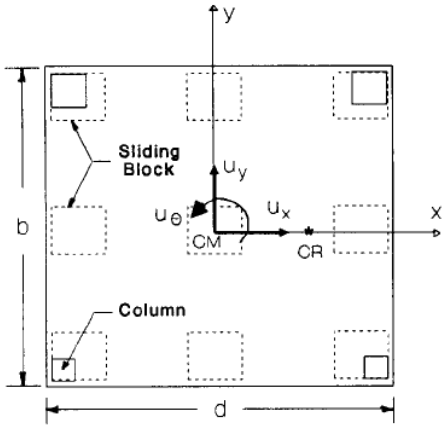


Figure 1. Plan view of the system [1]

The results of [1] shows that while rotational frequency and translational frequency ratio, w_0/w_x, increases, in other words, when torsional rigidity of the system increases, R value decreases in torsionally unrestrained cases ($0 < w_0/w_x < 1$).

The R ratio increases as the base mass to superstructure mass ratio, m_b/m increases. This was explained in that study as increasing of the limiting value of force in sliding elements in the system.

Finally, because of the increase in friction coefficient, sliding force in the system increases, as well. Hence, more force would be transmitted to the superstructure. This leads to an increase in R ratio. Thus, effectiveness of the system decreases.

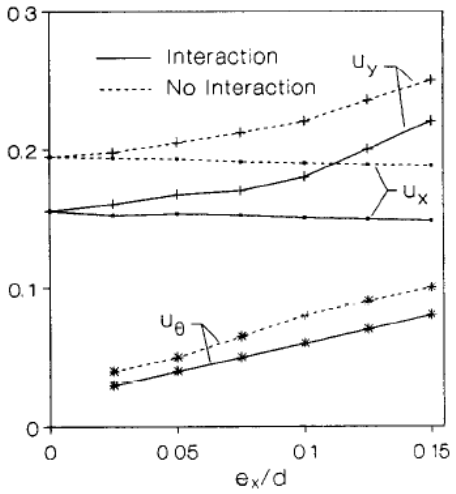


Figure 2. Response ratio vs eccentricity [1]

Tena-Colunga and Gomez-Soberon studied the torsional response of base-isolated structures due to asymmetries in the superstructure [2]. In that study, a simple, completely symmetrical in both directions, structure was selected. Structure itself has 3 bays in whole directions each having 7 meters long and a height of 3 meters. 3 different earthquake histories were used. Fixed-base modes were translational in first two modes and rotational in third mode. At each column, two types of bilinear isolation system was designed and selected for each case.

Asymmetry was provided by shifting the mass center of the system. Different cases were considered through this process. Mass center shifted only in one direction or in two directions are these cases (Figure 3). Furthermore, seismic input were given to the system in three different cases, as well.

According to the article, reduction of torque in the system is greatest when center of rigidity of isolators coincides with the center of mass of the system. Center of the rigidity of the superstructure is not that important and has a little effect on the magnitude of isolator displacements. Especially in elastomeric bearing systems, instead of structural eccentricity, eccentricity of isolators are more important.

In the cases with zero eccentricity, in other words, when the structure is completely symmetric, peak displacements were not occurring for same seismic input angle for all isolators. Therefore, using circular sections in design is best selection because the peak displacement values cannot be estimated with variable angles.

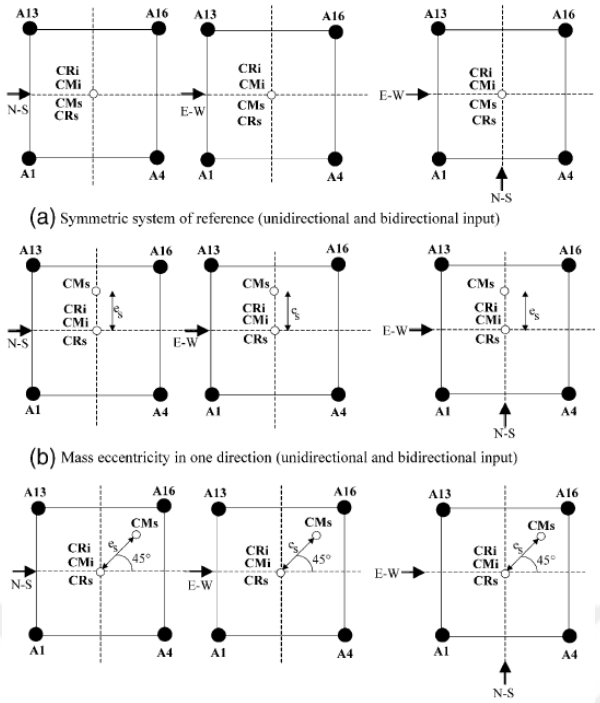


Figure 3. Static eccentricity definitions [2]

As eccentricities increase, ductility demands for the isolators which are farthest from the center of mass increase. In the same manner, isolators which are nearest to the center of mass of the system has decreasing displacement demands. In Figure 4, this relation is illustrated for different eccentricities with bidirectional seismic input.

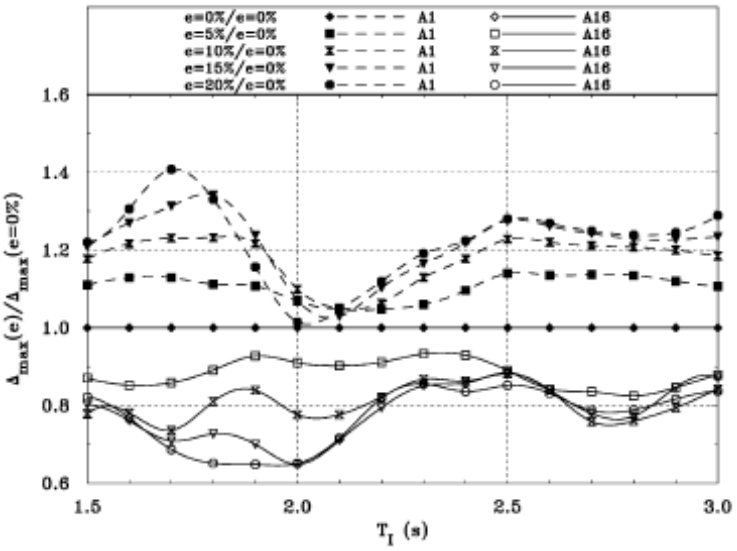
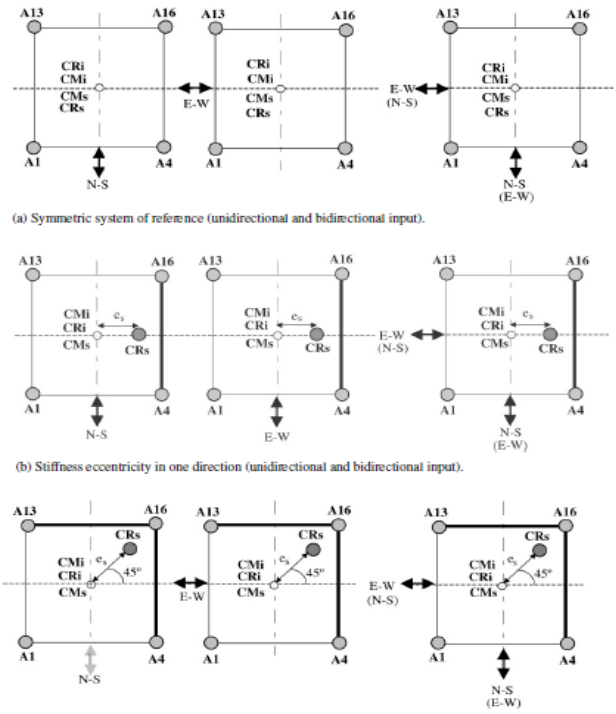


Figure 4. Ratio between peak isolator displacement for asymmetric and symmetric systems for different isolators [2]

In addition, unidirectional and bidirectional earthquakes cannot determine the peak displacements of the isolators. Hence, the code suggested combination for seismic input 100% one direction plus 30% other direction rule is not certain.

As a result, looking displacement values of isolators with different center of masses and earthquake inputs. The farthest isolator to the center of mass has the increasing displacement demand, nearest isolator has the decreasing displacement demand but, isolators with equal distances to the center of mass can show different displacement demands for different conditions.

Tena-Colunga and Escamilla-Cruz studied torsional amplifications in asymmetric base-isolated structures [3]. Issue in that study is very similar to the previous article that is torsional response of base-isolated structures due to asymmetries in the superstructure. Similar tests were done on the same structural model. Moreover, in addition to mass eccentricities, structural stiffness eccentricities were provided to system by stiffer perimeter frames (see in Figure 5). All studies were done for the cases with mass eccentricities similar in previous article and cases with stiffness eccentricities.



(a) Symmetric system of reference (unidirectional and bidirectional input).

(b) Stiffness eccentricity in one direction (unidirectional and bidirectional input).

Figure 5. Definition of static eccentricities [3]

Main aim in that article was showing the difference between the mass and stiffness eccentricities in the structure looking the response of it. Furthermore, other aim was to see that if the suggested isolated to fixed-base period design ratios were effective.

Because the procedure is very similar to previous study by the author, only results were argued here. After the all cases analyzed, it can be easily said that torsional amplifications are higher in the systems having mass eccentricities than the system with stiffness eccentricities. Moreover, the peak amplifications occur in the systems with higher eccentricities, such as e = 20%.

When the isolated period and fixed-base period ratio equals or larger than 8, the peak torsional displacement differences between the systems with mass and stiffness eccentricities can be ignored. Moreover, if the period ratios of isolated and fixed-base structure is smaller than 2, undesirable results are occurring about torsional behavior. According to the studies in this article, to get smaller torsional amplifications, recognizing the ratio of isolated and fixed-base period equal or larger than 3 is the best solution.

Finally, to have desirable torsional amplifications, eccentricities in any story should not exceed 10% of the plan dimensions. In addition, if any eccentricity exceeding 20% of the plan dimension exists, then, very strong torsional irregularities emerges in the structure.

Kilar and Koren studied seismic behavior of asymmetric base isolated structures with various distributions of isolators [4]. In that study, the difference from the other ones is the isolator distribution in addition to mass eccentricities. While providing mass eccentricities at different levels, at the same time 6 different isolator distribution was selected for the system. Tested structure here was a 4 story and rectangular planned building. It has 4 cases; symmetric, 10% mass eccentricity, 20% mass eccentricity and 30% mass eccentricity in only one direction. Moreover, system would be noted under 6 isolator distribution cases; center of rigidity of isolators (CI) is at the center of geometry, CI is at the center of mass (CM), CI is at –CM, CI is at CM/2, CI is at –CM/2 and CI is at the center of geometry but, the lateral rigidity of outer axes is higher than other ones.

All of these cases were examined under 3 cases, as well. These were torsionally unrestrained case ($\Omega_s<1$) and restrained cases ($\Omega_s=1$ and $\Omega_s>1$), where, Ω is torsional to lateral frequency ratio.

First result was of course that when mass eccentricities increases, even torsionally restrained cases becomes torsionally unrestrained case. In other words, torsional modes become first mode as coupling modes while mass eccentricities increase (Table 1, [4]). In Table 1, T shows that torsional mode has higher participation mass ratio.

Table 1. First and second periods of coupled modes [4]

	Fixed Base Building						Base Isolated Building					
	A10		A20		A30		A10		A20		A30	
	TY1		TY2		TY3		TY1		TY2		TY3	
$\Omega = 0.8$	0.71T	0.54	0.77T	0.48	0.86T	0.45	2.30T	1.66	2.47T	1.49	2.75T	1.38
$\Omega = 1$	0.61	0.48T	0.69	0.40T	0.78T	0.37	1.93	1.50T	2.16T	1.26	2.46T	1.17
$\Omega = 1.2$	0.5	0.41T	0.66	0.34	0.75T	0.32	1.85	1.31T	2.07	1.07T	2.35T	1.02

In the Table 1, as eccentricity increases, torsional mode becomes critical and overcomes the translational mode in both fixed-base and isolated structures.

After, looking the results of the selected ground motion, relations between the fixed-base top displacements and base and top displacements of isolated case were presented (Figure 6).

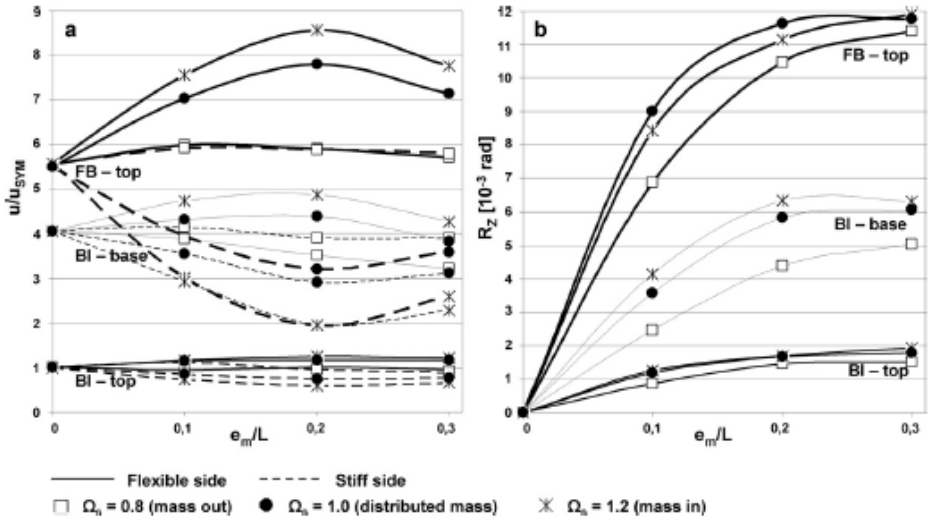


Figure 6. Displacements and rotations of the plan [4]

Looking at Figure 6, as expected, isolations get system to show smaller displacements when compared to fixed-base case. In asymmetric systems, isolators closer to mass center show higher displacements when compared to symmetric ones. Furthermore, increase in eccentricity do not result in much differences at the torsionally unrestrained cases. However, in torsionally restrained cases, mass eccentricity has great influence on displacements.

Various isolator distributions affects system in different ways. For example, if CI is at CM, isolator displacements show that isolator movements are not affected by the eccentricities and they displaces translationally and torsional amplifications are low. However, amplifications of the superstructure increases. On the other hand, if CI is at –CM, then, isolators show torsional and high displacements but, superstructure shows less torsional amplifications. In Figure 7, this relation is illustrated well.

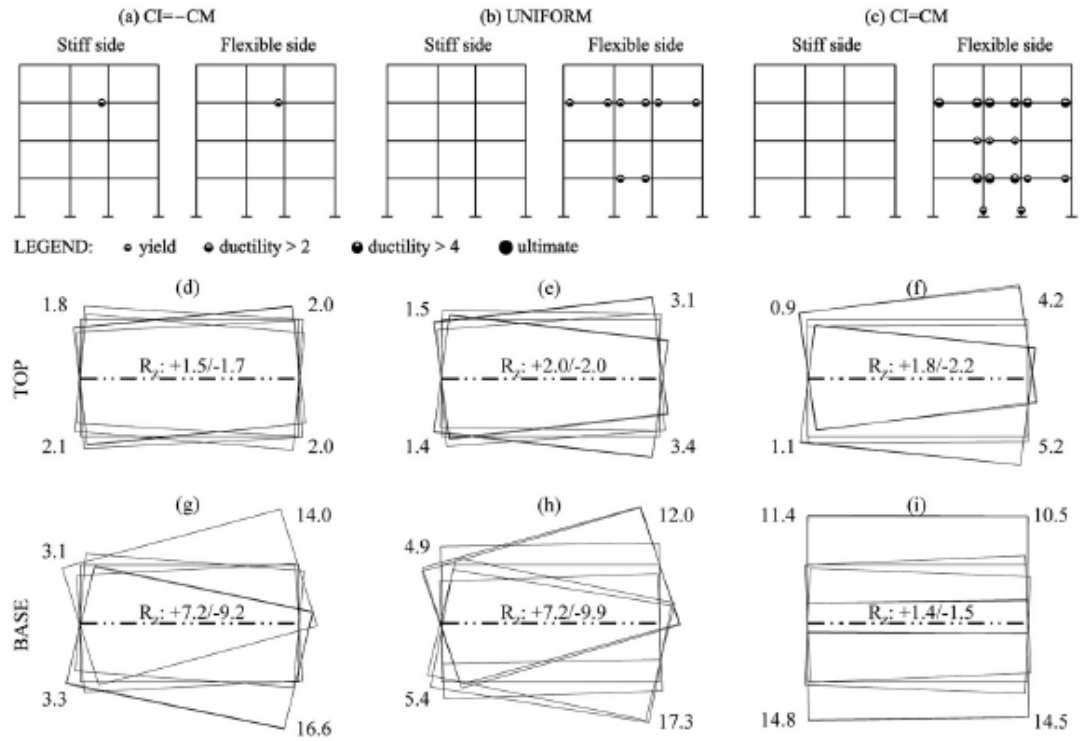


Figure 7. Floor plan displacements [4]

As a result, because the CI arrangement cannot affect positively isolator displacements and superstructure displacements at the same time, optimizing the CI at CM or CI at -CM is not a good solution. Generally, as a designing suggestion, center of mass and

the center of isolators should coincide. Thus, torsional amplifications in the isolation system are reduced much. However, this time amplifications in the superstructure increases and hence, forces increases in the structure, as well. Here, the best solution seems that the isolators should be at the intermediate level of the center of mass and center of rigidity. For instance, CI = -CM/2 or CM/2 is a good solution when looking this article results.

Wolff, Ipek, Constantinou and Mirallas studied the torsional response of seismically isolated structures [5]. In that study, the issue that is mainly focused on was about the torsional amplification factor investigation by comparing ASCE 7 [6] equivalent force method. In the ASCE 7 standard, to consider the accidental torsion, torsional displacements should be at least 1.1 times the normal displacements or a mass eccentricity of 5% should be taken into account.

According to an experiment by Zayas et al [7], a one story with four columns structure was modeled and a mass eccentricity was given. Isolator system of the structure was selected as friction pendulum system. After the system was examined on a shake table, the amplification ratios for isolator displacements were recorded as around 1.035 or less.

More recent experiment was done by Wolff and Constantinou [8], which was on a six story structure. This time, stiffness of the isolators and mass center were at the geometric center. Hence, mass eccentricities were not the case. Only eccentricities were provided by stiffness eccentricities with framing system itself by adding bracing only east side of the plan. Tests were carried out using different types of isolators such as lead-rubber, friction pendulum, low damping elastomeric and elastomeric and friction together. Results showed that the amplification factors were calculated around 1.13 or less. An example for lead-rubber bearing case can be seen in Figure 8. In the Figure 8, vertical axis shows the ratio of corner isolator displacement to average isolator displacement and horizontal axis shows velocity (mm/s) of shake table.

Another consideration in the article was about an important parameter which is $ye/\Omega_o r^2$. Here, y is the perpendicular edge distance to the plan dimension, e is eccentricity, Ω_o is translational period to torsional period and r is the radius of gyration.

The value of the parameter $ye/\Omega_o r^2$ is 0.085 based on the model in Wolff and Constantinou and this parameter is dimensionless. This test result parameter was applied to other structures to get e value in it. For example it was applied to Erzurum hospital and some other ones. When the e values were calculated, it can be seen that eccentricities was found around 0.025 times the side dimension considered, which is the half of the code suggestion.

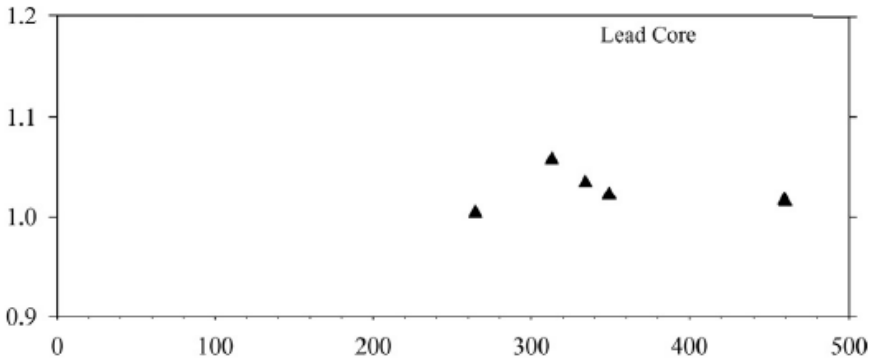


Figure 8. Amplification ratio vs velocity (mm/s) [5]

In conclusion, the amplification factor of the ASCE 7 is around the tested results of the past experiments. However, this factors can of course increase under different time histories. Moreover, the accidental eccentricity given in the code is about two times the eccentricity calculated by the tests.

1.2 AIM OF THE THESIS

As designing the conventional seismic isolation systems, isolators below each columns or shear walls are designed according to the axial load level on them. Then, axially durable but, laterally flexible isolators separate system from the ground to prevent the damages of the earthquakes. However, torsionally weak structures can stay weak in torsion and seismic isolation can be inefficient under different mass eccentricities when designed with conventional method. Thus, conventional designing method should be carefully applied to those kind of structures to control the behavior of the structure and increase the effectiveness of base isolation system. The main aim of this

study is to develop a new design method for torsionally unrestrained systems to make seismic isolation system more efficient.

When, a totally symmetric fixed-base structure itself has translational modes in first and second modes, then, it can be designed with the conventional method. However, if a totally symmetric fixed-base structure has torsional mode in its first mode, which is called torsionally unrestrained structure, then, using conventional designing method with elastomeric (lead-rubber) bearings may not prevent the torsional behavior of the structure. In other words, first mode of the structure after it is seismically isolated with elastomeric bearings, can emerge as torsion in first mode again. One of the ways to prevent this torsional mode and provide translational modes as the first two, the isolators standing at the outer axes of the structure should be laterally strengthened. While strengthening outer isolators, total lateral stiffness of the isolation system increases, as well. Hence, effective period of the structure decreases. In order to hold the effective period around the target period and providing translational modes as the first two in such structures, instead of the conventional designing, a new designing type can be used which is based on a lateral stiffness ratio between the isolators at outer and inner axes of the structure.

Logic in the design method developed in this study is that the lateral stiffnesses of the isolators are not designed according to axial load, instead they are separated as inner and outer isolator groups and their stiffnesses are determined as a ratio between them. This ratio is determined by using some parameters such as distances of isolators to the geometric center of the structure, total weight on outer and inner isolators, fixed-base first torsional and last translational period and target period. By using the parameters with a formulation developed by this research, a total outer and inner lateral stiffness ratio is calculated. Then, total required lateral stiffness found from conventional method is distributed with the stiffness ratio calculated to the outer and inner isolators. Axial resistance of each isolators are also checked. Thus, this developed design method allows system to stay around target period and saves structure from torsional mode.

Two design methods, conventional and developed, isolate the structure for different base shears and floor accelerations and result in torsionally different behaviors. In this study, effects of these two design methods on different systems were examined.

Systems were identical but, in addition to symmetrical case, the results of 4 different levels of mass eccentricities were defined to consider asymmetrical cases and also compared. Same asymmetries were examined under an additional stiffness eccentricity case also.

After designing systems with two different design methods, results such as displacements and shear forces on isolators are compared under different seismic loadings. Response spectrum analyses were used and then, to see more realistic behavior of the structure, 3 different time history records were used for same systems. As a result, effectiveness of each design method was discussed and that which one should be used was determined.

In Chapter 2, general informations about seismic base isolation are given. First, principles and backgrounds of seismic base isolation are described. Then, theory and design concepts of isolation system are provided.

Case studies are shown in Chapter 3. Definitions of building, formulation studies of proposed method and isolated cases of structure for both conventional and proposed method are provided under that section.

In Chapter 4, results of the isolated systems designed with conventional and proposed methods and the discussions of them are given.

Finally, in Chapter 5, conclusions of this study are provided.

CHAPTER 2

THEORY

2.1 SEISMIC BASE ISOLATION

Seismic base isolation is a design method, which protects the structures from damaging effects of the earthquakes. The protection is provided by attaching flexible devices under the structure. Main goal here is displacing the seismic device instead of the members of the structures and reducing the acceleration demand due to earthquake. Actually, independently from isolation, displacement of the members of the structure can be successively provided by designing a stiffer system, but this time acceleration demand would be increased. Thus, nonstructural components and devices are damaged more. On the other hand, if a flexible system is designed rather than a stiffer system, force demand from earthquake is reduced, but displacement of the system, interstory drifts, would be higher. As a result, seismic base isolation systems reduce the displacement and force demand of the structure and nonstructural components in it (Figure 9). Moreover, members of the structures show elastic deformations and story accelerations are sufficiently low to prevent any kind of damage.

Reduced accelerations with the help of the seismic base isolation are satisfied by shifting the period of the system to a larger value. As shown in Figure 10, while period is getting larger, displacement demand also increases. These higher period and deformation demands are satisfied by the flexibility of the seismic isolation devices. In the case of excessive deformation demands due to earthquake, energy dissipation ratios or in other words, damping ratios of the seismic isolation devices can be designed to optimize these excessive deformations to acceptable levels.

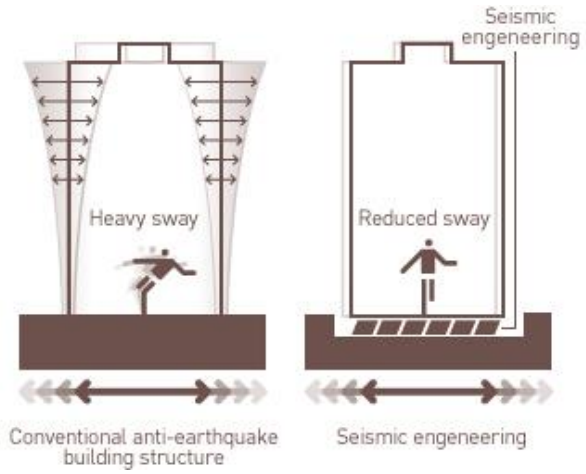


Figure 9. Deformations of conventional vs isolated structures [9]

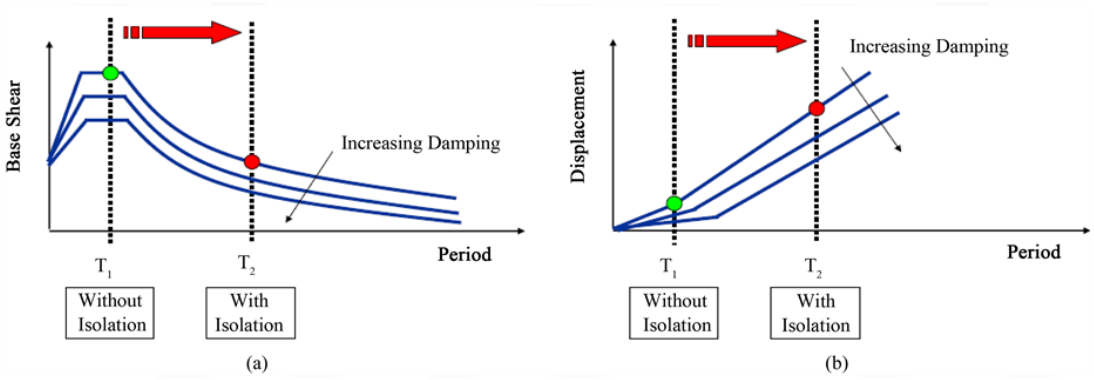


Figure 10. Effects of increasing period and damping on the demands of acceleration and displacement [10]

Therefore, the great flexibility difference between the seismic base isolation system and the structure itself allows only the isolator devices to move and dissipate the energy from the earthquake. In this way, ground movement is not transmitted to the structure. Thus, structure stays rigid and healthy.

2.2 BACKGROUND OF SEISMIC BASE ISOLATION

With the help of the improvements in the technology and the science, applications of seismic base isolation can be done efficiently and practically. These developments result from the catastrophic effects of the earthquakes in human life through the past years.

According to Naeim and Kelly [11], in August 1909, a medical doctor J. A. Calantarients, wrote a letter including an example of early base isolation technique to the Director of the Seismological Service of Scarborough. He suggested to build a structure on a layer which can be composed of sand, talc or gravel type fine rocks. By this method, energy transmitted from ground to the structure could be reduced.

Following years [11], big earthquakes in Italy, India and China showed scientists the damage differences on the buildings which stayed fixed on the ground and which slid over the ground. This energy dissipation by sliding made scientists notice the protection of buildings from seismic movements.

The base isolation is widely used in seismic zones. There are many examples of seismic base isolation especially in United States and Japan (Figure 11, 12).



Figure 11. Fire Command and Control Facility, Los Angeles, California [12]



Figure 12. Los Angeles City Hall [13]

After the developments of technology behind the seismic isolation systems, beyond the sliding type thoughts, also multilayered elastomeric seismic isolators emerged within the last 50 years [11]. These elastomers were improved by reinforcing them with steel layers. In addition, attaching lead core parts to the multilayered seismic devices improved damping capacity of the elastomers. Isolator systems are stiffer in vertical direction and very flexible in horizontal directions. As a result, with the help of the manufacturing developments of seismic isolators and experiencing the efficiency of seismic base isolation during earthquakes, isolation systems have become very popular around the world.

2.3 TYPES OF SEISMIC BASE ISOLATION SYSTEMS

Seismic base isolation systems can be examined in two main parts; elastomeric based systems and sliding based systems. Each year, with the help of new technologies, many different isolation systems are developed and patented. Nevertheless, in whole these types, isolation systems must satisfy some basic requirements: [14]

- High lateral deformation capacity

Isolation system should have low lateral rigidity (high lateral deformation capacity) to have a low frequency when compared to the fixed-base frequency of the same structure and the dominant frequency of the severe earthquakes.

- Sufficient lateral rigidity for wind load and low level earthquakes

In order to prevent small movements of the structures under low level load such as wind and small earthquakes, and satisfying the serviceability conditions, isolation system must have sufficient lateral rigidity.

- High vertical rigidity

Isolation system must have high vertical rigidity to prevent crushing or lateral bulging of the isolators so that it can resist the weight of the structure properly.

- Restoring force effect

Isolation system must have a restoring force effect to stay in its original position after large displacements.

- Damping

An isolation system should have a sufficient damping ratio (15 to 30%) than the structure to reduce the high displacements of the system and to prevent a potential resonance case. In addition, higher damping of the isolation system dissipates more energy coming from the earthquake.

- Resistance to tension forces

In the case of tension forces on the isolators, system must be designed to resist these forces.

- Collapse – preventing system

Isolation systems are designed for resisting a specific level earthquake. However, in the case of an unexpected earthquake, isolation system must have a collapse – preventing system for avoiding primarily isolator collapse and then, whole system collapse.

2.3.1 Elastomeric Based Systems

Elastomeric based system was first used as natural rubber bearing in Pestalozzi School, Macedonia in 1969 [11]. Isolators were designed with only rubber material in block shape. However, system has only a few times vertical rigidity when compared to horizontal rigidity. Thus, natural rubber material laterally bulges under the gravitational load of the structure. This issue leads structure to display rocking motions during strong earthquakes. Low vertical rigidity and thus rocking problem get scientists to develop laminated elastomeric bearings which are composed of rubber layers with steel shims.

Laminated elastomeric bearings are commercial products mainly developed for bridge sector, which is issued at Skinner, Robinson & McVerry [15]. These type of bearings are generally used as low-damping and high-damping natural rubber systems. Because low-damping natural rubber systems have a very low damping ratios, they are generally used with additional damping devices [11]. On the other hand, high-damping natural rubber systems were designed to have relatively higher damping ratios to eliminate the additional damping devices (see Figure 13).

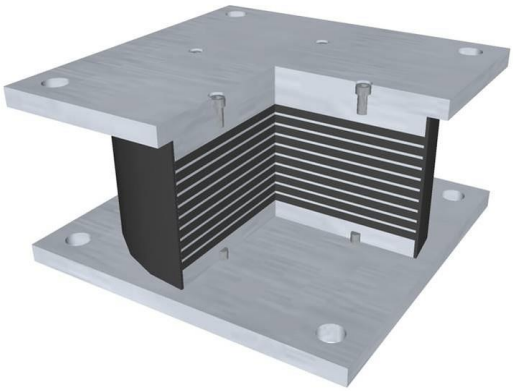


Figure 13. High-Damping Natural Rubber Bearing [16]

Another type of elastomeric bearings is lead-rubber bearings. It is invented in New Zealand in 1975 [11]. Lead-rubber bearings are composed of low-damping natural rubber system and cylindrical lead core at the center of bearing (Figure 14). Because of the yield strength of lead, system shows a bilinear response, which provides system to dissipate energy. This bilinear hysteretic response provides required high damping levels to the system.



Figure 14. Lead-Rubber Bearing [17]

2.3.2 Sliding Based Systems

As it is mentioned at Section 2.2, first idea for seismic isolation system based on sliding was proposed in 1909. Upcoming years, many scientific studies about sliding isolation have developed new systems. These sliding based systems can be named as flat surfaced and spherical surfaced sliding systems [18]. Isolation here is provided by sliding and friction parameters of this kind of devices.

In flat surfaced sliding systems, energy dissipation and required displacements are satisfied by sliding of the elements in them. However, because centering effect does not exist in this type of isolators, restoring force is provided by using them with other types of isolators or attaching cylindrical rubber core to the center. Resilient-friction base isolation system (R-FBI) is an example for this kind (Figure 15).

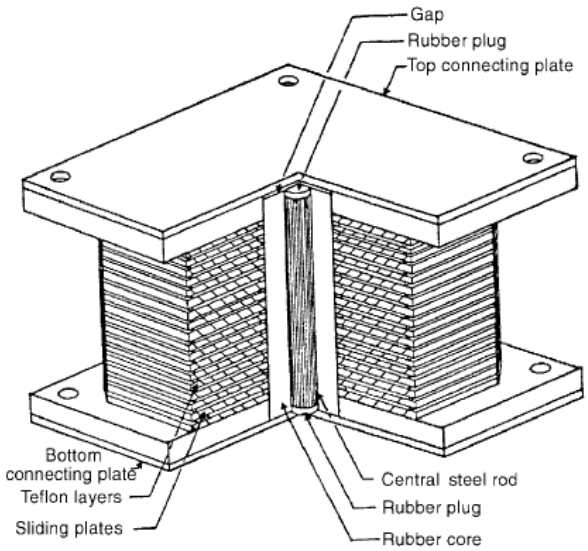


Figure 15. Resilient-Friction Base Isolation System [11]

Spherical sliding systems combines restoring force and sliding by its geometry. Because its sliding surface is spherical, displaced slider moves a bit upward direction. This additional potential energy brings system back to its original position. Hence, system gains a centering force. Moreover, friction between the slider and the spherical surface provides system damping. This type of sliding systems are called friction pendulum systems (FPS). In Figure 16, an illustration of FPS is supplied.

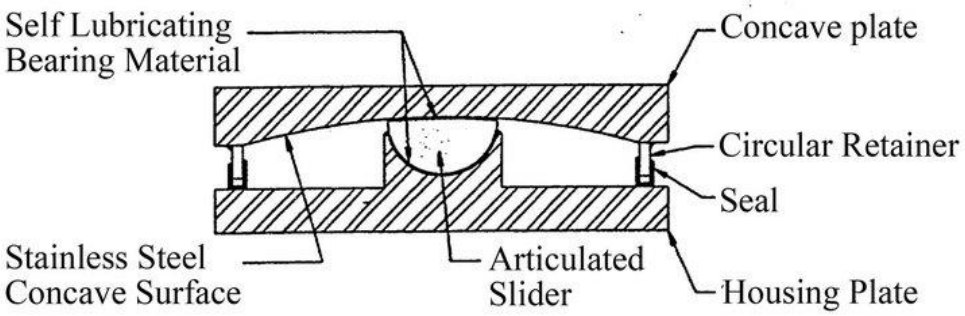


Figure 16. Friction Pendulum System [19]

2.4 FORMULATION OF SEISMIC BASE ISOLATION SYSTEM

Formulations used in this study about seismic base isolation systems were examined in two parts. Firstly, procedures behind the extension of theory to buildings were given. Then, mechanical formulations of the seismic isolators were figured out.

2.4.1 Linear Theory of Seismic Isolation Systems

Linear theory of seismic isolation is given in Kelly [20] in detail. This section covers the extension of this theory to the buildings.

According to Kelly [21] and Akyüz [22], the 2 degree of freedom analysis of a simple linear model can be extended through multistory structures. When defining the structural system, let mass matrix M, damping matrix C and stiffness matrix K. If the structure is a conventionally based structure, the relative displacement which is u of each degree of freedom with respect to the ground would be given,

$$M\ddot{u} + C\dot{u} + Ku = -Mr\ddot{u}_g \tag{2.1}$$

Here, r is a vector that couples the degree of freedoms to the ground motion. If a base isolation attached to the structure and if has a mass m_b, damping c_b and stiffness k_b; v is the relative displacement to base slab and v_b is the relative displacement of base slab to the ground, then Equation (2.1),

$$M\ddot{v} + C\dot{v} + Kv = -Mr(\ddot{u}_g + \ddot{v}_b) \tag{2.2}$$

When building and base slab is combined, equation becomes,

$$r^T M\ddot{v} + (m + m_b)\ddot{v}_b + c_b\dot{v}_b + k_b v_b = -(m + m_b)\ddot{u}_g \tag{2.3}$$

If Equation (2.3) is written in matrix form,

$$M^*\ddot{v}^* + C^*\dot{v}^* + K^*v^* = -M^*r^*\ddot{u}_g \tag{2.4}$$

where,

$$M^* = \begin{bmatrix} m + m_b & r^T M \\ Mr & M \end{bmatrix},\ C^* = \begin{bmatrix} c_b & 0 \\ 0 & C \end{bmatrix},\ K^* = \begin{bmatrix} k_b & 0 \\ 0 & K \end{bmatrix},\ r^* = \begin{bmatrix} 1 \\ 0 \end{bmatrix},\ v^* = \begin{bmatrix} v_b \\ v \end{bmatrix}$$

Assuming the natural mode shapes of a fixed base structure as $\underline{\phi^i}$, where i = 1,.....,N.

Then, displacement of each degree of freedom can be written by,

$$\mathrm{v} = \sum_{i=1}^{N} \mathrm{q}_i \underline{\phi^i} \tag{2.5}$$

And natural frequencies are given by,

$$\mathrm{M}\underline{\phi^i}\omega_i^2 = \mathrm{K}\underline{\phi^i} \tag{2.6}$$

Here, it is assumed that $\underline{\phi^i}\mathrm{C}\underline{\phi^j} = 0$ if $i \neq j$, and the matrix equations are reduced to N+1 equations,

$$\sum_{i=1}^{N} \mathrm{r}^{\mathrm{T}}\mathrm{M}\underline{\phi^i}\ddot{\mathrm{q}}_i + (m+m_b)\ddot{v}_b + c_b\dot{v}_b + k_b v_b = -(m+m_b)\ddot{u}_g \tag{2.7}$$

$$\ddot{\mathrm{q}}_i + 2\omega_i\beta_i\dot{\mathrm{q}}_i + \omega_i^2\mathrm{q}_i = -\mathrm{L}_i(\ddot{u}_g + \ddot{v}_b) \qquad i = 1,.....,\mathrm{N} \tag{2.8}$$

L_i here are the participation factors of fixed-base modes. Then, M_i fixed-base modal masses which are denoted by,

$$\mathrm{L}_i = \frac{\underline{\phi^i}^{\mathrm{T}}\mathrm{Mr}}{\underline{\phi^i}^{\mathrm{T}}\mathrm{M}\underline{\phi^i}}, \quad \mathrm{M}_i = \underline{\phi^i}^{\mathrm{T}}\mathrm{M}\underline{\phi^i}$$

Then, these equations can be written as,

$$\sum_{i=1}^{N} \frac{\mathrm{L}_i\mathrm{M}_i}{(m+m_b)}\ddot{\mathrm{q}}_i + \ddot{v}_b + 2\omega_b\beta_b\dot{v}_b + \omega_b^2 v_b = -\ddot{u}_g \tag{2.9}$$

$$\mathrm{L}_i\ddot{v}_b + \ddot{\mathrm{q}}_i + 2\omega_i\beta_i\dot{\mathrm{q}}_i + \omega_i^2\mathrm{q} = -\mathrm{L}_i\ddot{u}_g \qquad i = 1,.....,\mathrm{N} \tag{2.10}$$

The equations of natural frequencies and mode shapes of the superstructure, by eliminating damping and velocity parameters,

$$\ddot{\mathrm{q}}_i + \omega_i^2\mathrm{q}_i + \mathrm{L}_i\ddot{v}_b = 0 \qquad i = 1,.....,\mathrm{N} \tag{2.11}$$

$$\sum_{i=1}^{N} \frac{\mathrm{L}_i\mathrm{M}_i}{(m+m_b)}\ddot{\mathrm{q}}_i + \ddot{v}_b + \omega_b^2 v_b = 0 \tag{2.12}$$

If new eigenvector is applied in v_b and q_i by $\vec{\psi}^{j} = \overrightarrow{\overrightarrow{\psi}}^{j} e^{iwt}$

where,

$\overrightarrow{\overrightarrow{\psi}}^{jT} = (\bar{v}_b, \bar{q}_1, \bar{q}_2, \bar{q}_3, ..., \bar{q}_N)$ $\quad j = 0,\ldots,N$ (i.e ψ_0^j is the value of v_b of the j^{th} mode)

Then,

$$(-\omega^2 + \omega_i^2)\bar{q}_i - \omega^2 L_i \bar{v}_b = 0 \qquad i = 1,.....,N \tag{2.13}$$

$$-\omega^2 \sum_{i=1}^{N} \frac{L_i M_i}{(m+m_b)} \bar{q}_i + (-\omega^2 + \omega_b^2)\bar{v}_b = 0 \tag{2.14}$$

Substituting Equations (2.13) and (2.14),

$$-\omega^2 \sum_{i=1}^{N} \frac{L_i{}^2 M_i}{(m+m_b)} \frac{\omega^2}{(-\omega^2 + \omega_i^2)} \bar{v}_b + (-\omega^2 + \omega_b^2)\bar{v}_b = 0 \tag{2.15}$$

Distributing terms into two side of the equation and dividing both sides with $-\omega^2$,

$$\sum_{i=1}^{N} \frac{L_i{}^2 M_i}{(m+m_b)} \frac{1}{(1-\frac{\omega_i^2}{\omega^2})} = (1-\frac{\omega_b^2}{\omega^2}) \tag{2.16}$$

Then the equation can be solved for each root by iterative processes. Accepting the lowest root is close to ω_b^2 and recognizing $\omega_i^2 / \omega_b^2 >> 1$. Then,

$$\omega_b^{*2} = \omega_b^2 (1 - \sum_{i=1}^{N} \frac{L_i{}^2 M_i}{(m+m_b)} \frac{\omega_b^2}{\omega_i^2}) \tag{2.17}$$

Next root near ω_1 with setting $\omega_b^2 / \omega^2 \cong 0$ is approximately determined as,

$$\omega^2 = \omega_1^2 \frac{1}{(1-\gamma_1)} \quad \text{where } \gamma_i = \frac{L_i^2 M_i}{m+m_b} \tag{2.18}$$

Then, the general result for n^{th} mode,

$$\omega_n^{*2} = \frac{\omega_n^2}{1-\gamma_n (\frac{1}{1-(1-\gamma_n)\omega_b^2/\omega_n^2} - \sum_{i=1}^{N} \frac{\gamma_i}{1-\omega_i^2/\omega_1^2(1-\gamma_n)})} \tag{2.19}$$

The corresponding eigenvectors computed by substations of $\bar{q}_i^j$ and ω_i^* for ω_j^*,

$$\bar{q}_i^j = -\frac{\omega_j^{*2}}{\omega_j^{*2} - \omega_i^2} L_i \tag{2.20}$$

The value of $\bar{v}_b$ here is taken as unity for each modes. Then the resulting mode shapes for superstructure are given as,

$$\bar{\bar{\psi}}^{jT} = (1, \sum_{i=1}^{N} \bar{q}_i^j \phi_1^i, \sum_{i=1}^{N} \bar{q}_i^j \phi_2^i, ...) \tag{2.21}$$

2.4.2 Mechanical Formulations of Seismic Isolation

Because only elastomeric based bearings (lead-rubber bearings) were used in this study, mechanical formulations and characteristics of seismic isolation were examined according to lead-rubbers and in two parts; elastomeric based bearings and bilinear modeling of isolation bearings.

2.4.2.1 Elastomeric Based Bearings

Formulations and characteristics of the elastomeric bearings were figured out in detail by [21]. Briefly, horizontal stiffness of an elastomeric bearing,

$$K_H = \frac{GA}{t_r} \tag{2.22}$$

where, G is shear modulus of elastomer, A is cross sectional area of elastomer and t_r is the total thickness of rubber.

Maximum shear strain, γ, is related to maximum horizontal displacement, D,

$$\gamma = \frac{D}{t_r} \tag{2.23}$$

Because the vertical frequency of the structure is controlled by the vertical stiffness of the isolators and the buckling behavior is important for bearings, vertical stiffness and

bending stiffness of the isolators must be calculated for designing. This calculation is figured out through simple linear elastic theory.

Then, vertical stiffness of the bearing,

$$K_V = \frac{E_C A}{t_r} \tag{2.24}$$

where, E_C is the compression modulus of rubber-steel composite under a specific vertical load, A is the cross sectional area of elastomer and t_r is the total thickness of rubber.

The value of E_C for a single rubber layer is determined by a shape factor, S, which is defined in [11] as,

$$S = \frac{loaded\ area}{force - free\ area} \tag{2.25}$$

Values of S for different types of bearings are below.

For an infinite strip of width 2b and thickness t,

$$S = \frac{b}{t} \tag{2.26}$$

For a square bearing of side dimension b and thickness t,

$$S = \frac{b}{4t} \tag{2.27}$$

For a circular bearing of radius r and thickness t,

$$S = \frac{r}{2t} \tag{2.28}$$

Related E_C values for each type of bearings,

For an infinite strip,

$$E_C = 4GS^2 \tag{2.29}$$

For a square bearing,

$$E_C = 6.73GS^2 \tag{2.30}$$

For a circular bearing,

$$E_C = 6GS^2 \tag{2.31}$$

For the bearings with central hole, even if a very small hole, has great effect on E_C. Hence, for the bearings with central hole cases, [11] and [22] stated that E_C should be taken as $4GS^2$.

Bending stiffness of each type of bearings are,

For an infinite strip,

$$(EI)_{eff} = E_C(1/5I) \tag{2.32}$$

For a square bearing,

$$(EI)_{eff} = E_C(0.329I) \tag{2.33}$$

For a circular bearing,

$$(EI)_{eff} = E_C(1/3I) \tag{2.34}$$

In this study, S (shape factor) was selected as at least 10 for no rocking conditions, thus, eliminating bulging effects.

2.4.2.2 Bilinear Modeling of Isolation Bearings

In general, whole high damping rubber bearings are modelled as bilinear elements. There are three main parameters when it is modelled; K_1, K_2 and Q. Here, K_1 is elastic stiffness, K_2 is plastic stiffness and Q is the intercept of the extension of K_2 and force axis, in other words, yielding force of the lead. Generally, because of the difficulty when estimating the elastic stiffness of the bearings, elastic stiffness is taken as multiple times the plastic stiffness or gathered from past test results [15]. For instance, elastic stiffness of lead-rubber bearings are estimated as ten times of plastic stiffness and friction pendulum systems are assumed as an hundred times of plastic stiffness. Moreover, while Q is about yielding force on lead-rubber bearings, it is about friction and load on the friction pendulum systems. In Figure 17, parameters are explained for lead-rubber bearings,

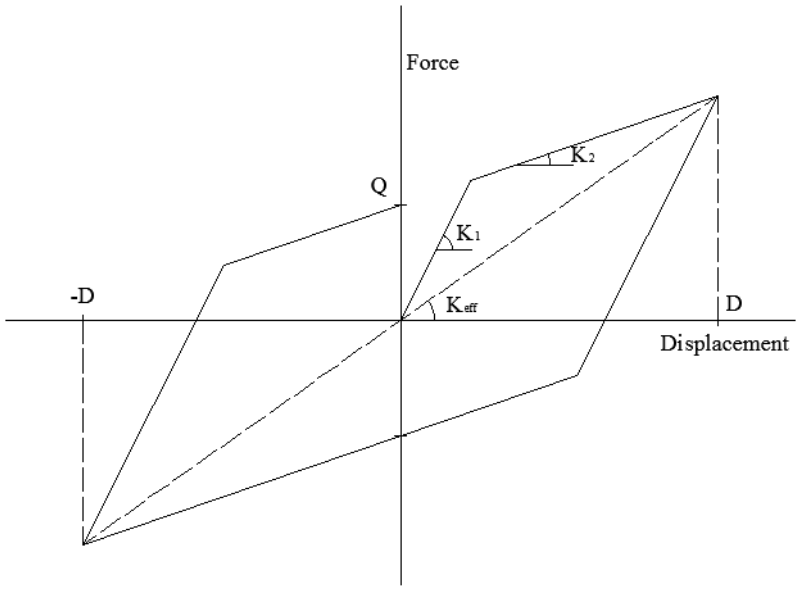


Figure 17. Friction Pendulum System

Natural frequency of lead-rubber, ω, is stated as [11],

$$\omega = \sqrt{\frac{K_{eff}\, g}{W}} = \sqrt{\omega_0{}^2 + \mu \frac{g}{D}} \tag{2.35}$$

where, $\mu = Q/W$ *and* $\omega_0{}^2 = \sqrt{K_2 g / W}$

Effective damping ol f the system, β_{eff}, for D > Dy

$$\beta_{eff} = \frac{W}{2\pi K_{eff} D^2} \tag{2.36}$$

where, W is area of hysteresis loop, D_y is yield displacement. The yielding force F_y equals D_y times K_1 and $F_y = Q + K_2 D_y$. Thus,

$$D_y = \frac{Q}{K_1 - K_2} \tag{2.37}$$

$$W = 4Q(D - D_y) \tag{2.38}$$

Then, substituting the Equations (2.37) and (2.38) into (2.36),

$$\beta_{eff} = \frac{4Q(D - Q/9K_2)}{2\pi K_{eff} D^2} \tag{2.40}$$

where, for $D > D_y$, effective stiffness,

$$K_{eff} = K_2 + Q / D \tag{2.41}$$

Furthermore, effective damping of the system can be calculated in a different way considering nondimensional parameters. Assuming $D > D_y$, $y = D/D_y$ and $a = Q/K_2D_y$

Then, effective damping becomes,

$$\beta_{eff} = \frac{2a(y-1)}{\pi y(y+a)} \tag{2.42}$$

In order to calculate the maximum effective damping, derivative of effective damping with respect to y is calculated. The y point equating the formula to zero is at $1+(1+a)^{1/2}$, which gives,

$$\beta_{\max} = \frac{2a}{\pi(2\sqrt{1+a}+(2+a))} \tag{2.43}$$

Rewriting the parameter a,

$$a = \frac{Q}{K_2 D_y} = \frac{Q}{K_2}\frac{K_1 - K_2}{Q} = (K_1 - K_2)/K_2 \tag{2.44}$$

Result shows that elastic stiffness of the isolator that has no effect on effective stiffness has influence on effective damping. According to Naeim and Kelly [11], this effect is high at small displacements and equal for different kind of elastic stiffness values at large displacements.

2.5 DESIGN OF SEISMIC BASE ISOLATION

In the study, instead of other structural elements, design of base isolation system was carried out only. Preliminary assumptions of the basic parameters of the isolation system such as displacements and effective stiffnesses were selected with the help of ASCE 7-10 [6] and UBC-97 [23].

Designing of isolation system is carried out for two types of seismic input. One of them is design base earthquake (DBE) that is an earthquake with 10% probability of being exceeded in 50 years (475 years return period) and the other one is maximum considered earthquake (MCE) that is an earthquake with 2% probability of being exceeded in 50 years (2475 years return period). MCE is used for designing of seismic isolators and DBE is used for designing of the building. Earthquake inputs can be assigned to structure by equivalent force, response spectrum and time history methods. In this study, response spectrum and time history loadings were used.

First, considering the fixed base period and seismic zone of the structure, two target periods are determined for desired floor accelerations and base shears. Then, selecting the type of the isolation bearings damping coefficients are determined. Using the target periods and the weight of the structure, effective stiffness of the isolation system is estimated. After that required displacements are calculated preliminarily with the help of the seismicity, damping level and the target period of the system.

Second, using preliminary parameters and values, system is analyzed with response spectrum technique. Then, the forces on each isolator are calculated and the detailed design of each isolator is done. With the new detailed values updated displacements, forces and periods are verified through new analyses.

Finally, after the whole parameters design values are verified, system is analyzed with time history method to see the real behavior of the structure under real seismic input. Actual design parameters are updated again and noted.

Design steps were explained in two parts; preliminary design and final design of seismic isolators.

2.5.1 Preliminary Design of Seismic Isolators

According to ASCE 7-10, effective stiffness of the system at DBE and MCE can be estimated as,

$$T_D = 2\pi\sqrt{\frac{W}{k_D g}} \tag{2.45}$$

$$T_M = 2\pi\sqrt{\frac{W}{k_M g}} \tag{2.46}$$

where, T_D is target period of DBE, T_M is target period of MCE, k_D is effective stiffness of the system under DBE, k_M is effective stiffness of the system under MCE, W is effective weight of the structure and g is gravitational acceleration.

Design and maximum displacements of the isolation system is estimated as,

$$D_D = \frac{gS_{D1}T_D}{4\pi^2 B_D} \tag{2.47}$$

$$D_M = \frac{gS_{M1}T_M}{4\pi^2 B_M} \tag{2.48}$$

where, D_D is design displacement under DBE, D_M is maximum displacement under MCE, S_{D1} is design 5% damped spectral acceleration at 1 second, S_{M1} is maximum 5% damped spectral acceleration at 1 second, B_D is a coefficient about damping level at DBE, B_M is a coefficient about damping level at MCE (For B values see Figure 18).

Moreover, total displacements of the isolation system must be taken into account in order to consider the actual and accidental torsional effects. These displacements are calculated as,

$$D_{TD} = D_D\left[1 + y\frac{12e}{b^2 + d^2}\right] \geq 1.1D_D \tag{2.49}$$

$$D_{TM} = D_M\left[1 + y\frac{12e}{b^2 + d^2}\right] \geq 1.1D_M \tag{2.50}$$

here, D_{TD} is design total displacement under DBE, D_{TM} is maximum total displacement under MCE, y is distance between center of rigidity and edge point measured

perpendicular to the earthquake direction, b is the shortest plan dimension, d is longest plan dimension of the structure and e is the eccentricity between center of mass and center of rigidity of the structure plus accidental eccentricity.

Effective Damping, β_D or β_M (percentage of critical)[a,b]	B_D or B_M Factor
≤2	0.8
5	1.0
10	1.2
20	1.5
30	1.7
40	1.9
≥50	2.0

Figure 18. Damping Coefficients [6]

Furthermore, building is designed for a shear force to stay safe under DBE. This shear force is described as,

$$V_S = \frac{k_D D_D}{R} \tag{2.51}$$

where, V_S is the shear force for building above isolation system and R is a reduction factor with a value changing between 1.0 and 2.0 according to ASCE 7 [6]. Additionally, except for building itself, whole other components of the isolations system, such as isolators foundation and the systems below the isolator level should withstand a minimum shear force which is,

$$V_B = k_D D_D \tag{2.52}$$

2.5.2 Final Design of Seismic Isolators

Because the isolators designed in this study are lead-rubber bearings, design procedure was explained through this type of isolators. When preliminary designs were carried out and the forces on each isolators with displacements were calculated according to desired period and stiffness, final design or detailed design of isolators can be done. This procedure is below according to Akyüz [22],

- Determining the maximum shear strain γ_{max}.
- Defining material properties such as E, G and breaking strain.
- Selecting the total rubber height as,

$$t_r = \frac{D_{TM}}{\gamma_{\max}} \tag{2.53}$$

where, t_r is total rubber thickness.

- Calculating required sectional area of the lead and thus, diameter of it by,

$$A_p = \frac{Q}{f_{py}} \tag{2.54}$$

where, f_{py} is yield strength of the lead that is around 10 MPa and A_p is the required lead area. Q is calculated by eliminating the D_y in Equation (2.37).

- Selecting a shape factor S while considering no rocking conditions,

$$K_V / K_H \geq 400 \tag{2.55}$$

Where, $K_V / K_H = 6S^2$, then, approximately $S \geq 10$

K_V is vertical stiffness and K_H is horizontal stiffness.

- To determine the cross sectional area of rubber, three kind of area value should be calculated,

Calculating A_0 that is required sectional area to resist axial stress,

$$\frac{P_{DL+LL}}{A_0} \leq 7.8\,MPa \tag{2.56}$$

Calculating A_1 from shear strain because of axial force,

$$6S\frac{P_{DL+LL}}{E_C A_1} \le \frac{\varepsilon_b}{3} \tag{2.57}$$

where, E_C is compression modulus and ε_b is breaking strain.

Calculating A_2 from net projection area of displaced rubber,

Elastic modulus of the bearing, K_e, is calculated as,

$$K_e = \frac{K_2}{(1+12\frac{A_p}{A_0})} \tag{2.58}$$

where, K_2 is elastic stiffness of the bearing, A_p is sectional area of the lead.

Then, using elastic modulus required shear failure area, A_{sf}, should be determined,

$$A_{sf} = \frac{K_e t_r}{G} \tag{2.59}$$

Now, A_2 can be calculated using A_{sf},

For rectangular bearings,

$$A_2 = L(B - D_{TM}) \tag{2.60}$$

where, L and B are the side dimensions of the bearing, parallel and perpendicular respectively.

For circular bearings,

$$A_2 = \frac{d^2}{4}\left[2\cos^{-1}(\frac{D_{TM}}{d}) - \sin(2\cos^{-1}(\frac{D_{TM}}{d}))\right] \tag{2.61}$$

where, d is diameter for area A_{sf}.

Thus, required cross sectional area of the rubber is maximum of three calculated areas.

$$A = \max(A_0, A_1, A_2) \tag{2.62}$$

- Defining each rubber layer thickness, t, using the Equations (2.27) or (2.28).
- Determining the rubber layer unit by,

$$N = t_r / t \tag{2.63}$$

- Calculating the thickness of steel plates, t_s,

$$t_s = \frac{4tP_{DL+LL}}{0.6F_y A_2} \geq 2\,mm \tag{2.64}$$

where, F_y is strength of steel used in bearing.

- Final verification about lead core dimension,

$$1.25 \leq H_p / d_p \leq 5.0 \tag{2.65}$$

Here, H_p is effective height of lead core and d_p is diameter of lead core.

After defining the parameters of the lead-rubber bearing, stability checks must be figured out through three steps.

Statically Stability Condition

Shear strain check,

$$6S\frac{P_{DL+LL}}{E_C A} \leq \frac{\varepsilon_b}{3} \tag{2.67}$$

Buckling check [11],

$$\frac{P_{DL+LL}}{A} \leq \sigma_{cr} \;\; where,\; \sigma_{cr} = \frac{\sqrt{2}\pi GSr}{t_r} \tag{2.66}$$

where, r is radius of gyration.

Dynamically Stability Condition

Shear strain check,

$$(\gamma_c + \gamma_{eq} + \gamma_{sr}) < 0.75\varepsilon_b \tag{2.67}$$

where,

$$\gamma_c = 6S\frac{P_{DL+LL+EQ}}{E_C A} \tag{2.68}$$

$$\gamma_{eq} = D_{TM} / t_r \tag{2.69}$$

$$\gamma_{sr} = \frac{d^2\theta}{2tt_r} \tag{2.70}$$

where, d is diameter calculated from cross sectional area of rubber and θ,

$$\theta = \frac{12D_{TM}e}{b^2 + d^2} \tag{2.71}$$

here, e is eccentricity defined before, and b is short plan dimension and d is long plan dimension.

Roll-out Stability Condition

If the bearings are dwelled (not to be bolted), roll-out stability check must be done.

$$\delta_{\max} = \frac{1}{2}\frac{(P_{DL+LL+EQ})d - QH}{(P_{DL+LL+EQ}) + K_2 H} \geq D_{TM} \tag{2.72}$$

where, H is the total height of the bearing including cover plates.

If bearings are bolted, roll-out stability check is not a necessity.

CHAPTER 3

CASE STUDIES

The aim of this study, as already mentioned, is to increase the effectiveness of seismic isolation on buildings for which the fundamental period is torsional. While investigating the effectiveness of isolation system, the parameters which were taken into account are the distances of isolators to geometric center of plan, weights on isolators, the periods of fixed-base structure and period assumed. In this chapter, the details of the building which were analyzed is given.

3.1 DEFINITION OF THE STRUCTURE

Structure itself that was used through the study is a reinforced concrete structure that was built in Istanbul, Eyup, Guzeltepe. It was built as a social house-dwelling project. Building is standing on seismic zone one ($A_0 = 0.4$), as stated in Turkish Seismic Code [24]. According to Turkish Code, soil classification was selected as two (Z2). Because the system is an house-dwelling project, importance factor was chosen as 1. Reduction factor of the building was taken as 4 for fixed-base case. Reinforced concrete class is C30 and reinforcing steel class is S420 [25].

Structure was modelled as 6 story building in SAP2000. First story has an height of 3.8 m and rest of the stories have an height of 3 m. Formwork plans are shown in Figure 19 and 20. Looking the architectural drawings of the building [26], additional dead load of the slabs were calculated as 0.22 ton/m^2: The details of additional dead load are as follows:

3 cm cement; 2 ton/m^2 * 0.033 = 0.66 ton/m^2

3 cm ceiling plaster; 2.1 ton/m^2 * 0.03 = 0.063 ton/m^2

4 cm leveling concrete; 2.2 ton/m^2 * 0.04 = 0.088 ton/m^2

1.5 cm parquet, 0.7 ton/m^2 * 0.015 = 0.011 ton/m^2

Moreover, live load on the system was chosen as 0.2 ton/m^2 at the interior regions of the building. However, on balcony regions, live load was taken as 0.5 ton/m^2. In addition, at the last floor, live load was selected as 0.15 ton/m^2 in all regions. Whole the interior and exterior walls have an height of 3.2 m for ground floor and 2.4 m for upper floors. 20 cm brick walls and walls with insulation have a load of respectively 0.79 and 0.85 ton/m. 10 cm brick walls have 0.47 ton/m.

Axis distances of the system:

1-2 = 4 m; 2-3 = 2 m; 3-4 = 5.3 m; 4-5 = 2 m; 5-6 = 4 m

A-B’ = 2.75 m; B’-B = 2.6 m; B-C = 1.7 m; C-C’ = 1.35 m;

C’-D = 1.35 m; D-E = 1.7 m; E-F’ = 2.6 m; F’-F = 2.75 m;

In addition, lengths of the cantilever sides of each direction is 1.6 m.

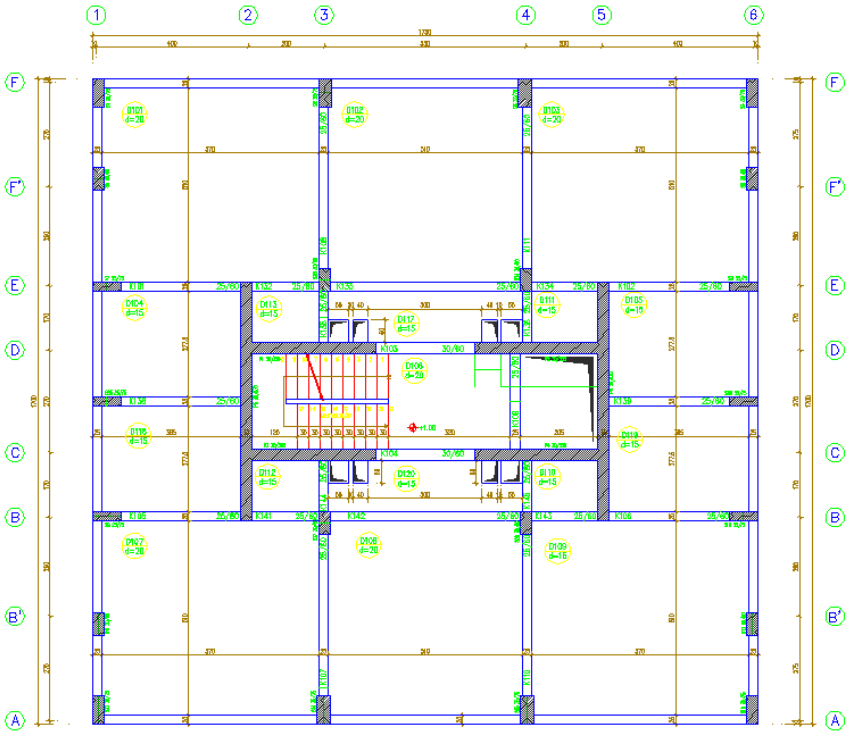


Figure 19. Ground floor formwork plan [27]

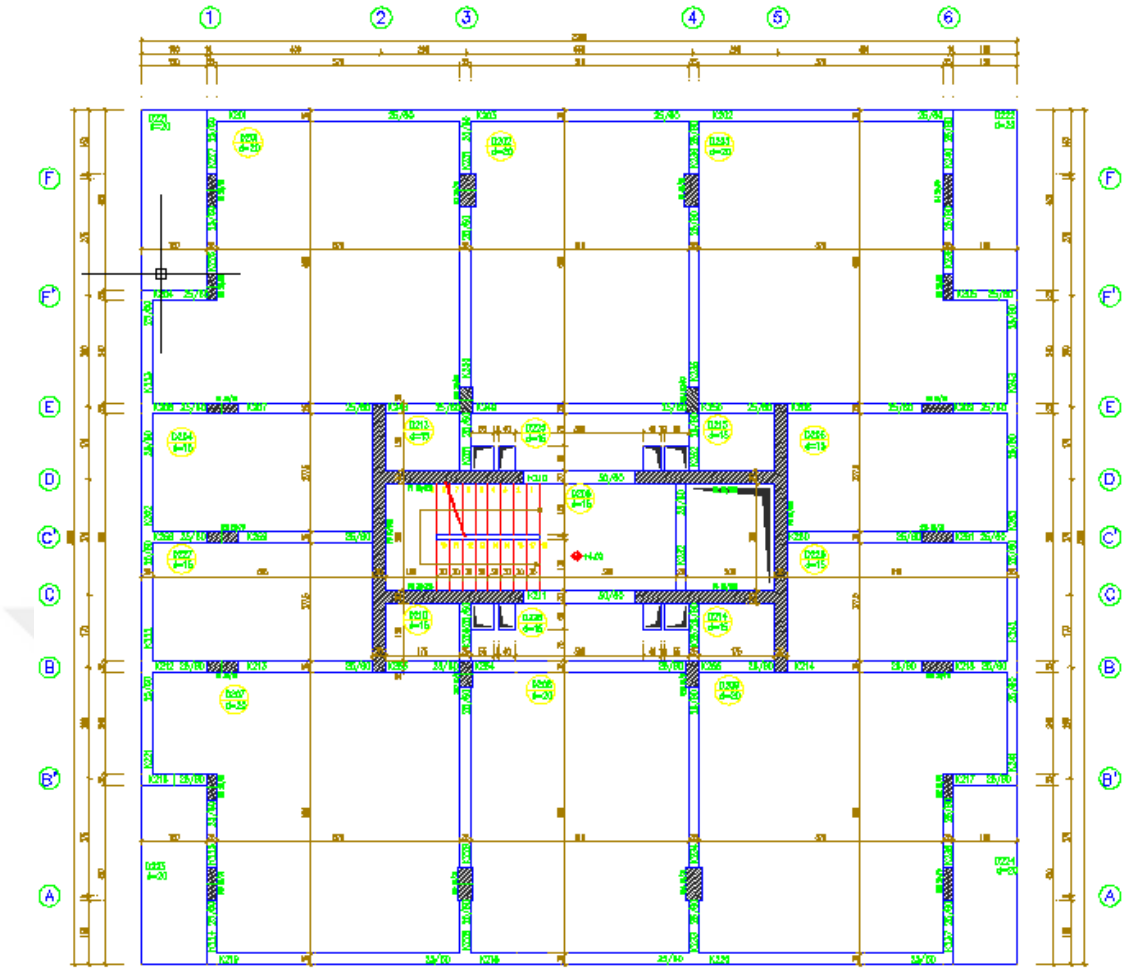


Figure 20. Upper floors formwork plan [27]

Slab thicknesses are 15 cm between the axes B and E. Rest of the slabs have a thickness of 20 cm. In order to provide fully asymmetry, stairs and empty places were ignored and 15 cm slabs were added to these places.

Whole the shear walls have a thickness of 30 cm.

Beams lying between the parallel shear walls at the axes C and D have a section of 30/60 cm. Rest of the beams have a cross section of 25/60 cm.

Columns are in variable sections. Because the system is symmetric, only columns at the axes A and C' will be stated with respect to horizontal axes.

First floor,

Axis A; 30/75 cm, 35/75 cm, 35/75 cm, 30/75 cm

Axis B’: 30/60 cm, 30/60 cm

Axis B: 25/75 cm, 30/60 cm, 30/60 cm, 25/75 cm

Axis C’: 25/75 cm, 25/75 cm

Second floor,

Axis A; 25/75 cm, 35/75 cm, 35/75 cm, 25/75 cm

Axis B’: 25/60 cm, 25/60 cm

Axis B: 25/75 cm, 30/60 cm, 30/60 cm, 25/75 cm

Axis C’: 25/75 cm, 25/75 cm

Third and upper floors,

Axis A; 25/75 cm, 30/75 cm, 30/75 cm, 25/75 cm

Axis B’: 25/60 cm, 25/60 cm

Axis B: 25/75 cm, 30/60 cm, 30/60 cm, 25/75 cm

Axis C’: 25/75 cm, 25/75 cm

3.1.1 Load Combinations

Load combinations were taken from ASCE 7-10 [6], in Chapter 2. In addition, live load factor was taken as 0.5. Thus, a combination to consider mass source, this factor was added to the combinations. Combinations are listed below:

1.4 G

1.2 G + 1.6 Q

1.2 G + 1 Q + 1 EQX + 0.3 EQY

1.2 G + 1 Q - 1 EQX - 0.3 EQY

1.2 G + 1 Q + 1 EQX - 0.3 EQY

1.2 G + 1 Q - 1 EQX + 0.3 EQY

1.2 G + 1 Q + 1 EQY + 0.3 EQX

1.2 G + 1 Q - 1 EQY - 0.3 EQX

1.2 G + 1 Q + 1 EQY - 0.3 EQX

1.2 G + 1 Q - 1 EQY + 0.3 EQX

1 G + 0.5 Q

3.1.2 Response Spectrum Function

Response spectrums for the fixed-base cases of the structure was selected according to the Turkish Seismic Code [24]. Considering the seismic zone, importance factor and soil class, response spectrum of the system was figured as in Figure 21.

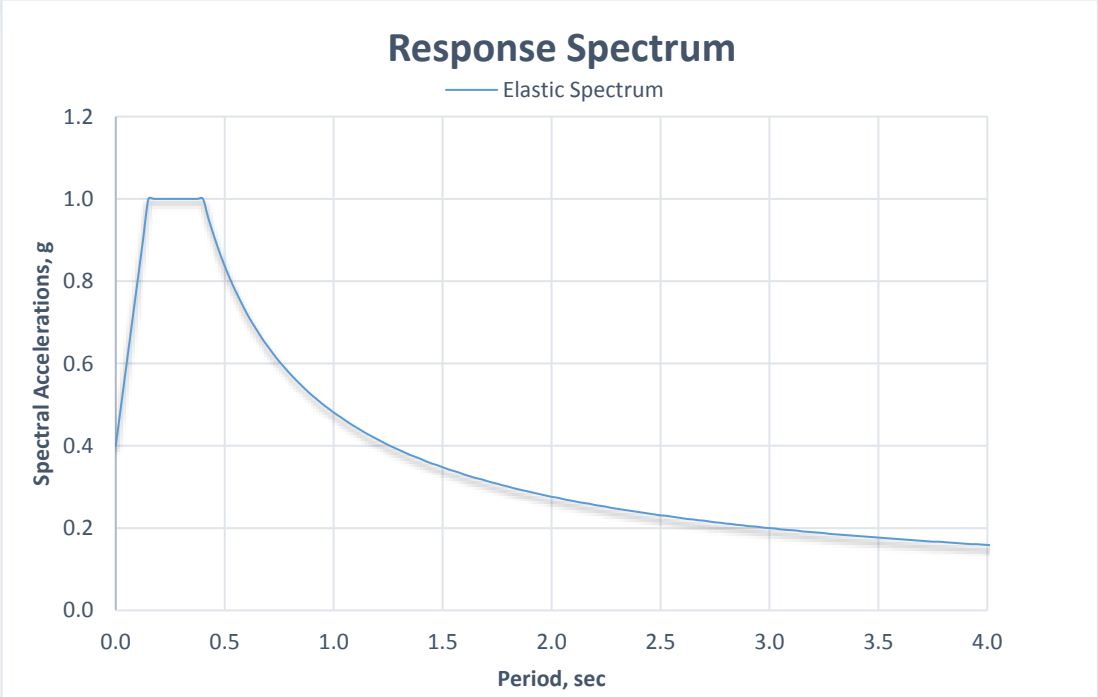


Figure 21. Response spectrum of fixed-base case [24]

3.1.3 3D Model of the Structure

As stated before, structure was modelled in SAP2000. Whole the analyses were carried out through this program. Below, an extrude view of the building is provided.

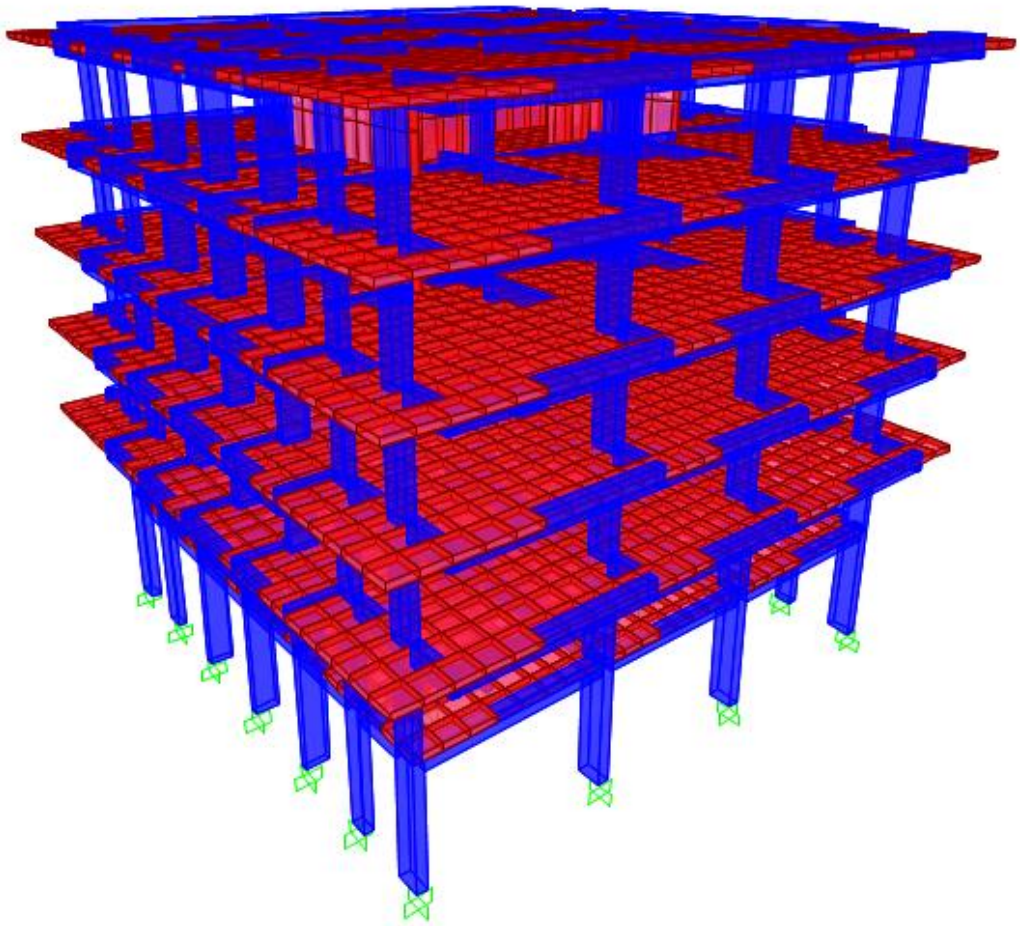


Figure 22. 3D view of the fixed-base model of the structure

3.2 FIXED-BASE CASE

After the structure modelled through the definitions, all the studies were carried out by using the same structure. Same building, structural system, materials, load combinations and response spectrums were used in each case.

Results after the system was analyzed are explained below.

Modal case results,

Table 2. Modal analysis results of fixed-base case

Modal Analysis Results			
Modes	Direction	Period, sec	Participating Mass Ratio Sum, %
1	Torsional, Z	0.50	81
2	Translational, Y	0.35	76
3	Translational, X	0.33	79
4	Torsional, Z	0.14	95
5	Translational, Y	0.11	90
6	Translational, X	0.11	93

As it can be seen from Table 2, structure has a torsionally unrestrained system. Thus, it has torsional mode in its first mode. In addition, modal participating ratios are below.

Moreover, floor accelerations of the structure in vectorial sum are listed in Table 3.

Table 3. Floor accelerations of symmetric case

Story	Floor Accelerations, g
6	0.38
5	0.31
4	0.25
3	0.21
2	0.15
1	0.08

Base reactions under the given response spectrum are listed below. Since the system was symmetric, there was no torsion. In response spectrum analysis, because the

direction is not important and system is totally symmetric, seismic combinations give same result with same factors, so only one of them is given in Table 4.

Table 4. Base reactions of fixed-base case

Forces at the Base			
Combination	X Direction, ton	Y Direction, ton	Vectorial Sum, ton
1.2G + 1Q + 1EQX + 0.3EQY	638.5	185.2	664.8
1.2G + 1Q + 1EQY + 0.3EQX	191.5	617.4	646.5

Furthermore, to get asymmetric systems, mass and stiffness eccentricities were given to the system. Mass eccentricities were given by shifting the joint masses. Eccentricity levels were choosen as 2.5%, 5%, 7.5% and 10%. In addition, to consider the stiffness eccentricity effects, shear walls at the right hand side of the plan were removed and columns were added.

3.3 DESIGN METHODS

In order to reduce the seismic forces transmitted to the structure and prevent the damaging effects of the earthquake, base isolation was applied to the system. Designing of the base isolation was made with lead-rubber bearing system. As stated in Naeim and Kelly [11], base isolation should be applied first considering the seismic weight and the assumed or target periods of the structure. Maximum considered earthquake periods were taken as 2.5 second. Maximum considered earthquake must be taken as 1.5 times the design basis earthquake. At each column, one isolator should be attached and at the shear walls, isolators were distributed at approximately one meter intervals for this study (see in Figure 23).

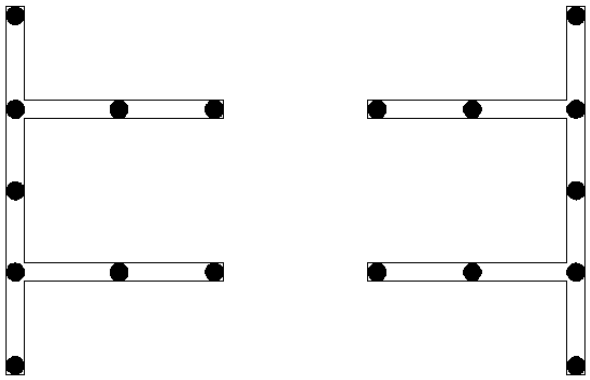


Figure 23. Isolator distributions under the shear walls

Both designing methods were used in two cases as stated before; symmetric and asymmetric. Then, in each case (symmetric and asymmetric cases), differences between conventional and proposed method were discussed. Design process of each method are explained in following sub-sections. Moreover, formulation studies and details of the proposed method are presented.

3.3.1 Conventional Method

In conventional method, firstly, system is analyzed under statical loads. Then, looking the axial load distributions, isolators were designed with axial load (effective seismic

weight) intervals. For instance, after noting the effective weight of the 40 isolator point separately, 3 types of isolators (50 tons, 100 tons, 150 tons) can be decided to design. Then, using the Equation (2.46), first guess of the lateral stiffness of each isolator type can be calculated. Vertical stiffness of the isolators can be estimated as 1000 times of the lateral stiffness at the beginning. Then, 1 second spectral acceleration and initial effective damping of the isolator is estimated. After that, displacements and total displacements can be estimated under maximum capable earthquake using the Equations (2.48) and (2.50).

Using the estimated values and analyzing the system with response spectrum, forces on isolators can be calculated under maximum capable earthquake. Then, at each iteration (each run), looking the axial loads under axial and seismic combinations, isolators can be designed in detail. Displacements are updated in accordance with analysis results.

3.3.2 Proposed Method

In this study, a new method was developed and proposed. In that method, isolators are not designed according to their axial load firstly. Finally, design checks were done looking the axial and axial seismic load combinations. However, in this technique, isolators standing at the outer axes of the structure are strengthened (effective stiffnesses are increased) so that a torsional stiffness is gathered to the system. While, increasing the lateral stiffness of the outer axes, the total lateral stiffness of the isolators increase, as well. Thus, target period of the system decreases and system starts to get more seismic load on it. A stiffness ratio between the outer and inner isolators must be provided to the system. This stiffness ratio can be achieved by a formula developed in the proposed method.

First, looking the seismic weight of the structure that is for example dead load plus 0.5 times live load, a total effective lateral stiffness should be calculated using Equation (2.46). Then, this total effective stiffness should be distributed to the outer and inner isolators using the stiffness ratio.

As it was seen from the results of the fixed-base modal, the structure is a torsionally unrestrained system. To get a torsionally restrained system, first, isolators are separated to inner and outer isolators as shown in Figure 24.

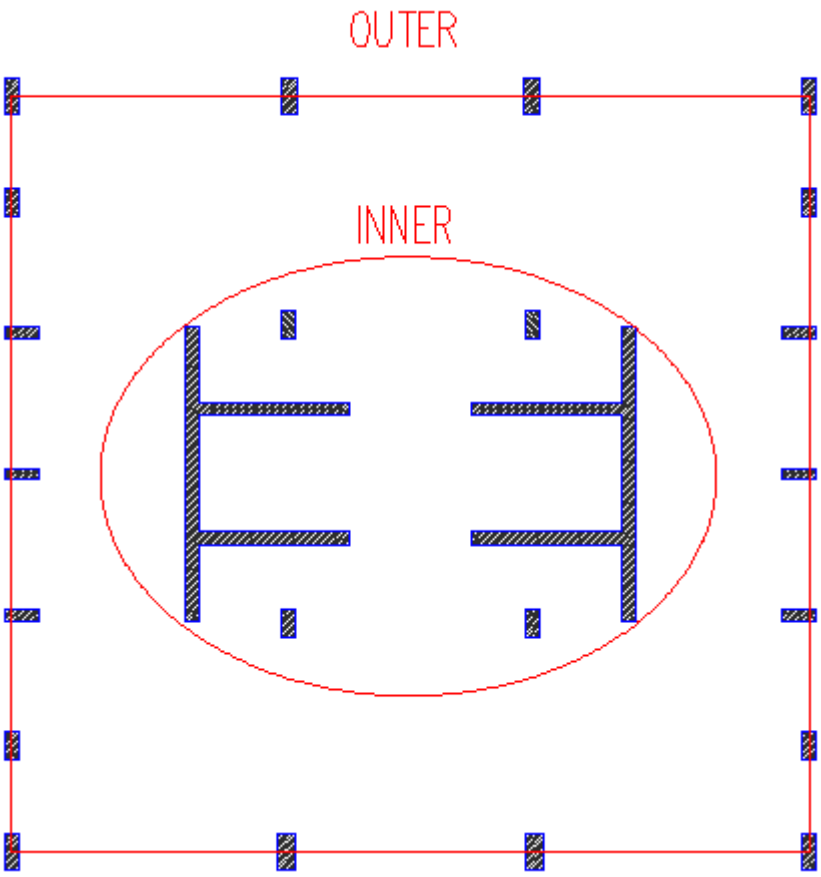


Figure 24. Isolator distributions under the shear walls

Then, looking the total seismic weight above the inner and outer isolators, a total lateral effective stiffness is calculated at target period of maximum capable earthquake by using Equation (2.46). This total stiffnesses are distributed to the isolator units equally. For instance, if total effective stiffness of the inner isolators are 8800 kN/m and there are 22 units of inner isolators, then, effective lateral stiffness of one isolator is 8800/22 = 400 kN/m. Same process is applied to the outer isolators, as well. For the vertical stiffness, that 1000 times the lateral stiffness rule can be applied to each isolator. After that, system is investigated with modal analysis. If the system results in a torsionally unrestrained system again, then, effective lateral stiffnesses of the outer isolators are increased step by step at each run. Increasing operation is stopped when, the structure

starts to show a torsionally restrained system. In other words, translational modes overcomes the torsional mode. Of course, this increasing operation decreases the target period but, this step is performed to get a stiffness ratio between inner and outer isolators.

General logic of the method is continued as mentioned above. This operations were figured out on 61 different structure cases that were obtained by changing the some specific parameters of the structure. Parameters changed on the system to get different building are; rigidity (shear wall thicknesses), distance (distances of outer axes), weight (weights on the inner and outer axes), height (heights of the stories), story (number of stories), story height (number of stories and story heights at the same time), mix (random changes) and period (modulus of elasticity of the concrete and assumed period). These parameters were used to form a relation to find stiffness ratio as in the Equation (3.1) which is calculated in following pages.

$$(K_O / K_I) = A + B*(D_O / D_I) + C*(W_O / W_I) + D*(T^2 / T_{translational}T_{assumed}) \quad (3.1)$$

All of the analyses were made on the building which was defined before. A base slab thickness of 60 cm was used during this operations.

Formula invented in this study consists of 3 general parameters; distance ratio of outer and inner isolators (D_O/D_I), weight ratio of outer and inner isolators (W_O/W_I) and ratio of periods (fixed-base period square divided by assumed period times fixed-base third period).

Distance ratio here is a ratio that is formed similar to the torsional stiffness in stiffness matrix as in Sucuoğlu and Akkar [28]. For example, for the outer isolators, each of them is considered with same lateral effective stiffness, and X and Y coordinates of each isolator is noted with respect to the geometric center of the plan. Because all of the outer isolators are same, inertias of all are same, as well, so it can be taken as unity or 1. Then, inertias of each isolator with respect to X axis times the square of X distance of that isolator are calculated. Same process is applied to Y direction of each isolator, as well. After that, whole these inertia times the distance square values are summed and divided to total X and Y inertias. This operation is showed in Equation (3.2).

$$D_O = \frac{\sum_1^n I_{xi} x_i^2 + I_{yi} y_i^2}{I_{xi} + I_{yi}} \tag{3.2}$$

where, I_{xi} and I_{yi} are unit inertias in x and y directions, x_i and y_i are distances to geometric center. Same equation is applied to the inner isolators and then, D_O/D_I ratio can be found.

Weight ratio is directly the ratio of the total seismic weight on the outer isolator divided by the total seismic weight on the inner isolator.

Period ratio in the formula consists of fixed-base periods and assumed period. Fixed-base translational and torsional periods were added to the formula because they directly affect the stiffness ratio of the inner and outer isolators to form a torsionally restrained system. Furthermore, because assumed period directly affects the effective stiffness of the isolator as it can be seen in Equation (2.46), it was added to formula, as well. Period ratio formula is showed in the Equation (3.3).

$$T_R = \frac{T_{torsional}^2}{T_{translational} T_{assumed}} \tag{3.3}$$

Translational period here is the third period of the torsionally unrestrained system.

After calculating each parameter of the formula for different structure cases, stiffness ratios between outer and inner isolators are obtained.

Calculations made to form the formula itself by changing the parameters of the system is presented step by step below.

3.3.2.1 Rigidity

To see the effects of rigidity, i.e stiffness of the structure to the stiffness ratios of the inner and outer isolators to provide a torsionally restrained system, thicknesses of the shear walls on building was changed. In addition, whole the seismic weights were calculated under the combination G + 0.5 L (dead load plus 0.5 times live load). Moreover, assumed periods on this rigidity title are 2.5 seconds. At the inner side of the building 22 units of isolators exist, at the outer side there are 18 units of isolators.

When the thicknesses of shear walls were arranged from 20 cm to 50 cm, related parameters are provided below in Table 5. Total axial loads on the inner and outer isolators are shown. Also, total stiffnesses of them to get a torsionally restrained system are illustrated.

Table 5. Weight and stiffness parameters of the formula when shear wall thicknesses were changed

Shear Wall Thickness (cm)	Inner			Outer		
	Axial Load (ton)	Stiffness (kN/m)	Total Stiffness (kN/m)	Axial Load (ton)	Stiffness (kN/m)	Total Stiffness (kN/m)
20	1456.93	418	9196	2187.65	957	17226
25	1528.60	439	9658	2178.48	946	17028
30	1589.39	459	10098	2171.19	935	16830
35	1666.71	479	10538	2165.37	925	16650
40	1733.87	498	10956	2160.70	916	16488
45	1800.14	517	11374	2156.94	907	16326
50	1865.69	536	11792	2153.89	900	16200

Moreover, fixed-base periods for the first 3 modes are shown in Table 6, respectively. Z means torsional mode and Y and X are the translational modes. Distance ratio parameters are illustrated in upcoming pages since they were not changed as the thicknesses of the shear walls are being changed.

Table 6. Period parameter of formula when shear wall thicknesses were changed

Shear Wall Thickness (cm)	Modes		
	1	2	3
	Z (sec)	Y (sec)	X (sec)
20	0.576	0.399	0.393
25	0.535	0.374	0.359
30	0.501	0.354	0.334
35	0.473	0.337	0.314
40	0.449	0.323	0.298
45	0.428	0.311	0.284
50	0.410	0.301	0.273

Because the distance parameter of the formula is independent from rigidity, it was not showed step by step with the results of the rigidity changes. For whole rigidity case, distance ratio is same and it is shown below in Table 7.

Table 7. Distance parameters of formula at rigidity case

INNER								
COLUMN		UNIT	INERTIA (m4)		DISTANCE (m)		INERTIA*DISTANCE	
X	Y		X	Y	X	Y	X	Y
1	1	4	4	4	1.3	1.35	6.76	7.29
1	1	4	4	4	2.98	1.35	35.40	7.29
1	1	4	4	4	4.65	1.35	86.49	7.29
1	1	4	4	4	2.65	3.05	28.09	37.21
1	1	4	4	4	4.65	3.05	86.49	37.21
1	1	2	2	2	4.65	0	43.25	0
Sum		22	22	22	Sum		286.48	96.29
Resultant Distances			6.51	2.19	**Resultant Core Dis. (m^2)**		**8.70**	
OUTER								
COLUMN		UNIT	INERTIA (m4)		DISTANCE (m)		INERTIA*DISTANCE	
X	Y		X	Y	X	Y	X	Y
1	1	4	4	4	2.65	8.4	28.09	282.24
1	1	4	4	4	8.65	8.4	299.29	282.24
1	1	4	4	4	8.65	5.65	299.29	127.69
1	1	4	4	4	8.65	3.05	299.29	37.21
1	1	2	2	2	8.65	0	149.65	0
Sum		18	18	18	Sum		1075.61	729.38
Resultant Rigidity			29.88	20.26	**Resultant Outer Dis. (m^2)**		**50.14**	

In Table 7, calculations that were specified in Equation (3.2) are figured out and showed. As stated, because the whole inner and outer isolators are same, they were thought with same unit inertia.

All the cases were carried out separately as tabled above. Relating on the results showed, parameter obtained to form the formula are listed below in Table 8.

Table 8. Parametric ratios of the formula at rigidity case

Thickness (cm)	D_O / D_I	W_O / W_I	T_R (Equation 3.2)	K_O / K_I
20	5.76	1.50	0.34	1.87
25	5.76	1.43	0.32	1.76
30	5.76	1.36	0.30	1.67
35	5.76	1.30	0.29	1.58
40	5.76	1.25	0.27	1.51
45	5.76	1.20	0.26	1.44
50	5.76	1.16	0.25	1.37

3.3.2.2 Distance

Distances of the outer axes of the structure were increased with respect to geometric center of the plan step by step to see the distance effects on the stiffness ratios of the inner and outer isolators. Core distances were same for whole the cases. Thus, core results are same in Table 7 so, only outer distance results are presented. In addition, whole analyses were figured out assuming a period of 2.5 second.

25 cm displacement of outer axes in X and Y directions

Weight, stiffness and period parameters of the case when outer axes of the structure were displaced 25 cm in both X and Y directions (total 50 cm for X and Y) are showed in Table 9. Distance calculations of the same case are presented after Table 9. As it is mentioned above, only the calculations and results of the outer isolator distances are presented in Table 10.

Table 9. Related parameters of formula when outer axes were displaced 25 cm

Inner			**25 cm**	Outer		
Axial Load (t)		1640.14		Axial Load (t)		2280.92
Isolator Unit		22		Isolator Unit		18
Stiffness (kN/m)		471		Stiffness (kN/m)		976
Total Stiffness (kN/m)		10362		Total Stiffness (kN/m)		17568
Total Axial Load (t)					3921.055	
Period	Z (sec)	0.52	Y (sec)	0.362	X (sec)	0.341

Table 10. Outer distance of formula when outer axes were displaced 25 cm

OUTER								
COLUMN		UNIT	INERTIA (m4)		DISTANCE (m)		INERTIA*DISTANCE	
X	Y		X	Y	X	Y	X	Y
1	1	4	4	4	2.65	8.65	28.09	299.29
1	1	4	4	4	8.9	8.65	316.84	299.29
1	1	4	4	4	8.9	5.65	316.84	127.69
1	1	4	4	4	8.9	3.05	316.84	37.21
1	1	2	2	2	8.9	0	158.42	0
Sum		18	18	18	Sum		1137.03	763.48
Resultant Rigidity			31.58	21.21	**Resultant Outer Dis. (m^2)**		**52.79**	

Parameters of both in Table 9 and Table 10 were explained in rigidity part. Hence, for each distance cases, distance, weight, period and stiffness parameters that are the parts of the formula are presented.

50 cm displacement of outer axes in X and Y directions

Parameters of the formula mentioned above are presented below in Tables 11 and 12, when the outer axes of the system were displaced 50 cm.

Table 11. Related parameters of formula when outer axes were displaced 50 cm

Inner			**50 cm**	Outer	
Axial Load (t)		1684.22		Axial Load (t)	2391.68
Isolator Unit		22		Isolator Unit	18
Stiffness (kN/m)		484		Stiffness (kN/m)	1021
Total Stiffness (kN/m)		10648		Total Stiffness (kN/m)	18378
Total Axial Load (t)				4075.90	
Period	Z (sec)	0.54	Y (sec)	0.37	X (sec)	0.348

Table 12. Outer distance of formula when outer axes were displaced 50 cm

OUTER								
COLUMN		UNIT	INERTIA (m4)		DISTANCE (m)		INERTIA*DISTANCE	
X	Y		X	Y	X	Y	X	Y
1	1	4	4	4	2.65	8.9	28.09	316.84
1	1	4	4	4	9.15	8.9	334.89	316.84
1	1	4	4	4	9.15	5.65	334.89	127.69
1	1	4	4	4	9.15	3.05	334.89	37.21
1	1	2	2	2	9.15	0	167.45	0
Sum		18	18	18	Sum		1200.21	798.58
Resultant Rigidity			33.34	22.18	**Resultant Outer Dis. (m^2)**		**55.52**	

75 cm displacement of outer axes in X and Y directions

In Table 13, weight, period and stiffness parameters are showed and in Table 14, distance parameter is shown.

Table 13. Related parameters of formula when outer axes were displaced 75 cm

Inner			**75 cm**	Outer		
Axial Load (t)		1730.5		Axial Load (t)		2503.61
Isolator Unit		22		Isolator Unit		18
Stiffness (kN/m)		497		Stiffness (kN/m)		1067
Total Stiffness (kN/m)		10934		Total Stiffness (kN/m)		19206
Total Axial Load (t)					4234.11	
Period	Z (sec)	0.559	Y (sec)	0.378	X (sec)	0.355

Table 14. Outer distance of formula when outer axes were displaced 75 cm

OUTER								
COLUMN		UNIT	INERTIA (m4)		DISTANCE (m)		INERTIA*DISTANCE	
X	Y		X	Y	X	Y	X	Y
1	1	4	4	4	2.65	9.15	28.09	334.89
1	1	4	4	4	9.4	9.15	353.44	334.89
1	1	4	4	4	9.4	5.65	353.44	127.69
1	1	4	4	4	9.4	3.05	353.44	37.21
1	1	2	2	2	9.4	0	176.72	0
Sum		18	18	18	Sum		1265.13	834.68
Resultant Rigidity			35.14	23.19	**Resultant Outer Dis. (m^2)**		**58.33**	

100 cm displacement of outer axes in X and Y directions

When outer axes of the system were displaced 100 cm in both directions, related parameters of the formula are illustrated in Tables 15 and 16.

Table 15. Related parameters of formula when outer axes were displaced 100 cm

Inner			**100 cm**	Outer		
Axial Load (t)		1778.85		Axial Load (t)		2616.84
Isolator Unit		22		Isolator Unit		18
Stiffness (kN/m)		511		Stiffness (kN/m)		1117
Total Stiffness (kN/m)		11242		Total Stiffness (kN/m)		20106
Total Axial Load (t)					4395.69	
Period	Z (sec)	0.579	Y (sec)	0.385	X (sec)	0.362

Table 16. Outer distance of formula when outer axes were displaced 100 cm

OUTER								
COLUMN		UNIT	INERTIA (m4)		DISTANCE (m)		INERTIA*DISTANCE	
X	Y		X	Y	X	Y	X	Y
1	1	4	4	4	2.65	9.4	28.09	353.44
1	1	4	4	4	9.65	9.4	372.49	353.44
1	1	4	4	4	9.65	5.65	372.49	127.69
1	1	4	4	4	9.65	3.05	372.49	37.21
1	1	2	2	2	9.65	0	186.25	0
Sum		18	18	18	Sum		1331.81	871.78
Resultant Rigidity			36.99	24.22	**Resultant Outer Dis. (m^2)**		**61.21**	

125 cm displacement of outer axes in X and Y directions

In Tables 17 and 18, related parameters as mentioned are shown below.

Table 17. Related parameters of formula when outer axes were displaced 125 cm

Inner			**125 cm**	Outer	
Axial Load (t)		1829.14		Axial Load (t)	2731.49
Isolator Unit		22		Isolator Unit	18
Stiffness (kN/m)		525		Stiffness (kN/m)	1170
Total Stiffness (kN/m)		11550		Total Stiffness (kN/m)	21060
Total Axial Load (t)				4560.63	
Period	Z (sec)	0.6	Y (sec)	0.393	X (sec)	0.369

Table 18. Outer distance of formula when outer axes were displaced 125 cm

OUTER								
COLUMN		UNIT	INERTIA (m4)		DISTANCE (m)		INERTIA*DISTANCE	
X	Y		X	Y	X	Y	X	Y
1	1	4	4	4	2.65	9.65	28.09	372.49
1	1	4	4	4	9.9	9.65	392.04	372.49
1	1	4	4	4	9.9	5.65	392.04	127.69
1	1	4	4	4	9.9	3.05	392.04	37.21
1	1	2	2	2	9.9	0	196.02	0
Sum		18	18	18	Sum		1400.23	909.88
Resultant Rigidity			38.90	25.27	**Resultant Outer Dis. (m^2)**		**64.17**	

<u>150 cm displacement of outer axes in X and Y directions</u>

Last displaced axes operation in both direction is at an amount of 150 cm. In Tables 19 and 20, details of parameters were shown.

Table 19. Related parameters of formula when outer axes were displaced 150 cm

Inner			**150 cm**	Outer	
Axial Load (t)		1881.24		Axial Load (t)	2847.69
Isolator Unit		22		Isolator Unit	18
Stiffness (kN/m)		540		Stiffness (kN/m)	1228
Total Stiffness (kN/m)		11880		Total Stiffness (kN/m)	22104
Total Axial Load (t)				4728.93	
Period	Z (sec)	0.620	Y (sec)	0.401	X (sec)	0.376

Table 20. Outer distance of formula when outer axes were displaced 150 cm

OUTER								
COLUMN		UNIT	INERTIA (m4)		DISTANCE (m)		INERTIA*DISTANCE	
X	Y		X	Y	X	Y	X	Y
1	1	4	4	4	2.65	9.9	28.09	392.04
1	1	4	4	4	10.15	9.9	412.09	392.04
1	1	4	4	4	10.15	5.65	412.09	127.69
1	1	4	4	4	10.15	3.05	412.09	37.21
1	1	2	2	2	10.15	0	206.05	0
Sum		18	18	18	Sum		1470.41	948.98
Resultant Rigidity			40.85	26.36	Resultant Outer Dis.		67.21	

50 cm displacement of outer axes in X direction only

Having some difference from the previous cases, this time, outer axes of the system were displaced only in X direction. In Table 21, weight, period and stiffness parameters are shown. In Table 22, outer distance is tabled.

Table 21. Related parameters of formula when outer axes were displaced 50 cm in X direction

Inner			**50 cm**	Outer		
Axial Load (t)		1639.6		Axial Load (t)		2276.91
Isolator Unit		22		Isolator Unit		18
Stiffness (kN/m)		471		Stiffness (kN/m)		935
Total Stiffness (kN/m)		10362		Total Stiffness (kN/m)		16830
Total Axial Load (t)					3916.51	
Period	Z (sec)	0.52	Y (sec)	0.362	X (sec)	0.341

Table 22. Outer distance of formula when outer axes were displaced 50 cm in X direction

OUTER								
COLUMN		UNIT	INERTIA (m4)		DISTANCE (m)		INERTIA*DISTANCE	
X	Y		X	Y	X	Y	X	Y
1	1	4	4	4	2.65	8.4	28.09	282.24
1	1	4	4	4	9.15	8.4	334.89	282.24
1	1	4	4	4	9.15	5.65	334.89	127.69
1	1	4	4	4	9.15	3.05	334.89	37.21
1	1	2	2	2	9.15	0	167.45	0
Sum		18	18	18	Sum		1200.21	729.38
Resultant Rigidity			33.34	20.26	**Resultant Outer Dis. (m^2)**		**53.60**	

100 cm displacement of outer axes in X direction only

Again, results of the case in which outer axes were displaced 100 cm in X direction are shown below in Tables 23 and 24.

Table 23. Related parameters of formula when outer axes were displaced 100 cm in X direction

Inner			100 cm		Outer	
Axial Load (t)		1684.58			Axial Load (t)	2378.86
Isolator Unit		22			Isolator Unit	18
Stiffness (kN/m)		484			Stiffness (kN/m)	940
Total Stiffness (kN/m)		10648			Total Stiffness (kN/m)	16920
Total Axial Load (t)					4063.44	
Period	Z (sec)	0.539	Y (sec)	0.37	X (sec)	0.349

Table 24. Outer distance of formula when outer axes were displaced 100 cm in X direction

OUTER								
COLUMN		UNIT	INERTIA (m4)		DISTANCE (m)		INERTIA*DISTANCE	
X	Y		X	Y	X	Y	X	Y
1	1	4	4	4	2.65	8.4	28.09	282.24
1	1	4	4	4	9.65	8.4	372.49	282.24
1	1	4	4	4	9.65	5.65	372.49	127.69
1	1	4	4	4	9.65	3.05	372.49	37.21
1	1	2	2	2	9.65	0	186.25	0
Sum		18	18	18	Sum		1331.81	729.38
Resultant Rigidity			31.00	20.26	**Resultant Outer Dis. (m^2)**		**57.26**	

150 cm displacement of outer axes in X direction only

Results when the outer axes of the system were displaced 150 cm in X direction are shown in Tables 25 and 26.

Table 25. Related parameters of formula when outer axes were displaced 150 cm in X direction

Inner			**150 cm**	Outer		
Axial Load (t)		1732.42		Axial Load (t)		2477.96
Isolator Unit		22		Isolator Unit		18
Stiffness (kN/m)		497		Stiffness (kN/m)		946
Total Stiffness (kN/m)		10934		Total Stiffness (kN/m)		17028
Total Axial Load (t)					4210.38	
Period	Z (sec)	0.558	Y (sec)	0.377	X (sec)	0.356

Table 26. Outer distance of formula when outer axes were displaced 150 cm in X direction

OUTER								
COLUMN		UNIT	INERTIA (m4)		DISTANCE (m)		INERTIA*DISTANCE	
X	Y		X	Y	X	Y	X	Y
1	1	4	4	4	2.65	8.4	28.09	282.24
1	1	4	4	4	10.15	8.4	412.09	282.24
1	1	4	4	4	10.15	5.65	412.09	127.69
1	1	4	4	4	10.15	3.05	412.09	37.21
1	1	2	2	2	10.15	0	206.05	0
Sum		18	18	18	Sum		1470.41	729.38
Resultant Rigidity			40.85	20.26	**Resultant Outer Dis. (m^2)**		**61.11**	

<u>50 cm displacement of outer axes in Y direction only</u>

Results when the outer axes of the system were displaced 50 cm in Y direction are shown in Tables 27 and 28.

Table 27. Related parameters of formula when outer axes were displaced 50 cm in Y direction

Inner			**50 cm**	Outer		
Axial Load (t)		1641.46		Axial Load (t)		2280.78
Isolator Unit		22		Isolator Unit		18
Stiffness (kN/m)		471		Stiffness (kN/m)		1021
Total Stiffness (kN/m)		10362		Total Stiffness (kN/m)		18378
Total Axial Load (t)					3922.24	
Period	Z (sec)	0.52	Y (sec)	0.361	X (sec)	0.34

Table 28. Outer distance of formula when outer axes were displaced 50 cm in Y direction

OUTER								
COLUMN		UNIT	INERTIA (m4)		DISTANCE (m)		INERTIA*DISTANCE	
X	Y		X	Y	X	Y	X	Y
1	1	4	4	4	2.65	8.9	28.09	316.84
1	1	4	4	4	8.65	8.9	299.29	316.84
1	1	4	4	4	8.65	5.65	299.29	127.69
1	1	4	4	4	8.65	3.05	299.29	37.21
1	1	2	2	2	8.65	0	149.65	0
Sum		18	18	18	Sum		1075.61	798.58
Resultant Rigidity			29.88	22.18	**Resultant Outer Dis. (m^2)**		**52.06**	

100 cm displacement of outer axes in Y direction only

When the outer axes were displaced 100 cm in Y direction, results were tabled below in Tables 29 and 30.

Table 29. Related parameters of formula when outer axes were displaced 100 cm in Y direction

Inner			**100 cm**	Outer		
Axial Load (t)		1686.22		Axial Load (t)		2388.69
Isolator Unit		22		Isolator Unit		18
Stiffness (kN/m)		484		Stiffness (kN/m)		1121
Total Stiffness (kN/m)		10648		Total Stiffness (kN/m)		20178
Total Axial Load (t)					4074.90	
Period	Z (sec)	0.541	Y (sec)	0.368	X (sec)	0.346

Table 30. Outer distance of formula when outer axes were displaced 100 cm in Y direction

OUTER								
COLUMN		UNIT	INERTIA (m4)		DISTANCE (m)		INERTIA*DISTANCE	
X	Y		X	Y	X	Y	X	Y
1	1	4	4	4	2.65	9.4	28.09	353.44
1	1	4	4	4	8.65	9.4	299.29	353.44
1	1	4	4	4	8.65	5.65	299.29	127.69
1	1	4	4	4	8.65	3.05	299.29	37.21
1	1	2	2	2	8.65	0	149.65	0
Sum		18	18	18	Sum		1075.61	871.78
Resultant Rigidity			29.88	24.22	**Resultant Outer Dis. (m^2)**		**54.09**	

150 cm displacement of outer axes in Y direction only

Results when the outer axes of the system were displaced 150 cm in Y direction are shown in Tables 31 and 32.

Table 31. Related parameters of formula when outer axes were displaced 150 cm in Y direction

Inner			**150 cm**	Outer	
Axial Load (t)		1732.23		Axial Load (t)	2495.34
Isolator Unit		22		Isolator Unit	18
Stiffness (kN/m)		497		Stiffness (kN/m)	1236
Total Stiffness (kN/m)		10934		Total Stiffness (kN/m)	22248
Total Axial Load (t)					4227.57
Period	Z (sec)	0.562	Y (sec)	0.376	X (sec)	0.353

Table 32. Outer distance of formula when outer axes were displaced 150 cm in Y direction

OUTER								
COLUMN		UNIT	INERTIA (m4)		DISTANCE (m)		INERTIA*DISTANCE	
X	Y		X	Y	X	Y	X	Y
1	1	4	4	4	2.65	9.9	28.09	392.04
1	1	4	4	4	8.65	9.9	299.29	392.04
1	1	4	4	4	8.65	5.65	299.29	127.69
1	1	4	4	4	8.65	3.05	299.29	37.21
1	1	2	2	2	8.65	0	149.65	0
Sum		18	18	18	Sum		1075.61	948.98
Resultant Rigidity			29.88	26.36	**Resultant Outer Dis. (m^2)**		**56.24**	

After all the distance cases, parameters in the formula as ratios using the results are given below in Table 33.

Table 33. Parametric ratios of the formula at distance case

Displacement (cm)	D_O / D_I	W_O / W_I	T_R (Equation 3.2)	K_O / K_I
50	6.38	1.42	0.34	1.73
100	7.04	1.47	0.37	1.79
150	7.73	1.51	0.41	1.86
25	6.07	1.39	0.32	1.70
75	6.71	1.45	0.35	1.76
125	7.38	1.49	0.39	1.82
X-50	6.16	1.39	0.32	1.62
X-100	6.58	1.41	0.33	1.59
X-150	7.02	1.43	0.35	1.56
Y-50	5.99	1.39	0.32	1.77
Y-100	6.22	1.42	0.34	1.90
Y-150	6.47	1.44	0.36	2.04

3.3.2.3 Weight

In this case, slabs with 15 cm thickness and located at the inner sides of the plans at whole stories were reloaded with different amounts. In other words, at each case dead loads on the slabs with 15 cm were replaced with another load. While changing the load, results according to this change were calculated in accordance with the parameters in the formula. Here, because there is no change on distances of the outer or inner axes, distance parameters are same as in the default case. Thus, distance parameters are not shown. Only, weight, period and stiffnesses are shown through these cases. Moreover, in the analyses, an assumed period of 2.5 second was used for whole cases.

Table 34. Weight and stiffness parameters of formula when slabs loaded 0.3 to 0.5 ton/m^2

Slab Loading (ton/m2)	Inner			Outer		
	Axial Load (ton)	Stiffness (kN/m)	Total Stiffness (kN/m)	Axial Load (ton)	Stiffness (kN/m)	Total Stiffness (kN/m)
0.3	1637.55	470	10340	2189.03	934	16812
0.35	1662.66	477	10494	2200.46	934	16812
0.4	1687.76	485	10670	2211.89	935	16830
0.45	1712.87	492	10824	2223.33	935	16830
0.5	1737.97	499	10978	2234.76	935	16830

Moreover, fixed-base periods for the first 3 modes are shown in Table 35, respectively. Z means torsional mode and Y and X are the translational modes.

Table 35. Period parameter of formula when slabs loaded 0.3 to 0.5 ton/m^2

Slab Loading (ton/m2)	Modes		
	1	2	3
	Z (sec)	Y (sec)	X (sec)
0.3	0.504	0.357	0.337
0.35	0.505	0.359	0.339
0.4	0.507	0.361	0.341
0.45	0.509	0.363	0.343
0.5	0.510	0.365	0.345

When the different cases analyzed, weight, period and stiffness ratios of each case noted. Default distance ratios were added to the weight title so that there is no distance changes in the models. Results of the ratios of the formula at the weight case are shown in Table 36.

Table 36. Parametric ratios of the formula at weight case

Loading (ton/m^2)	D_O / D_I	W_O / W_I	T_R (Equation 3.2)	K_O / K_I
0.3	5.76	1.34	0.30	1.63
0.35	5.76	1.32	0.30	1.60
0.4	5.76	1.31	0.30	1.58
0.45	5.76	1.30	0.30	1.56
0.5	5.76	1.29	0.30	1.53

3.3.2.4 Height

In order to see the effects of the heights of the stories, in other words, period changes because of the story heights, height of the stories were increased step by step. In some cases, only the height of the ground story that has 3.8 meters height diversely from the rest of the stories was changed. Moreover, in whole the cases, assumed period was 2.5 second again. As a reminder, fixed-base and isolated structures of the each case through these analyses while forming formula, not only in height, at all of the cases,

buildings are torsionally unrestrained. In addition, again there is no change in distance parameters of the formula because distances of axes were not displaced.

In first case, the height of the each stories were increased by 25 cm (story heights; 4.05 m and 3.25 m). Second, they were increased by 50 cm (story heights; 4.3 m and 3.5 m). Other cases, only the height of the ground floor was reduced by respectively, 30, 55 and 80 cm (story heights of ground floors; 3.5, 3.25 and 3 m). Results of the weight, fixed-base period and stiffness changes were shown in Table 37.

Table 37. Weight and stiffness parameters when the heights of the stories were changed

Height Cases	Inner			Outer		
	Axial Load (ton)	Stiffness (kN/m)	Total Stiffness (kN/m)	Axial Load (ton)	Stiffness (kN/m)	Total Stiffness (kN/m)
1	1626.63	467	10274	2179.84	953	17154
2	1654.81	475	10450	2188.54	972	17496
3	1589.30	456	10032	2171.13	925	16650
4	1581.70	454	9988	2171.11	919	16542
5	1574.07	452	9944	2171.10	913	16434

Moreover, fixed-base periods for the first 3 modes are shown in Table 38, respectively. Z means torsional mode and Y and X are the translational modes.

Table 38. Period parameter when the heights of the stories were changed

Height Cases	Modes		
	1	2	3
	Z (sec)	Y (sec)	X (sec)
1	0.537	0.383	0.359
2	0.574	0.413	0.385
3	0.49	0.345	0.327
4	0.481	0.338	0.321
5	0.472	0.331	0.315

After the whole cases in height part, ratios of the parameters of the formula put done down together in Table 39.

Table 39. Parametric ratios of the formula at height case

Heights Cases	D_O / D_I	W_O / W_I	T_R (Equation 3.2)	K_O / K_I
1	5.76	1.34	0.32	1.67
2	5.76	1.32	0.34	1.67
3	5.76	1.37	0.29	1.66
4	5.76	1.37	0.29	1.66
5	5.76	1.38	0.28	1.65

3.3.2.5 Story

In order to investigate the effect of period on the stiffness ratio of outer and inner isolators, story numbers of the structure were changed. Again there is no distance change on the axes. Thus, only weight, period and stiffness changes were figured out in tables. In addition, assumed period was taken as 2.5 second during the whole cases.

Stories of the structure were changed to get 4, 5 and 7 story buildings. When it was arranged as mentioned, results of the weight and stiffness changes in the system are shown in Table 40.

Table 40. Weight and stiffness parameters when the system was arranged for different stories

Stories	Inner			Outer		
	Axial Load (ton)	Stiffness (kN/m)	Total Stiffness (kN/m)	Axial Load (ton)	Stiffness (kN/m)	Total Stiffness (kN/m)
4	1127.08	324	7128	1482.40	536	9648
5	1357.78	390	8580	1831.75	719	12942
7	1849.58	531	11682	2500.04	1202	21636

Furthermore, fixed-base periods for the first 3 modes are shown in Table 41, respectively. Z means torsional mode and Y and X are the translational modes.

Table 41. Period parameter when the system was arranged for different stories

Stories	Modes		
	1	2	3
	Z (sec)	Y (sec)	X (sec)
4	0.297	0.202	0.2
5	0.396	0.273	0.266
7	0.613	0.442	0.406

Whole the results are shown as the ratios of the parameters of the formula in Table 42. Moreover, distance ratio were added as in default case.

Table 42. Parametric ratios of the formula at story case

Story	D_O / D_I	W_O / W_C	T_R (Equation 3.2)	K_O / K_I
4	5.76	1.32	0.18	1.35
5	5.76	1.35	0.24	1.51
7	5.76	1.35	0.37	1.85

3.3.2.6 Story - Height

In this case, while increasing the story height, story numbers were decreased at the same time. Whole the cases, assumed periods were 2.5 seconds. Moreover, distances of the axes of the structure were not changed. Hence, default case were considered for same distance parameters.

Story heights except first story were changed for all cases. Story heights were 3.25m, 3.5 m and 3.75 m. Results of the weight, period and stiffness parameters are shown in Table 43.

Table 43. Weight and stiffness parameters when the stories and heights of the system were changed

Story and Heights	Inner			Outer		
	Axial Load (ton)	Stiffness (kN/m)	Total Stiffness (kN/m)	Axial Load (ton)	Stiffness (kN/m)	Total Stiffness (kN/m)
5 - 3.25 m	1379.61	396	8712	1839.45	728	13104
5 - 3.50 m	1401.34	402	8844	1847.26	736	13248
5 - 3.75 m	1432.12	409	8998	1855.01	747	13446
4 - 3.25 m	1142.95	328	7216	1488.7	539	9702
4 - 3.50 m	1158.76	333	7326	1495.06	544	9792
4 - 3.75 m	1174.62	337	7414	1501.38	548	9864

Furthermore, fixed-base periods for the first 3 modes are shown in Table 44, respectively. Z means torsional mode and Y and X are the translational modes.

Table 44. Period parameter when the stories and heights of the system were changed

Story and Heights	Modes		
	1	2	3
	Z (sec)	Y (sec)	X (sec)
5 - 3.25 m	0.422	0.293	0.285
5 - 3.50 m	0.449	0.314	0.305
5 - 3.75 m	0.477	0.336	0.324
4 - 3.25 m	0.314	0.215	0.213
4 - 3.50 m	0.332	0.228	0.227
4 - 3.75 m	0.35	0.242	0.24

After the cases stated above, results of the ratios of the formula are shown in Table 45.

Table 45. Parametric ratios of the formula at story - height case

Story and Heights	D_O / D_I	W_O / W_I	T_R (Equation 3.2)	K_O / K_I
5 – 3.25 m	5.76	1.33	0.25	1.50
5 – 3.50 m	5.76	1.32	0.26	1.50
5 – 3.75 m	5.76	1.30	0.28	1.49
4 – 3.25 m	5.76	1.30	0.19	1.35
4 – 3.50 m	5.76	1.29	0.19	1.34
4 – 3.75 m	5.76	1.28	0.20	1.33

3.3.2.7 Randomly Changed Parameters

To increase the effectiveness of the formulation of the proposed method, randomly changes were applied to 3 systems in this case. These random changes include distances of outer axes, story number, height of the stories, shear wall thicknesses and weight of the slabs with 15 cm at the inner side. In whole cases, assumed periods of the isolated structures were taken as 2.5 seconds.

Random Case 1

In random case 1, story numbers were arranged as 5 story. Heights of the stories except first story were increased by 25 cm. Weight loaded to the inner slabs with 15 cm thicknesses was 0.2 ton/m^2. Shear wall thicknesses were arranged as 35 cm. Outer axes were displaced 50 cm only in X direction. Results are shown in Tables 46 and 47.

Table 46. Related parameters of random case 1

Inner			**R.C. 1**	Outer	
Axial Load (t)		1467.51		Axial Load (t)	1919.53
Isolator Unit		22		Isolator Unit	18
Stiffness (kN/m)		421		Stiffness (kN/m)	727
Total Stiffness (kN/m)		9262		Total Stiffness (kN/m)	13086
Total Axial Load (t)				3387.044	
Period	Z (sec)	0.412	Y (sec)	0.284	X (sec)	0.273

Table 47. Distance parameter of random case 1

OUTER								
COLUMN		UNIT	INERTIA (m4)		DISTANCE (m)		INERTIA*DISTANCE	
X	Y		X	Y	X	Y	X	Y
1	1	4	4	4	2.65	8.4	28.09	282.24
1	1	4	4	4	9.15	8.4	334.89	282.24
1	1	4	4	4	9.15	5.65	334.89	127.69
1	1	4	4	4	9.15	3.05	334.89	37.21
1	1	2	2	2	9.15	0	167.45	0
Sum		18	18	18	Sum		1200.21	729.38
Resultant Rigidity			33.34	20.26	**Resultant Outer Dis. (m^2)**		**53.60**	

Random Case 2

In random case 2, story numbers were arranged as 4 story. Heights of the stories except first story were increased by 50 cm. Weight loaded to the inner slabs with 15 cm thicknesses was 0.05 ton/m^2. Shear wall thicknesses were arranged as 40 cm. Outer axes were displaced 50 cm only in Y direction. Results are shown in Tables 48 and 49.

Table 48. Related parameters of random case 2

Inner			**R.C. 2**	Outer	
Axial Load (t)	1235.06			Axial Load (t)	1540.45
Isolator Unit	22			Isolator Unit	18
Stiffness (kN/m)	355			Stiffness (kN/m)	586
Total Stiffness (kN/m)	7810			Total Stiffness (kN/m)	10548
Total Axial Load (t)				2775.511	
Period	Z (sec)	0.304	Y (sec)	0.204	X (sec)	0.202

Table 49. Distance parameter of random case 2

OUTER								
COLUMN		UNIT	INERTIA (m4)		DISTANCE (m)		INERTIA*DISTANCE	
X	Y		X	Y	X	Y	X	Y
1	1	4	4	4	2.65	8.9	28.09	316.84
1	1	4	4	4	8.65	8.9	299.29	316.84
1	1	4	4	4	8.65	5.65	299.29	127.69
1	1	4	4	4	8.65	3.05	299.29	37.21
1	1	2	2	2	8.65	0	149.65	0
Sum		18	18	18	Sum		1075.61	798.58
Resultant Rigidity			29.88	22.18	**Resultant Outer Dis. (m^2)**		**52.06**	

Random Case 3

In random case 3, story numbers were arranged as 6 story. Heights of the stories except first story were increased by 30 cm. Weight loaded to the inner slabs with 15 cm thicknesses was 0.3 ton/m^2. Shear wall thicknesses were not changed. Outer axes were displaced 40 cm in X direction and 50 cm in Y direction. Results are shown in Tables 50 and 51.

Table 50. Related parameters of random case 3

Inner			R.C. 3	Outer		
Axial Load (t)		1749.18		Axial Load (t)		2399.55
Isolator Unit		22		Isolator Unit		18
Stiffness (kN/m)		502		Stiffness (kN/m)		1045
Total Stiffness (kN/m)		11044		Total Stiffness (kN/m)		18810
Total Axial Load (t)					4148.723	
Period	Z (sec)	0.585	Y (sec)	0.408	X (sec)	0.381

Table 51. Distance parameter of random case 3

OUTER								
COLUMN		UNIT	INERTIA (m4)		DISTANCE (m)		INERTIA*DISTANCE	
X	Y		X	Y	X	Y	X	Y
1	1	4	4	4	2.65	8.9	28.09	316.84
1	1	4	4	4	9.05	8.9	327.61	316.84
1	1	4	4	4	9.05	5.65	327.61	127.69
1	1	4	4	4	9.05	3.05	327.61	37.21
1	1	2	2	2	9.05	0	163.81	0
Sum		18	18	18	Sum		1174.73	798.58
Resultant Rigidity			32.63	22.18	**Resultant Outer Dis. (m^2)**		**54.81**	

After the results of the cases, ratios of each parameter in the formula are shown in Table 52.

Table 52. Parametric ratios of the formula at randomly change cases

Random Cases	D_O / D_I	W_O / W_I	T_R (Equation 3.2)	K_O / K_I
1	6.16	1.31	0.25	1.41
2	5.99	1.25	0.18	1.35
3	6.30	1.37	0.36	1.70

3.3.2.8 Period

This stage consists of two cases, first, all analyses were done by assuming isolated period as 2.5 seconds at MCE and modulus elasticity of the concrete was changed. Then, each parameter stayed as default but, assumed period of the system was changed.

Results of weight and stiffness parameters when elasticity was changed step by step is below in Table 53.

Table 53. Weight and stiffness parameters when elasticity was changed

Modulus of Elasticity (ton/cm2)	Inner			Outer		
	Axial Load (ton)	Stiffness (kN/m)	Total Stiffness (kN/m)	Axial Load (ton)	Stiffness (kN/m)	Total Stiffness (kN/m)
300	1598.39	459	10098	2171.19	941	16938
280	1598.39	459	10098	2171.19	950	17100
260	1598.39	459	10098	2171.19	960	17280
240	1598.39	459	10098	2171.19	972	17496
220	1598.39	459	10098	2171.19	987	17766
200	1598.39	459	10098	2171.19	1005	18090
340	1598.39	459	10098	2171.19	928	16704
360	1598.39	459	10098	2171.19	922	16596
380	1598.39	459	10098	2171.19	917	16506
400	1598.39	459	10098	2171.19	913	16434

Furthermore, fixed-base periods for the first 3 modes are shown in Table 54, respectively. Z means torsional mode and Y and X are the translational modes.

Table 54. Period parameter when elasticity was changed

Modulus of Elasticity (ton/cm2)	Modes		
	1	2	3
	Z (sec)	Y (sec)	X (sec)
300	0.516	0.364	0.344
280	0.534	0.377	0.356
260	0.554	0.391	0.369
240	0.577	0.407	0.384
220	0.603	0.425	0.401
200	0.632	0.446	0.421

Table 54(continued). Period parameter when elasticity was changed

Modulus of Elasticity (ton/cm2)	Modes		
	1	2	3
	Z (sec)	Y (sec)	X (sec)
340	0.485	0.342	0.323
360	0.471	0.332	0.314
380	0.459	0.323	0.305
400	0.447	0.315	0.298

The effect of period on the system was also investigated. In Equation (2.46), if assumed period changes, lateral effective stiffness of the isolator changes under same seismic weight, as well. This relation were obtained here.

Results when the assumed period of isolated structure was changed is given in Table 55.

Table 55. Weight and stiffness parameters when assumed period was changed

Assumed Period (sec)	Inner			Outer		
	Axial Load (ton)	Stiffness (kN/m)	Total Stiffness (kN/m)	Axial Load (ton)	Stiffness (kN/m)	Total Stiffness (kN/m)
2.4	1598.39	498	10956	2171.19	1024	18432
2.3	1598.39	542	11924	2171.19	1128	20304
2.2	1598.39	593	13046	2171.19	1251	22518
2.1	1598.39	650	14300	2171.19	1392	25056
2	1598.39	717	15774	2171.19	1565	28170
2.6	1598.39	424	9328	2171.19	856	15408
2.7	1598.39	394	8668	2171.19	789	14202
2.8	1598.39	366	8052	2171.19	728	13104
2.9	1598.39	341	7502	2171.19	674	12132
3	1598.39	319	7018	2171.19	627	11286

Moreover, fixed-base periods for the first 3 modes are shown in Table 56, respectively. Z means torsional mode and Y and X are the translational modes.

Table 56. Period parameter when assumed period was changed

Assumed Period (sec)	Modes		
	1	2	3
	Z (sec)	Y (sec)	X (sec)
2.4	0.501	0.354	0.334
2.3	0.501	0.354	0.334
2.2	0.501	0.354	0.334
2.1	0.501	0.354	0.334
2	0.501	0.354	0.334
2.6	0.501	0.354	0.334
2.7	0.501	0.354	0.334
2.8	0.501	0.354	0.334
2.9	0.501	0.354	0.334
3	0.501	0.354	0.334

Ratios of the formula including whole parameters are shown in Table 57 and 58.

Table 57. Parametric ratios of the formula at period case

E (ton/cm^2)	D_O / D_I	W_O / W_C	T_R (Equation 3.2)	K_O / K_C
318	5.76	1.36	0.30	1.67
300	5.76	1.36	0.31	1.68
280	5.76	1.36	0.32	1.69
260	5.76	1.36	0.33	1.71
240	5.76	1.36	0.35	1.73
220	5.76	1.36	0.36	1.76
200	5.76	1.36	0.38	1.79
340	5.76	1.36	0.29	1.65
360	5.76	1.36	0.28	1.64
380	5.76	1.36	0.28	1.64
400	5.76	1.36	0.27	1.63

Table 58. Parametric ratios of the formula at period case

Assumed Period (sec)	D_O / D_I	W_O / W_C	T_R (Equation 3.2)	K_O / K_C
2.4	5.76	1.36	0.31	1.68
2.3	5.76	1.36	0.33	1.70
2.2	5.76	1.36	0.34	1.73
2.1	5.76	1.36	0.36	1.75
2	5.76	1.36	0.38	1.79
2.6	5.76	1.36	0.29	1.65
2.7	5.76	1.36	0.28	1.64
2.8	5.76	1.36	0.27	1.63
2.9	5.76	1.36	0.26	1.62
3	5.76	1.36	0.25	1.61

3.3.2.9 Formulation Process

All of results were considered together to get a relation between the stiffness ratios and the other parameters (distance ratio, weight ratio and period ratio). In order to do this, relations between each parameter versus stiffness ratio were shown using the data under related parameter title.

Distance ratio vs Stiffness ratio

Results of distance ratios when the outer axes of the system were displaced in X and Y directions versus stiffness ratios are shown in Figure 25.

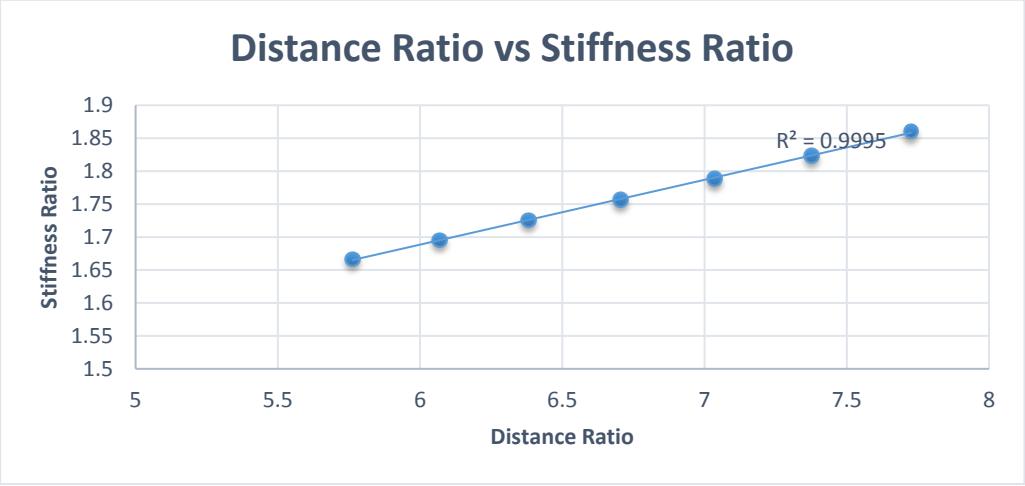


Figure 25. Distance ratio vs Stiffness ratio

In Figures 25, 26 and 27, the variation of distance (inner to outer) with respect to stiffness ratio for the cases where the plan dimensions were changed are provided.

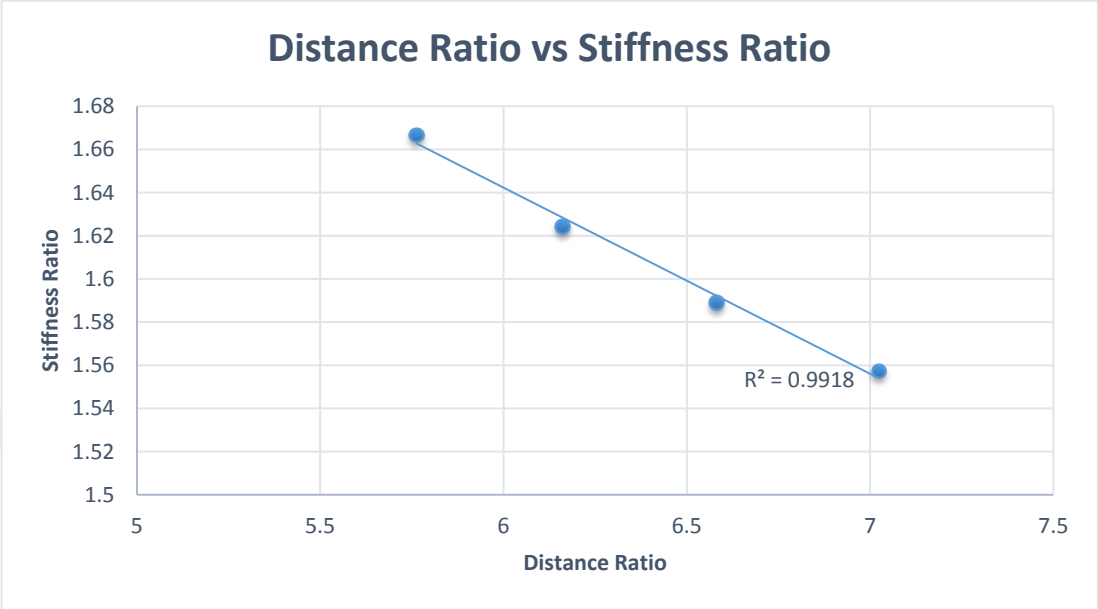


Figure 26. Distance ratio vs Stiffness ratio, only in X direction

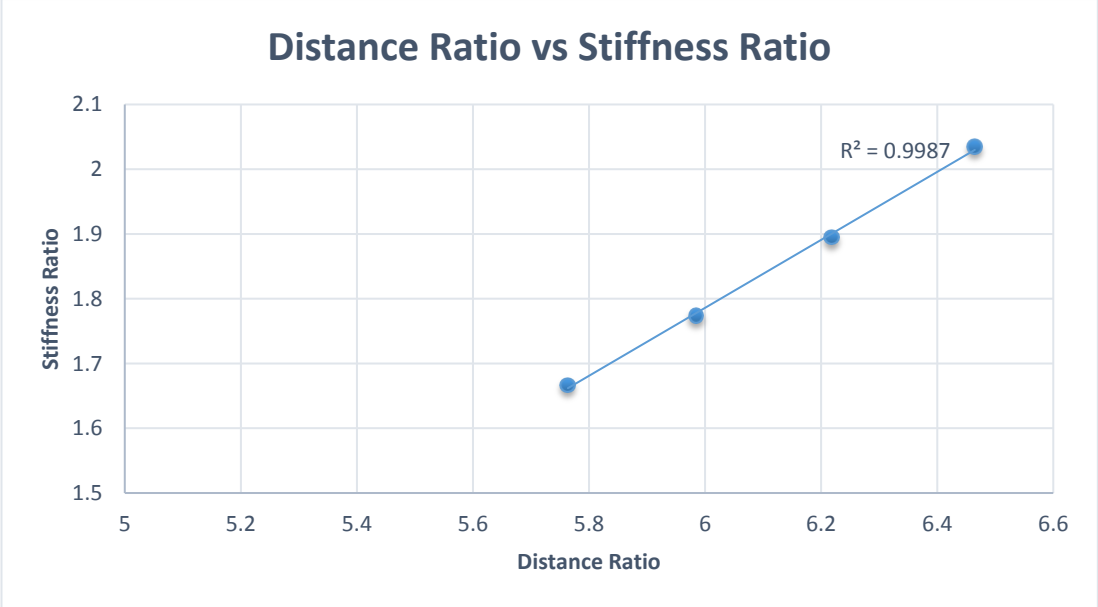


Figure 27. Distance ratio vs Stiffness ratio, only in Y direction

These results in distance case show the linear relation between the distance ratio and the stiffness ratios.

Weight ratio vs Stiffness ratio

Looking the results of the weight case at previous papers, relation between the weight ratio and stiffness ratio of the systems are illustrated in Figure 28.

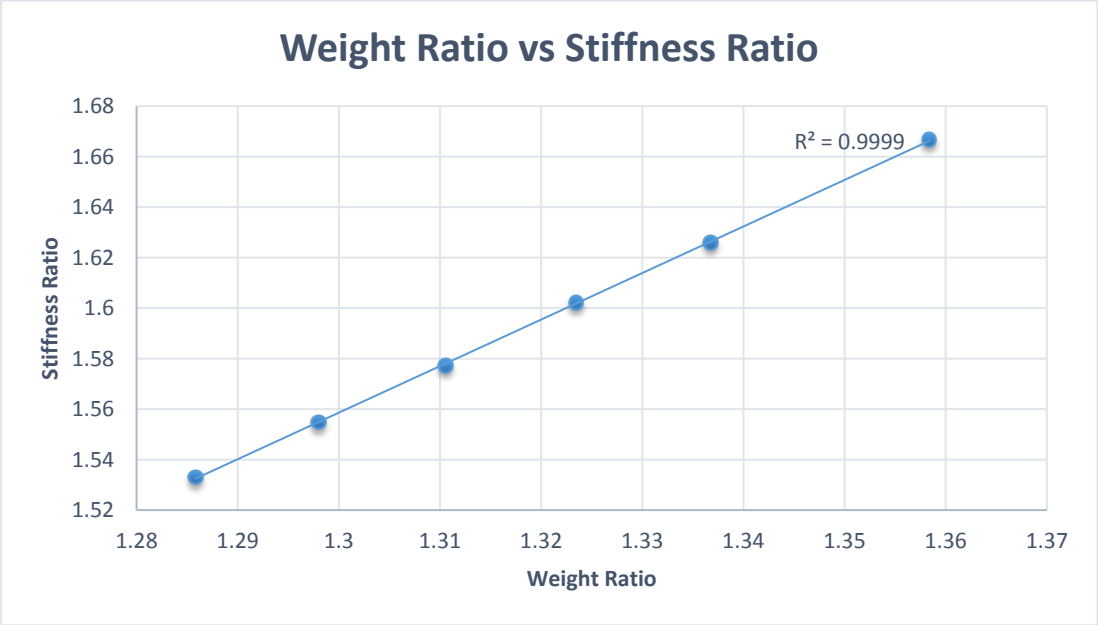


Figure 28. Weight ratio vs Stiffness ratio

Comparing the ratios of the weight parameter and stiffness, it can be seen that the relation between these results show a linear behavior.

Period ratio vs Stiffness ratio

In order to see the period ratio that is composed of fixed-base torsional period square divided by the assumed period times fixed-base third translational period (Equation 3.3) change with the stiffness ratio, Figure 29 can be considered.

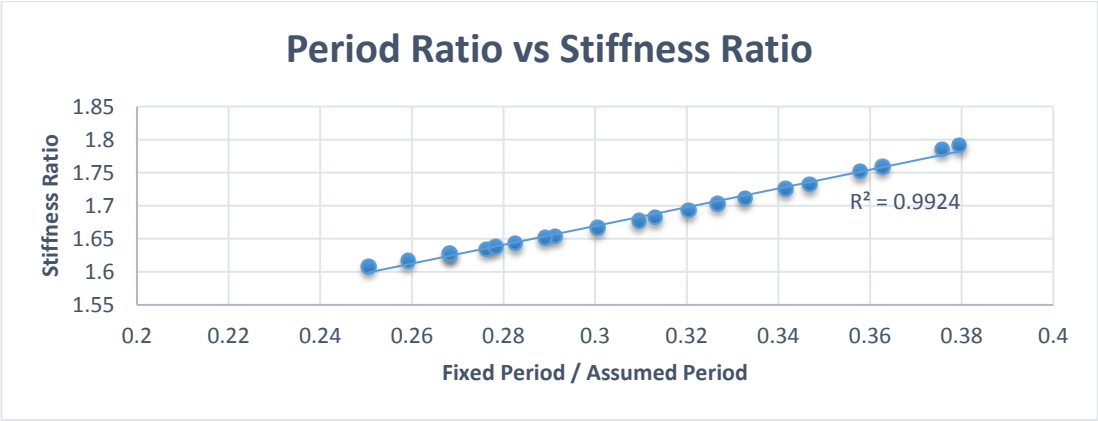


Figure 29. Period ratio vs Stiffness ratio

Looking at Figure 29, that almost a linearity exits between period ratio and stiffness ratio can be commented.

After seeing the linearity between the parameters of the formula with the stiffness ratios of the systems, a Multilinear Regression Analysis was performed to formulize the dataset.

Formulization was considered as Equation (3.1),

$$(K_O / K_I) = A + B*(D_O / D_I) + C*(W_O / W_I) + D*(T^2 / T_{translational}T_{assumed})$$

where, A is constant, B, C and D are the multipliers of each parameter.

After using the Multilinear Regression Analysis, the unknown parameters are,

A = 0.1, B = -0.12, C = 1.21 and D = 1.95

Then, Equation (3.1) becomes,

$$(K_O / K_I) = 0.1 - 0.12*(D_O / D_I) + 1.21*(W_O / W_I) + 1.95*(T^2 / T_{translational}T_{assumed}) \quad (3.4)$$

To see the sensitivity of the formula, each analysis case was controlled with the formula whether it can give the stiffness ratio true. Inner stiffness, K_I, at the left hand side of the formula was multiplied with the result of the right side of the formula. Then, total inner lateral effective stiffness of each system was multiplied by the value got from the right side of the formula. Thus, outer lateral effective stiffness of each system was calculated. This outer stiffnesses then, checked with the actual total outer effective stiffness. Calculations are shown in Table 59.

Table 59. Outer stiffness check when the formulation is used

Cases	Coefficient by Formula	K_I	K_O	K_O*	Difference %
Rigidity	1.91	9196	17226	17535.8	1.8
	1.78	9658	17028	17172.5	0.85
	1.66	10098	16830	16780.0	0.3
	1.56	10538	16650	16437.8	1.27
	1.47	10956	16488	16080.9	2.47
	1.39	11374	16326	15756.4	3.49
	1.31	11792	16200	15443.6	4.67
Distance	1.66	10098	16830	16780.0	0.3
	1.73	10648	18378	18448.2	0.38
	1.79	11242	20106	20098.8	0.04
	1.84	11880	22104	21803.5	1.36
	1.70	10362	17568	17595.2	0.15
	1.76	10934	19206	19251.9	0.24
	1.81	11550	21060	20954.9	0.5
	1.69	10362	16830	17459.9	3.74
	1.70	10648	16920	18057.2	6.72
	1.70	10934	17028	18586.6	9.15
	1.71	10362	18378	17699.1	3.69
	1.75	10648	20178	18670.8	7.47
	1.79	10934	22248	19595.5	11.92
Weight	1.66	10098	16830	16780.0	0.3
	1.64	10340	16812	16930.8	0.71
	1.62	10494	16812	17002.4	1.13
	1.61	10670	16830	17134.0	1.81
	1.59	10824	16830	17230.4	2.38
	1.58	10978	16830	17302.1	2.81
Height	1.66	10098	16830	16780.0	0.3
	1.70	10450	17496	17763.7	1.53
	1.68	10274	17154	17261.1	0.62
	1.66	10032	16650	16628.9	0.13
	1.66	9988	16542	16529.6	0.08
	1.65	9944	16434	16431.8	0.01
Story	1.37	7128	9648	9746.3	1.02
	1.52	8580	12942	13076.5	1.04
	1.66	10098	16830	16780.0	0.3
	1.79	11682	21636	20905.0	3.38
Story Height	1.53	8712	13104	13352.1	1.89
	1.54	8844	13248	13642.7	2.98

Table 59 (continued). Outer stiffness check when the formulation is used

Cases	Coefficient by Formula	K_I	K_O	K_O*	Difference %
Story Height	1.56	8998	13446	14010.2	4.2
	1.37	7216	9702	9878.7	1.82
	1.37	7326	9792	10050.4	2.64
	1.38	7414	9864	10207.2	3.48
Random Changes	1.45	9262	13086	13466.8	2.91
	1.27	7810	10548	9940.2	5.76
	1.73	11044	18810	19114.5	1.62
Period	1.66	10098	16830	16780.0	0.3
	1.68	10098	16938	16957.4	0.11
	1.70	10098	17100	17170.2	0.41
	1.72	10098	17280	17412.6	0.77
	1.75	10098	17496	17690.5	1.11
	1.78	10098	17766	18003.8	1.34
	1.82	10098	18090	18334.9	1.35
	1.64	10098	16704	16596.7	0.64
	1.63	10098	16596	16425.3	1.03
	1.61	10098	16506	16301.2	1.24
	1.60	10098	16434	16141.5	1.78
	1.69	10956	18432	18473.6	0.23
	1.71	11924	20304	20422.6	0.58
	1.74	13046	22518	22722.4	0.91
	1.77	14300	25056	25360.4	1.21
	1.81	15774	28170	28525.3	1.26
	1.64	9328	15408	15290.0	0.77
	1.62	8668	14202	14027.1	1.23
	1.60	8052	13104	12874.0	1.76
	1.58	7502	12132	11859.1	2.25
	1.56	7018	11286	10975.7	2.75

In Table 59, coefficient by formula means the result of the right hand side of the Equation (3.4). K_I and K_O are the actual inner and outer stiffnesses of each cases. K_O* is the total outer lateral effective stiffness and obtained by the product of actual inner stiffness with coefficient by formula for each case.

Formulation can satisfy the required stiffness ratio between the inner and outer isolators as in the Table 59. In most of the cases, errors are within 5% range. There are

a few cases with errors around 10%. This can result from the change of the outer plan dimensions having columns carrying the highest axial loads on the system.

As a result, design method developed in this study estimates a stiffness ratio between the inner and outer isolators of the system. This ratio can be reached by three parameters of the structure; distance ratios of inner and outer isolators, weight ratios of inner and outer isolators and, period ratio that is fixed-base torsional period square divided by assumed period times fixed-base period of third mode. Of course, this method was developed for the structures with torsionally unrestrained systems. Thus, using the stiffness ratio obtained from formula, total lateral effective stiffness of the isolation system that can be calculated from Equation (2.46) can be distributed to inner and outer isolators in which case this distribution provides structure to show torsionally restrained system.

3.4 ISOLATED CASES

Isolated cases of the structure were carried out in two systems; symmetric and asymmetric. As mentioned before, two systems have same structure but, asymmetric systems have mass and stiffness eccentricities (same structure but shear walls at the right side were removed). Designs of isolators were carried out according to symmetric system case and the same isolators were used for asymmetric cases. Comparison of conventional and proposed methods were examined on these systems.

A base slab thickness of 60 cm was used in both systems. Seismic parameters and load combinations are same as in fixed-base cases. Assumed period of maximum capable of earthquake was 2.5 seconds for all cases. To see the behavior and design of the isolators, maximum considered earthquake were used.

1 second response acceleration parameter was selected as 0.8 g for site in which the structure built as defined in Boğaziçi Earthquake Research Institute [29].

Isolation system was selected as lead-rubber bearing system for all the cases. Designs of the system were calculated according to that type of seismic isolators. Modelling and design of the isolators were carried out through the formulations in Chapter 2.

3.4.1 Symmetric Systems

Loading on the slabs of isolated symmetric system is as in the fixed-base symmetric system. Foundation on the isolators have same dead and live loads on it. For lead-rubber bearings in all cases, an effective damping of 20% was estimated at the beginning.

3.4.1.1 Conventional Method

In conventional method, isolators are designed looking the seismic weight on each of them. Thus, axial loads on the isolators (seismic weights) are primary parameter and they are given in Table 60.

Table 60. Seismic weights on isolators in symmetric case

Seismic Weights			
OutputCase	Axial Load (ton)	OutputCase	Axial Load (ton)
1G+0,5Q	200.85	1G+0,5Q	89.56
1G+0,5Q	200.85	1G+0,5Q	89.56
1G+0,5Q	200.85	1G+0,5Q	89.15
1G+0,5Q	200.85	1G+0,5Q	89.15
1G+0,5Q	114.28	1G+0,5Q	89.15
1G+0,5Q	114.28	1G+0,5Q	89.15
1G+0,5Q	114.28	1G+0,5Q	70.62
1G+0,5Q	114.28	1G+0,5Q	70.62
1G+0,5Q	101.38	1G+0,5Q	69.75
1G+0,5Q	101.38	1G+0,5Q	69.75
1G+0,5Q	101.38	1G+0,5Q	69.75
1G+0,5Q	101.38	1G+0,5Q	69.75
1G+0,5Q	92.06	1G+0,5Q	59.82
1G+0,5Q	92.06	1G+0,5Q	59.82
1G+0,5Q	92.06	1G+0,5Q	59.82
1G+0,5Q	92.06	1G+0,5Q	59.82
1G+0,5Q	90.83	1G+0,5Q	44.18
1G+0,5Q	90.83	1G+0,5Q	44.18
1G+0,5Q	90.83	1G+0,5Q	44.18
1G+0,5Q	90.83	1G+0,5Q	44.18

Looking the axial load distributions, 3 types of isolators were decided to be used. Limiting axial loads of the 3 types of isolators are 71 ton, 115 ton and 201 ton (smaller than 71 tons, in between 71 and 115 tons, greater than 201 tons). These isolators were called SC1, SC2 and SC3, respectively. In Figure 30, isolators are shown.

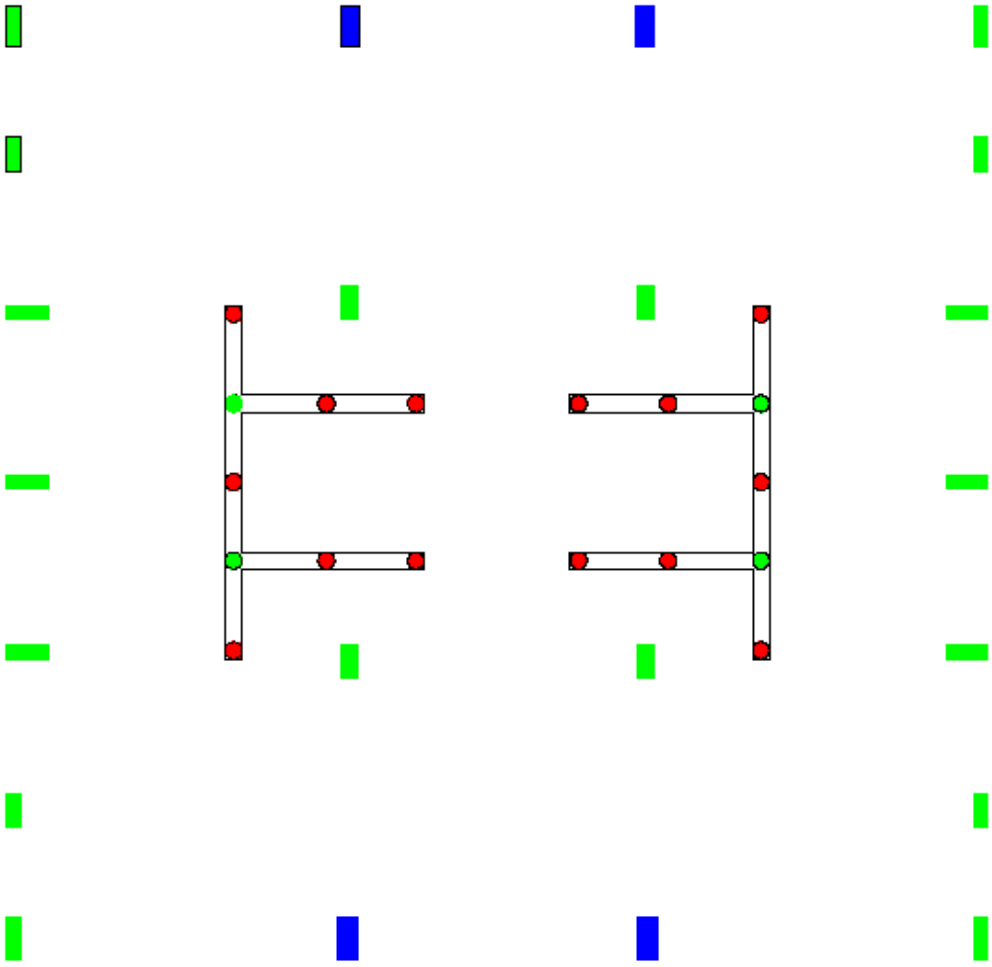


Figure 30. Isolator types in symmetric case

In Figure 30, red ones represent the SC1, green ones represent SC2 and blue ones represent SC3 type isolators. All isolators were designed with circular sections. Now, each stage of iterations done through the analyses of the isolators are presented. First, looking the seismic weights of the isolators and the assumed MCE period, an effective lateral stiffnesses of each isolator type were calculated. Vertical stiffnesses of each of

them were calculated as 1000 times the lateral ones at the beginning. Then, lateral and vertical stiffnesses were calculated considering the formulations stated in Chapter 2. In other words, after the first iteration, isolators were designed according to the maximum loads on them coming from axial and axial seismic combinations.

Using the Equation (2.46), effective lateral stiffnesses at MCE assumed period of each isolator type were calculated as below.

Table 61. Effective lateral stiffnesses of isolators at first iteration in symmetric case

	SC1	SC2	SC3
K_{eff} (kN/m)	449	726	1270

Then, assuming an initial 20% effective damping of the system and considering the seismicity of the structure, a response spectrum analysis was applied to the system. Response spectrum was damped spectrum as stated in [14], using the damping coefficient calculated from Figure 18. According to [14], spectral accelerations in response spectrum can be reduced to accelerations divided by B_D or B_M values from the point of 0.8 T_D or 0.8 T_M. Response spectrum in first isolated case is given in Figure 31.

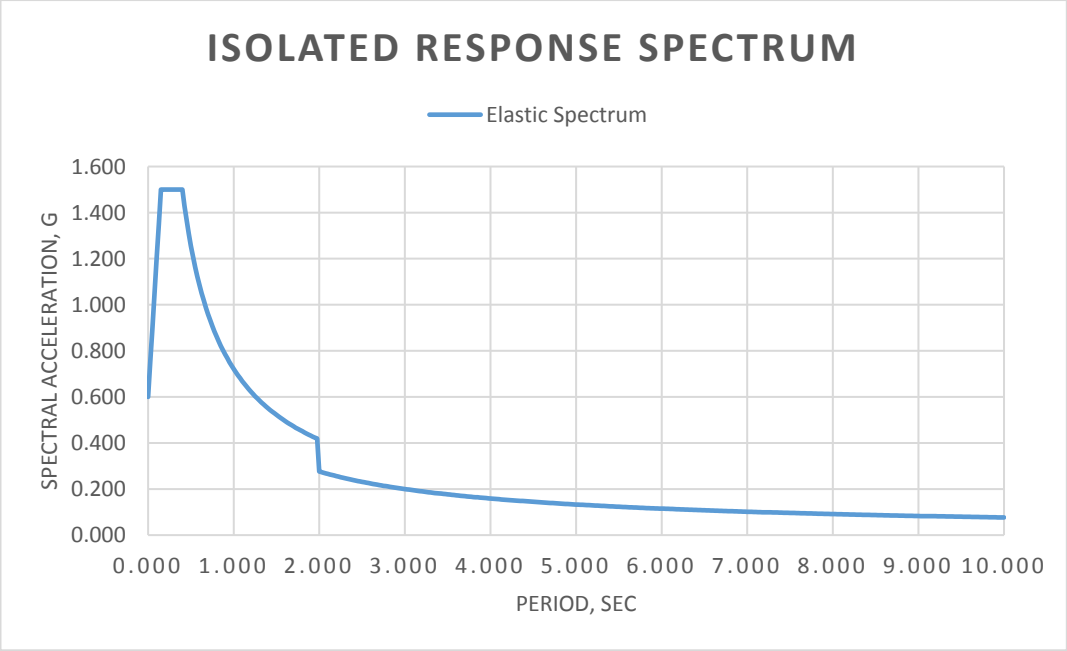


Figure 31. Isolated response spectrum in symmetric case

After the definitions about stiffness and the seismic loading of the structure, system was analyzed by means of a commercial computer software named as SAP2000. Results of the final iteration are shown in Table 62. Calculation details and design checks were given for the final iteration case.

Table 62. Analysis results in symmetric case for conventional method

Case	Definitions	SC1	SC2	SC3
Conventional	K_{eff} (kN/m)	471	751	1275
	W_M (kN.m)	86	126	199
	β_{eff}	28%		
	P_{DL++LL} (ton)	74	139	278
	$P_{DL+LL+EQ}$ (ton)	143	239	360
	D_{TM} (m)	0.31	0.31	0.31
	T_M (sec)	2.5		

Design results (Table 63) of each type of isolators were given through the formulations in Chapter 2. All lead-rubber bearings were designed assuming with bolted connections, so roll-out stability conditions was not required. Rubber used in the design has a shear modulus of 4.45 MPa and breaking strain of 500%. Ultimate strength of the steel shims used was 365 MPa. Design maximum shear strains were selected 100%. Calculation details of isolators are given in Appendix B.

Table 63. Design results of the isolators designed with conventional method

Isolator	W_M kN.m	Q kN	K_2 (K_P) kN/m	K_1 kN/m	D_y m	K_{eff} kN/m	β_{eff} %	G GPa
SC1	85.91	80.12	212.37	2123.7	0.04	470.82	30	0.4
SC2	125.52	113.1	386.08	3860.8	0.03	750.91	28	0.7
SC3	199.44	176.72	705.13	7051.3	0.03	1275.18	26	0.8

Design calculations were figured out according to maximum total displacements under the maximum capable earthquake with a maximum period of 2.5 seconds. Design checks were made under the critical axial and axial seismic load combinations that were given in definitions part of the structure.

Fixed-base structure itself was a torsionally unrestrained structure as mentioned before. After the conventional design method, structure is again a torsionally unrestrained structure. In other words, first mode of the isolated system is torsion again.

On the other hand, with the proposed method, first two modes of the isolated system was translational. All results are given in following chapter.

Moreover, final iteration and results of the design basis earthquake cases that were used for time history analyses, final effective damping calculations of both DBE and MCE using Equation (2.36) are shown in Tables 64, 65 and 66.

Table 64. Final results of isolators at DBE in symmetric case

Iterations	Definitions	SC1	SC2	SC3
Final	K_{eff} (kN/m)	747	1140	1883
	W_D (kN.m)	35	53	86
	β_{eff}	33%		
	D_{TD} (m)	0.15	0.15	0.15
	T_D (sec)	2		

Table 65. Final effective damping of the system at DBE in symmetric case

Design Basis Earthquake						
Unit	K_{eff} (kN/m)	W_D (kN.m)	Multi K_{eff} (kN/m)		Multi W_D (kN.m)	
14	747	35	10458		490	
22	1140	53	25080		1166	
4	1883	86	7532		344	
Total Composite Stiffnesses			43070		2000	
Total Composite Damping Values			β_{eff}	32.85	B_D	1.76

Table 66. Final effective damping of the system at MCE in symmetric case

Maximum Capable Earthquake						
Unit	K_{eff} (kN/m)	W_M (kN.m)	Multi K_{eff} (kN/m)		Multi W_M (kN.m)	
14	471	86	6594		1204	
22	751	126	16522		2772	
4	1275	199	5100		796	
Total Composite Stiffnesses			28216		4772	
Total Composite Damping Values			β_{eff}	28.01	B_M	1.66

Moreover, additionally, isolators were designed by taking Q/W ratio as 0.1 and yielding displacements (D_y) as 0.025 m to consider an other conventional design case to check the systems. Thus, each isolator type was designed as in Table 67. Total displacements were 0.31 m and effective damping was 28 % again.

Table 67. Design results of isolators designed with conventional method (Q/W = 0.1)

Isolator	W_M kN.m	Q kN	K_2 (K_P) kN/m	K_1 kN/m	D_y m	K_{eff} kN/m	β_{eff} %	G GPa
SC1	79.96	70.14	244.55	2445.5	0.025	470.80	28	0.4
SC2	128.93	113.10	386.08	3860.8	0.025	750.91	28	0.7
SC3	224.93	197.31	638.35	6383.5	0.025	1274.83	29	0.7

3.4.1.2 Proposed Method

In proposed design method, instead of the parameter seismic weight in convential design method, as stated before, a stiffness ratio between the inner and outer isolators was calculated depending on the formula shown in formulation process part. Parameters of the default system were shown here again.

$D_O / D_I = 5.76$, $W_O / W_I = 1.36$, T Ratio = 0.30

Then, using the Equation (3.4),

$(K_O / K_I) = 0.1 – 0.12*(D_O / D_I) + 1.21*(W_O / W_I) + 1.95*(T^2 / T_{translational}T_{assumed})$

$(K_O / K_I) = 0.1 – 0.12*5.76 + 1.21*1.36 + 1.95*0.30$

$(K_O / K_I) = 1.66$

Thus, effective lateral stiffness ratio of the outer and inner isolators should be around 1.66. When applying this ratio to the system, looking the seismic weight of the structure, total lateral effective stiffness must be calculated. Calculation process is shown below in.

Seismic weight of the structure is 3769.58 ton. Using the Equation (2.46), total effective lateral stiffness of the isolators is 23811 kN/m. Then,

$$\sum K_{eff} = 23811 kN/m \text{ and } \sum K_O / \sum K_I = 1.66$$

$$\sum K_O / \sum K_I = \sum K_{eff}$$

$$1.66 \sum K_I + \sum K_I = \sum K_{eff} = 23811 kN/m$$

$$2.66 \sum K_I = \sum K_{eff} = 23811 kN/m$$

$$\sum K_I = 8952 kN/m$$

$$\sum K_O = 14860 kN/m$$

Because there are 22 isolators at the inner side and 18 isolators at the outer side, these total effective stiffness values divided by the corresponding numbers of isolators. Hence, one inner isolator should have an effective lateral stiffness of 407 kN/m and one outer isolator should have an effective lateral stiffness of 826 kN/m. Again assuming target period of 2.5 seconds at MCE and an initial effective damping of 20%, system was analyzed for first case. Then, at the other iterations, isolators were designed according to the maximum axial and axial seismic load combinations at each step. In Figure 24, inner and outer isolators were represented. Inner and outer isolators were called as STI and STO, respectively. Calculations and design details were given for the final iteration. Final results are shown below in Table 68.

Table 68. Analysis results in symmetric case for proposed method

Case	Definitions	STI	STO
Proposed	K_{eff} (kN/m)	427	897
	W_M (kN.m)	75	161
	β_{eff}	25%	
	P_{DL+LL} (ton)	91	267
	$P_{DL+LL+EQ}$ (ton)	171	347
	D_{TM} (m)	0.34	0.34
	T_M (sec)	2.4	

Again design results (Table 69) of isolators are given through the formulations in Chapter 2. All of the lead-rubber bearings were designed assuming with bolted connections, so roll-out stability conditions was not required. Rubber used in the design has a young modulus of 4.45 MPa and breaking strain of 500%. Ultimate

strength of the steel shims used was 365 MPa. Design maximum shear strains were selected 100%. Calculation details of isolators are given in Appendix B.

Table 69. Design results of the isolators designed with proposed method

Isolator	W_M kN.m	Q kN	K_2 (K_P) kN/m	K_1 kN/m	D_y m	K_{eff} kN/m	β_{eff} %	G GPa
STI	74.62	59.45	252.14	2521.4	0.03	426.98	24	0.4
STO	160.82	128.68	518.81	5188.1	0.03	897.28	25	0.5

Design calculations were figured out according to maximum total displacements under the maximum capable earthquake with a maximum period of 2.5 seconds. Design checks were made under the critical axial and axial seismic load combinations that were given in definitions part of the structure.

That the fixed-base structure is a torsionally unrestrained system was mentioned above. After designing isolated system with proposed method, structure became a torsionally restrained system. In other words, first and second modes of the structure are translational mode and the third mode is torsional mode. As stated, aim of the proposed method was already getting the building to a torsionally restrained system.

On the other hand, with the proposed method, first two modes of the isolated system were translational. All results are given in following chapter.

Moreover, final iteration and results of the design basis earthquake cases that were used for time history analyses, final effective damping calculations of both DBE and MCE using Equation (2.36) are shown in Tables 70, 71 and 72.

Table 70. Final results of isolators at DBE in symmetric case

Iterations	Definitions	STI	STO
Final	K_{eff} (kN/m)	612	1299
	W_D (kN.m)	34	69
	β_{eff}	0.30	
	D_{TD} (m)	0.165	0.165
	T_D (sec)	2.1	

Table 71. Final effective damping of the system at DBE in symmetric case

Design Basis Earthquake						
Unit	K_{eff} (kN/m)	W_D (kN.m)	Multi K_{eff} (kN/m)		Multi W_D (kN.m)	
22	612	33	13464		726	
18	1299	71	23382		1278	
Total Composite Stiffnesses			36846		2004	
Total Composite Damping Values			β_{eff}	29.95	B_D	1.70

Table 72. Final effective damping of the system at MCE in symmetric case

Maximum Capable Earthquake						
Unit	K_{eff} (kN/m)	W_M (kN.m)	Multi K_{eff} (kN/m)		Multi W_M (kN.m)	
22	427	75	9394		1650	
18	897	161	16146		2898	
Total Composite Stiffnesses			25540		4548	
Total Composite Damping Values			β_{eff}	24.52	B_M	1.59

3.4.2 Asymmetric Systems

Asymmetricities were provided with mass and stiffness eccentricities. Mass eccentricities were applied by shifting the mass center of the system. Eccentricity levels were 2.5%, 5%, 7.5% and 10% of the side dimensions. Furthermore, to consider stiffness eccentricity, shear walls at the right side of the plan were removed and changed with columns (Figure 32). Center of stiffness (CI) is at 415 cm from left. Isolators in symmetrical cases were examined with mass and stiffness eccentricities.

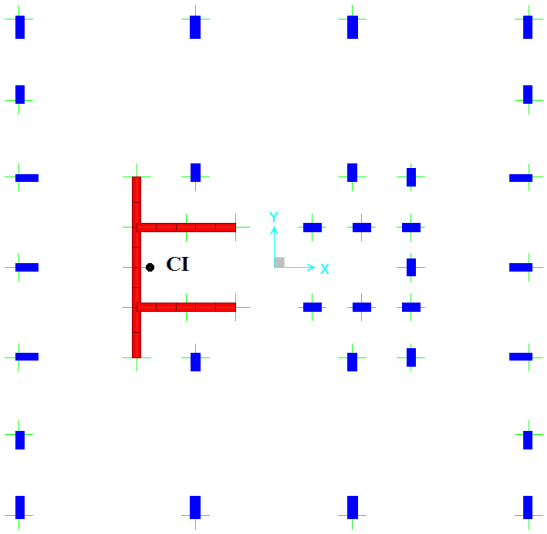


Figure 32. Stiffness eccentricity

3.4.2.1 Conventional Method

As mass eccentiricities increase, total displacements of isolators increase, as well. Thus, isolators designed in symmetrical case were updated(Table 73). Because stiffness eccentricity did not affect the general displacements of the isolator types, as stated in previous studies, effective stiffnesses were updated for mass eccentricities.

Table 73. Updated values of isolators under different mass eccentricities

Conventional Method							
Eccentricity, %	Definitions	Conventional			Q/W = 0.1		
		SC1	SC2	SC3	SC1	SC2	SC3
2.5	K_{eff} (kN/m)	463	734	1249	464	724	1236
	D_{TM} (cm)	0.31	0.32	0.32	0.315	0.32	0.32
	B_{eff} (%)	30%	28%	25%	28%	28%	29%
5.0	K_{eff} (kN/m)	463	719	1225	460	714	1219
	D_{TM} (cm)	0.32	0.34	0.34	0.325	0.34	0.34
	B_{eff} (%)	30%	27%	25%	28%	27.5%	28%
7.5	K_{eff} (kN/m)	452	700	1196	450	705	1186
	D_{TM} (cm)	0.335	0.36	0.36	0.335	0.355	0.36
	B_{eff} (%)	29.5%	27%	24%	27%	26.5%	27%
10.0	K_{eff} (kN/m)	445	684	1170	448	684	1158
	D_{TM} (cm)	0.345	0.38	0.38	0.345	0.38	0.38
	B_{eff} (%)	29%	25%	23.5%	27%	26%	26.5%

3.4.2.2 Proposed Method

In the same manner, updated values of each type of isolators designed in symmetrical case are shown in Table 74.

Table 74. Updated values of isolators under different mass eccentricities

Proposed Method			
Eccentricity	Definitions	ATI	ATO
2.5%	K_{eff} (kN/m)	422	876
	D_{TM} (cm)	0.35	0.36
	B_{eff} (%)	24%	24%

Table 74(continued). Updated values of isolators under different mass eccentricities

Proposed Method			
Eccentricity	Definitions	ATI	ATO
5.0%	K_{eff} (kN/m)	417	857
	D_{TM} (cm)	0.36	0.38
	B_{eff} (%)	24%	24%
7.5%	K_{eff} (kN/m)	413	841
	D_{TM} (cm)	0.37	0.4
	B_{eff} (%)	23%	23%
10.0%	K_{eff} (kN/m)	409	825
	D_{TM} (cm)	0.38	0.42
	B_{eff} (%)	23%	23%

3.5 DYNAMIC ANALYSES

Seismic analyses methods used in the study were described here. As mentioned, design of the isolators were figured out with response spectrum analysis. Then, behavior of the structure and isolation system were considered under time history analysis cases.

3.5.1 Response spectrums

Response spectrum curves used in modal analyses are shown in Figure 33. As stated before, response spectrums were taken from Turkish Seismic Code as maximum considered earthquake (2475 years return period) that were taken calculated as 1.5 times the design basis earthquake (475 years return period).

3.5.1.1 Symmetric Systems

Response spectrums used in symmetric systems designed with both conventional and proposed methods are shown in Figure 33.

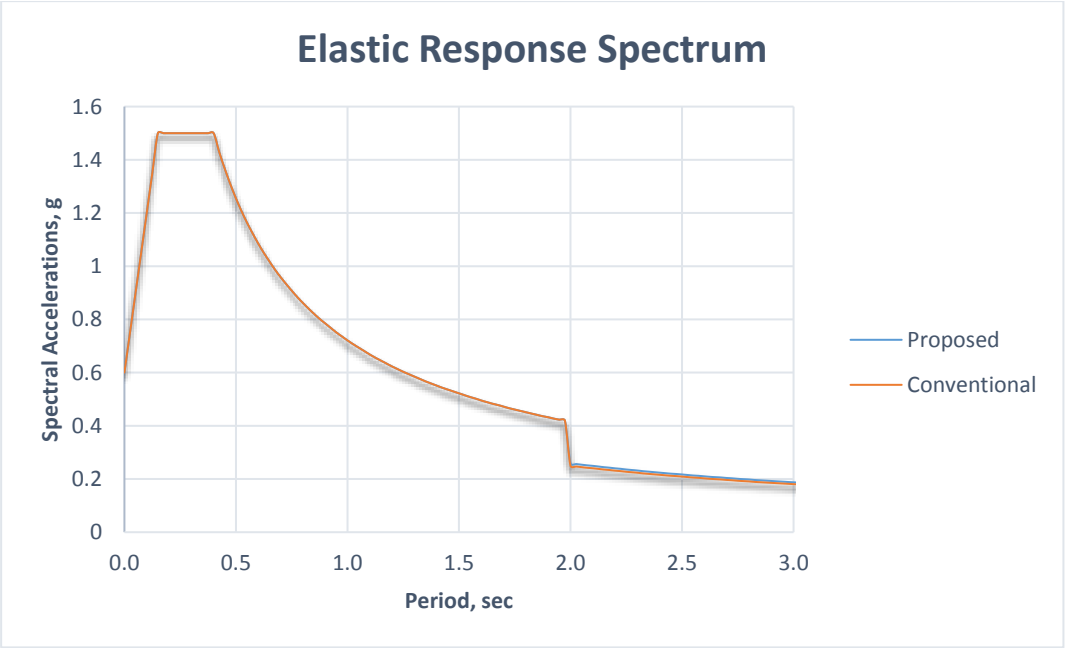


Figure 33. Isolated response spectrums in symmetric system

3.5.1.2 Asymmetric Systems

Response spectrums of asymmetric systems are same as symmetrical but, updated with the new effective damping ratios as in Table 75.

Table 75. Effective damping levels of each system with different mass eccentricities

Ecc. (%)	Effective damping (%)	
	Conventional	Proposed
2.5	28	24
5	28	24
7.5	27	23
10	27	23

3.5.2 Time Histories

Actual behavior of the structure and isolation system can be seen better in time histories. Thus, 3 different ground motion histories were selected which are Chi Chi (Station TCU057), Kocaeli (Station Gebze) and Northridge (Station Sylmar). According to ASCE 7-10 [6], time histories must be scaled in the interval 0.5 T_D and

1.25 T_M. Related spectral acceleration values of response spectrums of each case should not be smaller than the 5% damped response spectrums of the ground motion histories. Response spectrum of ground motion histories are calculated taking the average of square root sum of squares of the 5% response spectrum for two directions. Required time history records were taken from the PEER website (http://ngawest2.berkeley.edu/).

When the process was carried out for scaling, scale factors for time histories are; 2.55 for Chi Chi, 3.41 for Kocaeli and 0.42 for Sylmar.

In time history analysis cases, isolators were defined as bilinear elements. Whole parameters of the bilinear models of the isolators were defined in design calculations of each type of isolators. Nonlinear time history analyses were performed by using SAP2000.

Acceleration vs time intervals defined in SAP2000 figures of each ground motion histories are shown in Figures 34, 35 and 36 according to datas in PEER.

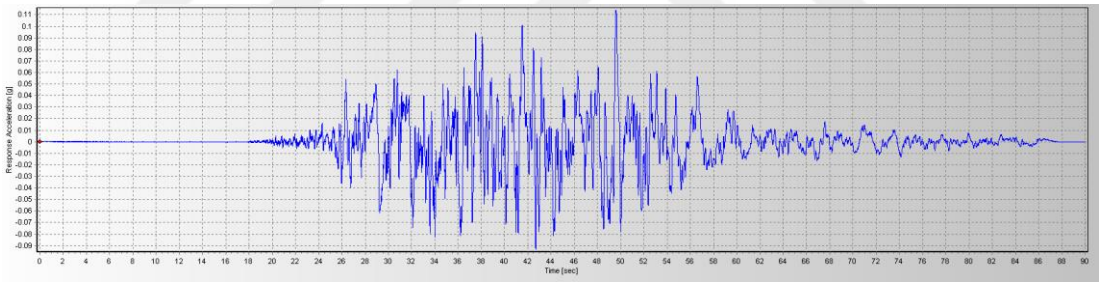


Figure 34. Ground motion history of Chi Chi

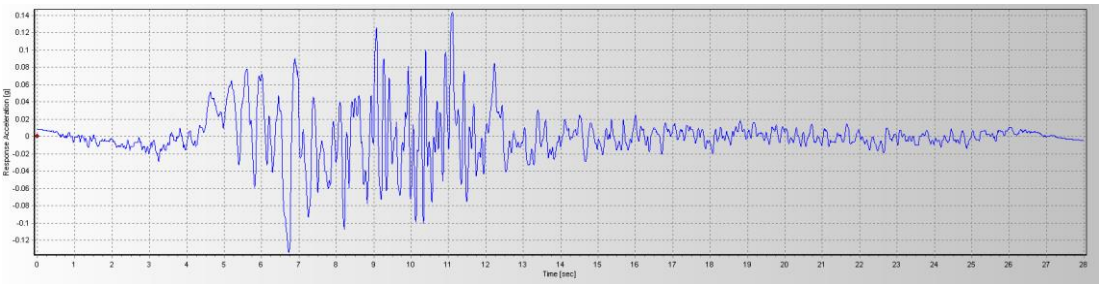


Figure 35. Ground motion history of Kocaeli

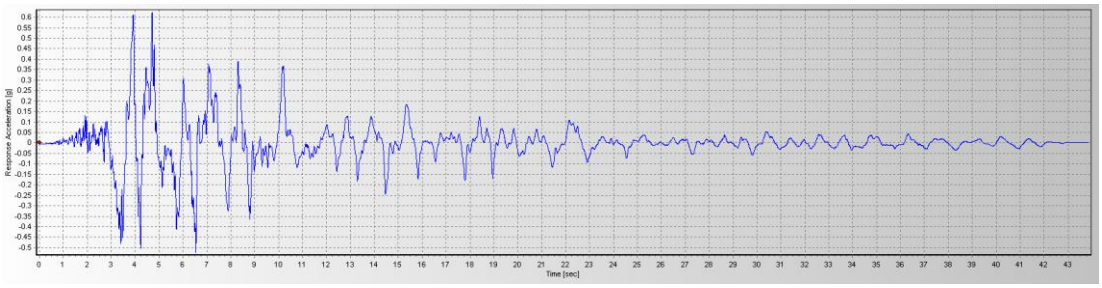


Figure 36. Ground motion history of Northridge

As mentioned, symmetrical (0% mass eccentricity) and asymmetrical (5% mass eccentricity) systems were examined with time history analyses to see more realistic behavior of structure and prove the datas obtained from response spectrum cases.

CHAPTER 4

RESULTS AND DISCUSSIONS

Systems were formed according to the calculations and seismic loadings in Chapter 3. Each system was analyzed in SAP2000. Isolators were bilinear link elements as stated. Design parameters of each isolator were defined as calculated and then, systems were analyzed with time history cases to see the behavior of the structure.

4.1 RESULTS

Results of the systems in terms of the displacements and shears of isolators, base shears and base torques are shown below for each case in MCE. In addition, to compare the behavior of the common isolators on each design method, 8 isolators were numbered as in Figure 37. Displacements of each of these numbered isolators were noted under different seismic inputs.

As a reminder, in Figure 37, points or isolators 1, 2, 3 and 4 are SC2 in conventional method, STO in proposed method; 5, 6, 7 and 8 are SC1 in conventional, STI in proposed method for symmetrical system cases. Response spectrum analyses were carried out for symmetrical, stiffness and mass eccentricity cases (2.5%, 5%, 7.5% and 10%). Time history cases were applied for the symmetrical and asymmetrical system with 5% mass eccentricity.

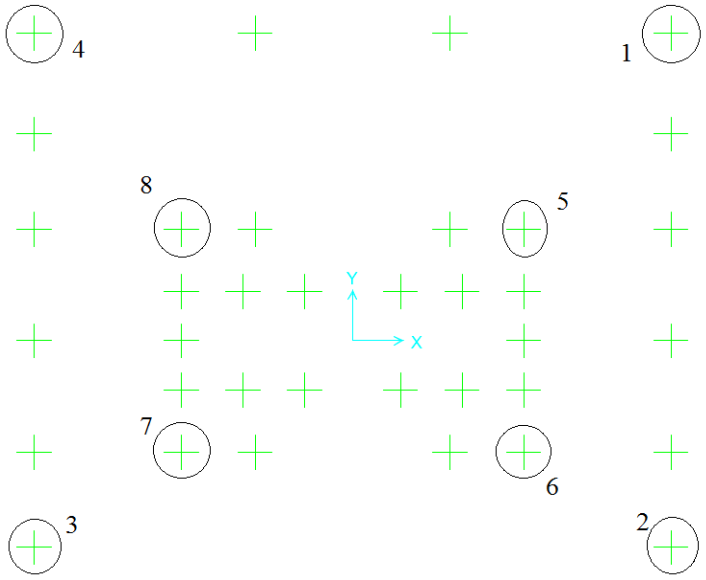


Figure 37. Labeled isolators for whole systems

4.1.1 Symmetric Systems

When the structure is a symmetrical system, seismic results for two design methods, conventional and proposed, are tabled below. In Tables 76 and 77, results from the modal analyses are shown.

Table 76. Modal results for symmetric system with conventional design method

Modal Results			Participating Mass Ratios		
Modes	Direction	Period, sec	Modes	Direction	Sum %
1	Torsional, Z	2.45	1	Torsional, Z	99
2	Translational, Y	2.35	2	Translational, Y	99
3	Translational, X	2.33	3	Translational, X	99

Table 77. Modal results for symmetric system with proposed design method

Modal Results			Participating Mass Ratios		
Modes	Direction	Period, sec	Modes	Direction	Sum %
1	Translational, Y	2.46	1	Translational, Y	99
2	Translational, X	2.45	2	Translational, X	99
3	Torsional, Z	2.42	3	Torsional, Z	99

As it can be seen from the Tables 76 and 77, using proposed method makes structure torsionally restrained. However, in conventional method, torsional mode came first again. Here, you can use the reason for inconvenience of seismic isolation system in torsionally unrestrained cases. This is not a desired case because for example in response spectrum analysis, the modes taking the force come below the assumed period. These modes written in Tables 76 and 77 are shown on response spectrum comparatively in Figure 38. In figure, PR means proposed method and CN means conventional method.

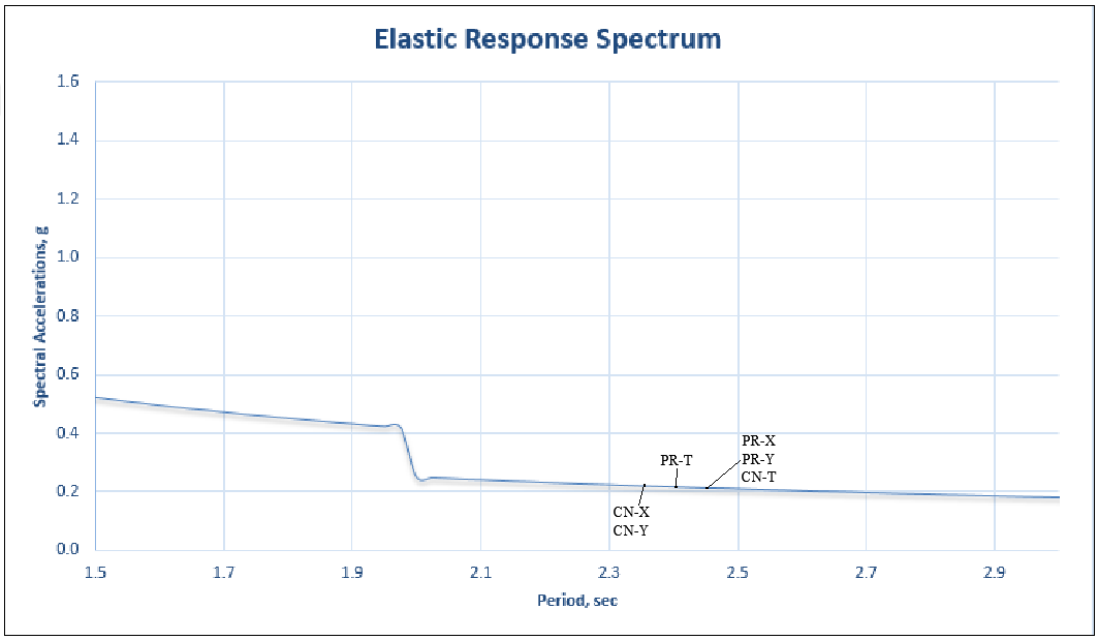


Figure 38. Modes calculated for conventional and proposed methods

Floor accelerations of each system was calculated, as well. For design purposes, a floor accelerations of maximum 0.2g is desired at DBE, looking the response spectra. Moreover, base shear over seismic weight ratio is desired between 0.1 and 0.2 at DBE. In Table 78, floor accelerations of symmetric systems in MCE are shown.

Table 78. Floor accelerations of symmetric systems in MCE

SYMMETRIC SYSTEMS		
Story	Conventional	Proposed
	Floor Acceleration, g	Floor Acceleration, g
6	0.246	0.242
5	0.239	0.237
4	0.233	0.233
3	0.230	0.230
2	0.229	0.228
1	0.228	0.227
0	0.228	0.227

Furthermore, floor accelerations of the symmetric systems at the DBE are shown in Table 79. Total base shear of symmetric system designed with conventional method is 432 ton and 421 ton for proposed method. Because seismic weight of the structure is 3770 ton, a ratio of 0.115 and 0.112 is obtained for conventional and proposed methods.

Table 79. Floor accelerations of symmetric systems in DBE

SYMMETRIC SYSTEMS		
Story	Conventional	Proposed
	Floor Acceleration, g	Floor Acceleration, g
6	0.127	0.120
5	0.121	0.117
4	0.117	0.114
3	0.115	0.111
2	0.114	0.11
1	0.113	0.11
0	0.113	0.11

In response spectrum analysis, a small decrease in base shears and floor accelerations are seen from the Tables 78 and 79 in proposed method. This was resulted from the periods reached at translational modes were different in two design methods. While proposed method provides system to be a torsionally restrained structure at assumed period, conventional method does that at lower periods.

Total base shears and torques for the symmetric system case with two design methods and maximum displacements and maximum shears of each isolator types are shown in Table 80.

Table 80. Results of isolator types for symmetric system with each design method

SYMMETRIC SYSTEM						
Seismic Loads	Parameters	CONVENTIONAL METH.			PROPOSED METH.	
		SC1	SC2	SC3	STI	STO
Response Spectrum	D_{TM} (cm)	30.2	30.2	30.2	33.3	33.0
	V (ton)	14.5	23.1	39.2	14.5	30.4
Chi Chi	D_{TM} (cm)	20.9	20.9	20.9	23.8	23.8
	V (ton)	12.4	19.7	33.1	12.9	27.1
Kocaeli	D_{TM} (cm)	19.6	19.6	19.6	21.6	21.6
	V (ton)	12.8	19.7	32.9	11.9	25.1
Northridge	D_{TM} (cm)	12.5	12.5	12.5	14.3	14.3
	V (ton)	10.6	16.3	26.9	9.8	20.8
R.S.	V_b (ton)	867			866	
	T_b (ton.cm)	0			0	
ChiChi	V_b (ton)	753			783	
	T_b (ton.cm)	0			0	
Kocaeli	V_b (ton)	745			713	
	T_b (ton.cm)	0			0	
Northridge	V_b (ton)	624			601	
	T_b (ton.cm)	0			0	

Under the maximum capable earthquake, isolators were modelled with response spectrum analysis loadings and they controlled with the ground motion histories as shown in Table 80. Here, D_{TM} is the total displacements and V is shear force of the each type of isolators under MCE. V_b and T_b is maximum base shear and base torque obtained at each system with two design methods.

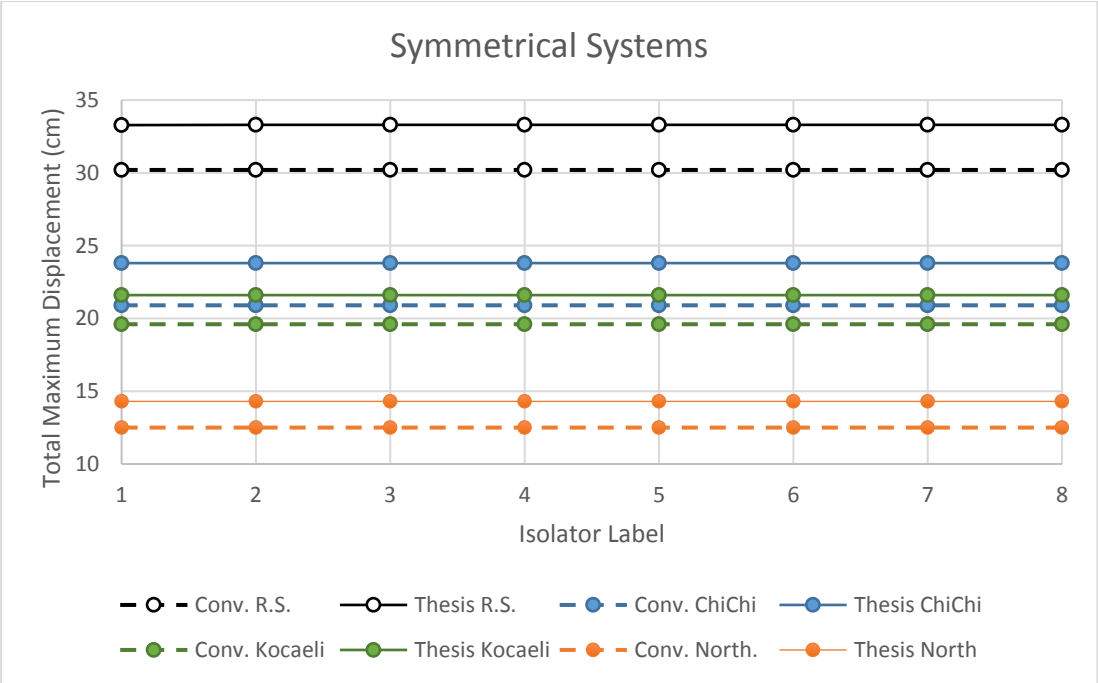


Figure 39. Labeled isolator displacements for symmetric systems

Looking at the Figure 39, displacements are higher in proposed method than conventional method for whole isolators in symmetric systems. Since system was totally symmetrical, all of the isolators displaced equally. On the other hand, base shears are almost equal for both design method. However, maximum shears on isolators calculated for system designed with conventional method. This shows the uniform shear distributions on isolators for the system designed with proposed method.

Maximum axial loads coming from the seismic load combinations for each isolator type in symmetrical systems are shown in Table 81. Units are in ton. Checks of the isolators for these maximum loads were supplied in Appendix C.

Table 81. Maximum axial loads (tons) on isolators in symmetric systems

Symmetric System					
Seismic Input	Conventional			Proposed	
	SC1	SC2	SC3	STI	STO
Northridge	156	260	391	177	360
ChiChi	197	325	451	203	397
Kocaeli	170	287	427	171	358
Max	197	325	451	203	397

4.1.2 Asymmetric Systems

Asymmetric systems were formed by shifting the mass centers to 2.5%, 5%, 7.5% and 10% of side dimensions of base slab and providing stiffness eccentricity. Response spectrum analyses were carried out for all eccentricities and time history analysis was performed for 5% mass eccentricity case only. Modal analyses results for systems designed with both method for mass eccentricity cases are shown in Table 82.

Table 82. Modal results for asymmetric systems for each design method

	Modal Results								
	Modes	Conventional Method				Proposed Method			
		Period sec	Participating Mass Ratio %			Period sec	Participating Mass Ratio %		
			X	Y	Torsion		X	Y	Torsion
2.5%	1	2.47	3	4	93	2.5	16	58	29
	2	2.35	9	89	2	2.48	65	31	4
	3	2.34	88	7	5	2.43	19	11	67
5.0%	1	2.53	8	9	87	2.56	22	38	45
	2	2.38	33	66	1	2.5	54	45	1
	3	2.35	59	25	12	2.42	24	17	54
7.5%	1	2.6	11	13	82	2.61	23	32	53
	2	2.41	43	57	1	2.52	52	48	1
	3	2.36	46	30	17	2.42	25	20	46
10.0%	1	2.66	13	15	80	2.67	23	29	58
	2	2.44	46	54	1	2.54	51	49	1
	3	2.36	41	31	19	2.41	26	22	41

In asymmetric systems, as it can be seen from the Table 82, as eccentricity levels increase, systems start to be torsionally unrestrained systems. Systems designed with conventional method shows always torsionally unrestrained case but, systems designed with proposed method are torsionally restrained at symmetrical and 2.5 and 5% mass eccentricity cases.

Maximum displacements and shear forces of each type of isolators designed with both methods using response spectrum analyses under mass eccentricity cases are shown below in Table 83.

Table 83. Displacements and shear forces of isolators analyzed with response spectrum

		Conventional			Proposed	
	Definition	SC1	SC2	SC3	STI	STO
2.5%	D_{TM} (cm)	31.5	33.4	32.5	35.4	37.4
	V (ton)	15.1	25.2	41.6	15.2	33.4
5.0%	D_{TM} (cm)	33	36.7	34.9	36.8	40.7
	V (ton)	15.6	26.9	43.7	15.7	35.6
7.5%	D_{TM} (cm)	34.9	40.0	37.5	38.4	43.9
	V (ton)	16.1	28.6	45.8	16.2	37.7
10.0%	D_{TM} (cm)	36.1	42.4	39.3	39.6	46.2
	V (ton)	16.4	29.6	46.8	16.5	38.9

Looking at the Table 83, displacements are higher at the systems designed with proposed method because translational periods are higher at that systems. On the other hand, maximum shear forces on the isolators were calculated at the systems designed with conventional method. Again, this shows the uniform distributions of shear forces on isolators for the proposed method.

Maximum displacements of isolators labeled as 1, 2, 3 and 4 that were analyzed with response spectrums for mass eccentricity cases are shown in Table 84 for two design methods.

Table 84. Corner isolator displacements at two design methods

	Methods	1	2	3	4
2.5%	Conventional, D_{TM} (cm)	31.9	33.3	33.4	33.2
	Proposed, D_{TM} (cm)	37.4	37.3	36.2	37.3
5.0%	Conventional, D_{TM} (cm)	34.2	36.6	36.7	36.6
	Proposed, D_{TM} (cm)	40.7	40.5	38.8	40.4
7.5%	Conventional, D_{TM} (cm)	37.1	39.9	40	40
	Proposed, D_{TM} (cm)	43.9	43.6	41.7	43.5
10.0%	Conventional, D_{TM} (cm)	39.2	42.2	42.1	42.4
	Proposed, D_{TM} (cm)	46.2	45.6	43.9	45.6

Furthermore, displacement differences of these isolators and difference over maximum displacement ratios are shown in Table 85.

Table 85. Displacement differences of corner isolators at two design methods

	Methods	Min	Max	Difference	%
2.5%	Conventional, D_{TM} (cm)	31.9	33.4	1.5	4
	Proposed, D_{TM} (cm)	36.2	37.4	1.2	3
5.0%	Conventional, D_{TM} (cm)	34.2	36.7	2.5	7
	Proposed, D_{TM} (cm)	38.8	40.7	1.9	5
7.5%	Conventional, D_{TM} (cm)	37.1	40	2.9	7
	Proposed, D_{TM} (cm)	41.7	43.9	2.2	5
10.0%	Conventional, D_{TM} (cm)	39.2	42.4	3.2	8
	Proposed, D_{TM} (cm)	43.9	46.2	2.3	5

As it can be seen from Table 85, maximum displacement differences are higher at the systems designed with conventional design method. Moreover, these differences increase with increasing mass eccentricities. Thus, compared to the conventional method, isolation systems are more effective at the proposed method because system displaces in more uniformity.

Base shears and torques for 4 mass eccentricity levels at response spectrum analyses are shown below in Table 86.

Table 86. Base reactions for 4 mass eccentricities at response spectrum analyses

	Definitions	Conventional	Proposed
2.5%	V (ton)	869	877
	T (ton.cm)	99689	111887
5.0%	V (ton)	873	887
	T (ton.cm)	181045	204361
7.5%	V (ton)	877	892
	T (ton.cm)	243801	274779
10.0%	V (ton)	881	899
	T (ton.cm)	284648	321676

When looked at Table 86, base shears are very close to each other. The reason of negligible higher base shears at proposed method resulted from the lower effective damping levels of the isolators at that method. On the other hand, as it can be seen from Table 86, shear forces on single isolator are decreased with the proposed method.

This shows that there is a more uniform distribution of total base shear to the isolators. Base torques are higher at proposed method because torsional rigidities of isolation systems were increased by increasing the effective stiffnesses of outer axes.

As stated, time history analyses were carried out on symmetrical (0% eccentricity) and asymmetrical (5% mass eccentricity) systems. Symmetrical case results were provided under symmetrical systems title. Thus, when systems were asymmetrical with 5% mass eccentricity, total base shears and torques, maximum displacements and shears of each isolator types are shown in Table 87.

Table 87. Results of isolator types for 5% asymmetric systems for each design method

ASYMMETRIC SYSTEM						
Seismic Loads	Parameters	CONVENTIONAL METH.			THESIS METH.	
		SC1	SC2	SC3	STI	STO
Response Spectrum	D_{TM} (cm)	33.0	36.7	34.9	36.8	40.7
	V (ton)	15.6	26.9	43.7	15.7	35.6
Chi Chi	D_{TM} (cm)	20.5	21.4	21.0	24.6	25.6
	V (ton)	13.7	20.7	36.9	12.2	28.3
Kocaeli	D_{TM} (cm)	20.0	20.8	20.6	21.8	22.4
	V (ton)	13.1	21	34.5	12.3	27.2
Northridge	D_{TM} (cm)	13.7	14.0	13.9	13.9	14.1
	V (ton)	12.1	19.6	31.4	10.8	24.0
R.S.	V_b (ton)	873			887	
	T_b (ton.cm)	181046			204361	
ChiChi	V_b (ton)	782			804	
	T_b (ton.cm)	132911			137968	
Kocaeli	V_b (ton)	746			725	
	T_b (ton.cm)	85886			103670	
Northridge	V_b (ton)	679			623	
	T_b (ton.cm)	117003			131820	

In the current ASCE code, if three time history analyses performed for a system, the maximum data shall be considered in the design. In Table 87, it is seen that Chi Chi record gives the higher results. Therefore, if one focus on the comparison of Chi Chi results, total base shears and total torques on both conventional and proposed are

almost equal even though proposed method is torsionally restrained and the conventional method is unrestrained.

In Figure 40, behavior of the common isolators for each design method for 5% asymmetric systems (mass eccentricity) are shown.

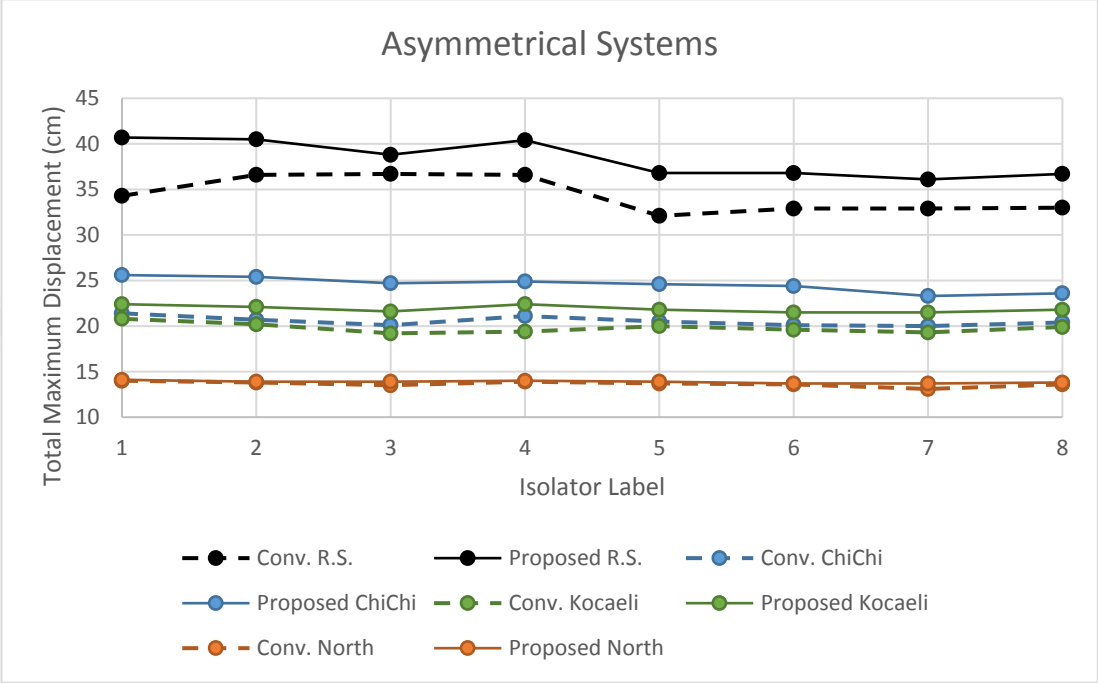


Figure 40. Labeled isolator displacements for asymmetric systems

Again looking at Figure 40, displacements are higher in proposed method. As stated before, this relation resulted from the higher mass participation ratios and translational periods in proposed method, in other words, because of spectral displacement curve. Furthermore, looking the displacements of corner isolators (1, 2, 3 and 4) and noting them relatively, for both dynamic analyses, differences between these displacements are less in proposed method. That means, since torsional rigidity of the structure was increased in proposed method, structure rotated less in this method. This displacement uniformity provides more effective system because it reduces torsional effects.

In Figure 41 and 42, displacements of corner isolators in 5% asymmetric system designed with conventional and proposed methods are illustrated, respectively.

Looking the Figure 41 and 42, it can be seen that the total displacements have higher differences at the conventional method.

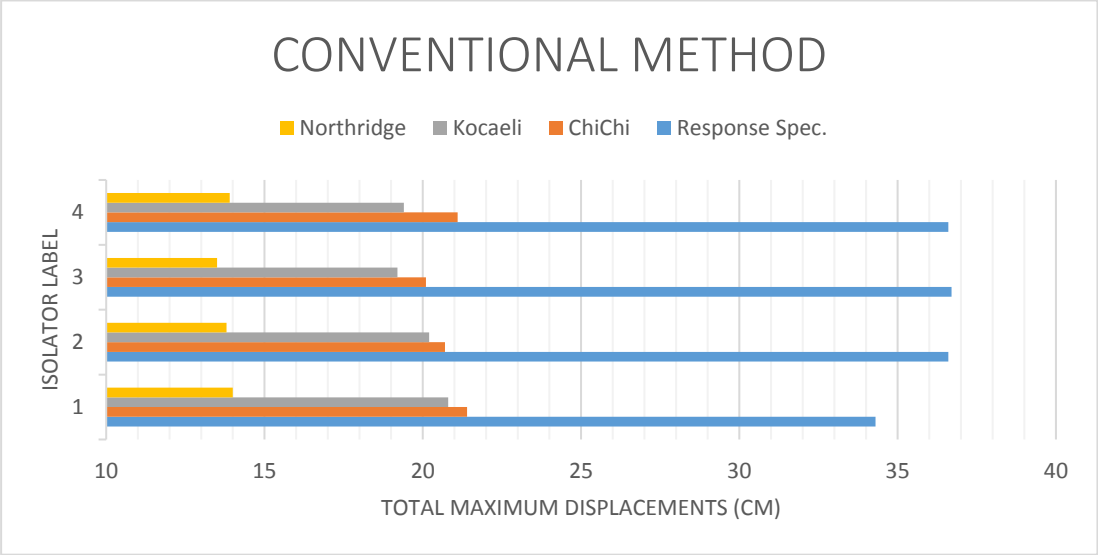


Figure 41. Displacements of corner isolators at conventional method

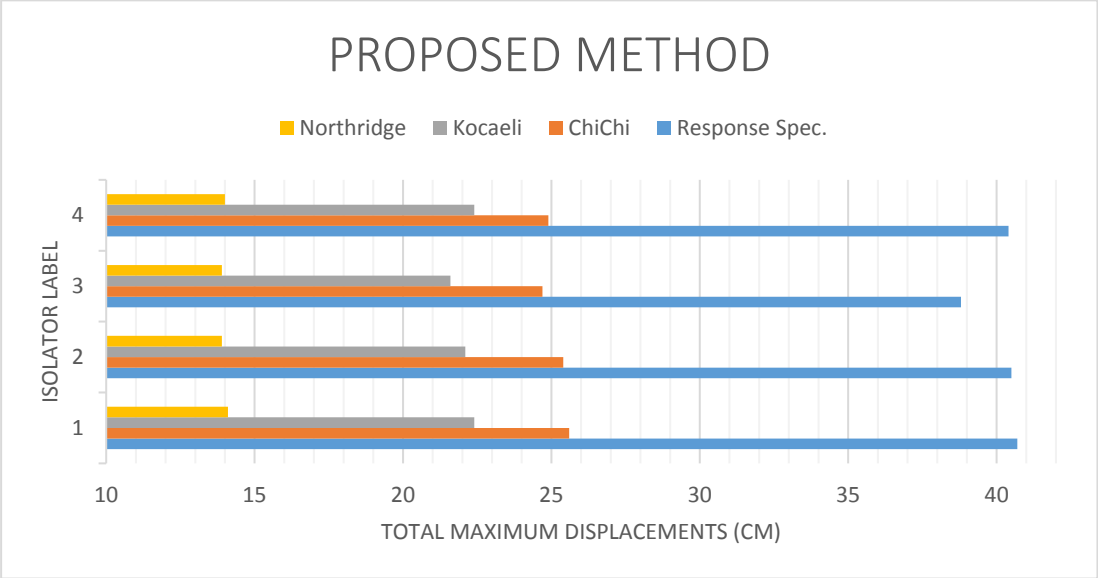


Figure 42. Displacements of corner isolators at proposed method

Displacement differences between isolators resulted from the mass eccentricity in systems. Because of the eccentricity, systems started to rotate and then, isolators

farther and closer to the mass center showed different displacements. As it can be seen from the above figures, isolators have closer displacements in the system designed with proposed method. These differences between the isolators displaced most and least are represented in Figure 43 for each seismic input.

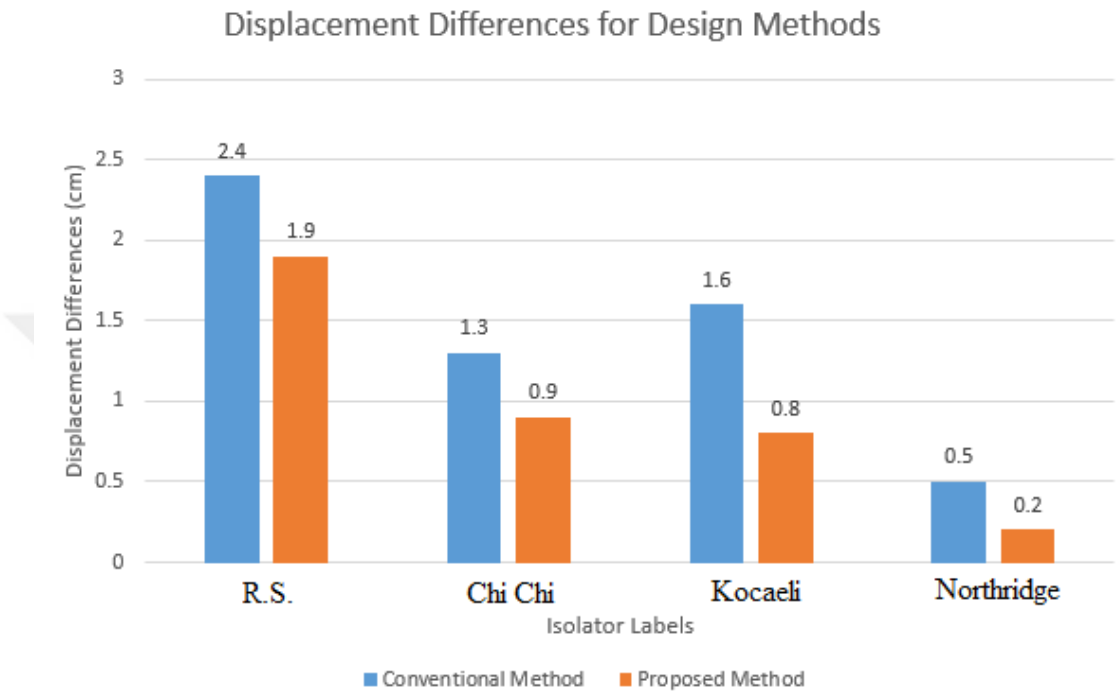


Figure 43. Displacement differences between the isolators for each seismic input

As stated and looking at the results of Figure 43, displacement uniformity is higher at the system designed with proposed method, which increases the effectiveness of base isolation system. The uniformity can be seen from the displacement differences and the shears on isolators.

In Table 88, displacement differences of these isolators and difference over maximum displacement ratios are shown.

Table 88. Displacement differences of corner isolators at two design methods

	Methods	Min	Max	Difference	%
Response Spectra	Conv.	34.3	36.7	2.4	7
	Thesis	38.8	40.7	1.9	5
Chi Chi	Conv.	20.1	21.4	1.3	6
	Thesis	24.7	25.6	0.9	4
Kocaeli	Conv.	19.2	20.8	1.6	8
	Thesis	21.6	22.4	0.8	4
Northridge	Conv.	13.5	14	0.5	4
	Thesis	13.9	14.1	0.2	1

To prove and develop the results obtained, when the isolators designed with Q/W ratio as 0.1 in conventional method, same comparison of two design methods was carried out below.

Shear forces and total maximum displacements of isolators designed with both conventional and proposed methods are shown in Table 89.

Table 89. Displacements and shear forces of isolators analyzed with response spectrum

		Conventional			Proposed	
	Definition	SC1	SC2	SC3	STI	STO
2.5%	D_{TM} (cm)	31.7	33.7	32.8	35.4	37.4
	V (ton)	15.0	25	41.3	15.2	33.4
5.0%	D_{TM} (cm)	33.2	36.9	35.1	36.8	40.7
	V (ton)	15.5	26.8	43.7	15.7	35.6
7.5%	D_{TM} (cm)	34.8	40.0	37.5	38.4	43.9
	V (ton)	16.0	28.8	45.3	16.2	37.7
10.0%	D_{TM} (cm)	36.1	42.5	39.3	39.6	46.2
	V (ton)	16.5	29.6	46.4	16.5	38.9

As in the Table 89, displacements are higher in proposed method because of the spectral displacement curve. However, maximum shear forces were again obtained on the systems designed with conventional method again. Hence, that more uniformity on shear force distribution to isolators was obtained in proposed method is proved when Q/W ratio and yielding force for isolators were selected 0.1 and 0.025 meters respectively. Corner isolator displacements were also noted for isolators designed with Q/W ratios as 0.1 in conventional method. This comparison is shown in Table 90.

Table 90. Corner isolator displacements of two design methods

	Methods	1	2	3	4
2.5%	Conventional, D_{TM} (cm)	32.2	33.6	33.7	33.5
	Proposed, D_{TM} (cm)	37.4	37.3	36.2	37.3
5.0%	Conventional, D_{TM} (cm)	34.5	36.8	36.9	36.8
	Proposed, D_{TM} (cm)	40.7	40.5	38.8	40.4
7.5%	Conventional, D_{TM} (cm)	37.1	39.9	39.9	40
	Proposed, D_{TM} (cm)	43.9	43.6	41.7	43.5
10.0%	Conventional, D_{TM} (cm)	39.2	42.2	42.2	42.5
	Proposed, D_{TM} (cm)	46.2	45.6	43.9	45.6

Moreover, as stated, stiffness eccentricity was considered by removing shear walls at the right side of the plan. When stiffness eccentricity was given to systems, modal analysis results for two design method are shown in Table 91.

Table 91. Modal results for asymmetric systems (stiffness eccentricity) for each design method

	Modal Results								
	Modes	Conventional Method				Proposed Method			
		Period sec	Participating Mass Ratio %			Period sec	Participating Mass Ratio %		
			X	Y	Torsion		X	Y	Torsion
Default	1	2.51	0	2	98	2.49	0	31	69
	2	2.34	0	98	2	2.45	0	69	31
	3	2.33	100	0	0	2.44	100	0	0
2.5%	1	2.54	1	7	92	2.54	5	33	62
	2	2.35	23	74	3	2.47	68	30	2
	3	2.34	75	19	6	2.44	27	37	36
5.0%	1	2.59	4	11	85	2.6	10	31	59
	2	2.38	47	52	1	2.49	63	36	1
	3	2.35	49	37	14	2.43	26	33	41
7.5%	1	2.66	7	14	78	2.67	12	31	57
	2	2.41	52	47	1	2.51	61	38	1
	3	2.36	41	39	20	2.42	27	32	41
10.0%	1	2.72	9	16	75	2.72	15	28	57
	2	2.43	54	45	1	2.53	58	41	1
	3	2.36	37	38	35	2.42	27	31	42

Isolator displacements and shear forces for systems designed with both design method when stiffness eccentricity was given to building are shown in Table 92. In addition to stiffness eccentricity, as in previous cases, mass eccentricities were given step by step to compare the behavior of isolators.

Table 92. Displacements and shear forces of isolators on stiffness eccentricity cases

		Conventional			Proposed	
	Definition	SC1	SC2	SC3	STI	STO
Default	D_{TM} (cm)	30.4	30.4	30.4	33.7	33.7
	V (ton)	14.7	24.8	40.3	14.4	31.5
2.5%	D_{TM} (cm)	31.9	34.5	32.8	35.9	38.0
	V (ton)	15.3	26.8	42.1	15.1	33.9
5.0%	D_{TM} (cm)	33.3	38.4	35.1	36.2	40.9
	V (ton)	15.7	28.2	43.8	15.4	35.7
7.5%	D_{TM} (cm)	35.1	41.5	37.4	37.7	44.2
	V (ton)	16.2	29.6	45.6	15.9	37.9
10.0%	D_{TM} (cm)	36.2	43.4	38.9	38.6	45.9
	V (ton)	16.4	30.3	46.4	16.1	38.6

Maximum displacements of corner isolators (1, 2, 3 and 4) for both design methods when stiffness eccentricity was given are shown in Table 93.

Table 93. Corner isolator displacement of two design methods at stiffness eccentricity cases

	Methods	1	2	3	4
Default	Conventional, D_{TM} (cm)	30.4	30.4	32.4	32.4
	Proposed, D_{TM} (cm)	33.7	33.7	34.5	34.5
2.50%	Conventional, D_{TM} (cm)	31.6	33.3	35.5	35.5
	Proposed, D_{TM} (cm)	36.9	36.9	37.8	38
5.00%	Conventional, D_{TM} (cm)	33.3	36.2	38.2	38.4
	Proposed, D_{TM} (cm)	39.7	39.5	40.5	40.9
7.50%	Conventional, D_{TM} (cm)	35.7	39.2	41.1	41.5
	Proposed, D_{TM} (cm)	42.7	42.3	43.5	44.2
10.00%	Conventional, D_{TM} (cm)	37.6	41.2	42.9	43.4
	Proposed, D_{TM} (cm)	44.4	44.1	45	45.9

Furthermore, displacement differences of the corner isolators are shown in Table 94 to consider and compare the effectiveness of both design methods.

Table 94. Displacement differences of isolators at stiffness eccentricity cases

	Methods	Min	Max	Difference	%
Default	Conventional, D_{TM} (cm)	30.4	32.4	2	6
	Proposed, D_{TM} (cm)	33.7	34.5	0.8	2
2.5%	Conventional, D_{TM} (cm)	31.6	35.5	3.9	11
	Proposed, D_{TM} (cm)	36.9	38	1.1	3
5.0%	Conventional, D_{TM} (cm)	33.3	38.4	5.1	13
	Proposed, D_{TM} (cm)	39.5	40.9	1.4	3
7.5%	Conventional, D_{TM} (cm)	35.7	41.5	5.8	14
	Proposed, D_{TM} (cm)	42.3	44.2	1.9	4
10.0%	Conventional, D_{TM} (cm)	37.6	43.4	5.8	13
	Proposed, D_{TM} (cm)	44.1	45.9	1.8	4

As it can be seen from Table 94, although displacements are higher in proposed method due to spectral displacement curve, displacement differences of corner isolators are less in proposed method at stiffness eccentricity cases, as well. This means as expected, proposed method gives more uniform displacemet distributions and thus, increases the effectiveness of base isolation system in mass and stiffness eccentricity cases.

4.2 DISCUSSIONS

When results of the systems were examined, to increase the effectiveness of base isolation on a torsionally unrestrained system, the stiffnesses of outer isolators were increased and inner isolators were decreased. Then, a torsionally restrained system was obtained and lead-rubber bearings were designed according to the proposed method. Formulation stating the stiffness ratio of the outer and inner isolators was as in Equation (3.4).

$$(K_O / K_I) = 0.1 - 0.12*(D_O / D_I) + 1.21*(W_O / W_I) + 1.95*(T^2 / T_{translational}T_{assumed})$$

After arranging the stiffnesses of isolators, system became strong in torsion. After designing symmetric (default) system with conventional approach and proposed method separately, behaviors of systems were examined under 4 different level of mass eccentricities and additional stiffness eccentricity cases.

Modal analyses results showed that the torsionally restrained system started to be torsionally unrestrained systems as eccentricity levels increase for proposed method. Furthermore, target periods increase as mass eccentricity increases.

Floor accelerations of symmetric systems were calculated with response spectrum analysis. Looking the results, accelerations are lower at the cases designed with proposed method at DBE and MCE. This was resulted from the target translational periods reached. In both systems, conventional design method could not get the target periods in translational modes. These modes were calculated lower than target periods, so as expected, accelerations were calculated higher at the systems designed with conventional method. Moreover, because the target translational periods were higher in proposed method, displacements were higher for all symmetrical and asymmetrical systems, as well (Figures 39 and 40).

Base shears differ as seismic input changes for each case. When Chi Chi earthquake that gave the higher results when compared with other earthquakes is considered, in symmetrical systems, base shears are higher for response spectrum analysis in conventional method and lower for ChiChi earthquake again in same method. However, base shear differences are negligibly low. On the other hand, in asymmetric systems, base shears are lower in response spectrum analysis and Chi Chi earthquake in conventional method but, again differences are negligibly low. That base shear changes can be explained by different energy dissipiations of designed isolators calculated from the hysteresis loops. Nevertheless, when considering the force – period relation principles of the response spectrum curve, at the beginning of the designs, to get lower shear forces or floor accelerations, using proposed method is more logical. Moreover, looking the shear forces on isolators, maximum shear forces occur on the systems designed with conventional method (Tables 80 and 87). Despite the closer base shears, higher shear forces on isolators designed with conventional method show

that the base shear is distributed to isolators in more uniform way for the systems designed with proposed method.

Since the torsional stiffnesses of the systems designed with proposed method is higher, base torques are higher at these systems, as expected. In other words, that the torsional stiffness was increased using proposed method resulted in higher torsional forces at the base. However, again that difference is negligibly low for both design method. Furthermore, while proposed method is providing higher torsional stiffnesses, it makes the system show more uniform displacements. Displacements of the isolators relatively less for whole eccentricities, as well (Tables 85, 88 and 94). Hence, effectiveness of the base isolation system increases. Moreover, looking the eccentricity levels, ratio of displacement difference over maximum displacement increases as eccentricities increase (Table 85, 88 and 94). At each level of eccentricity, proposed method shows better results when compared to conventional method. This relation shows that using conventional method in asymmetric systems decrease the effectiveness of the base isolation system when compared to proposed method.

Asymmetries were given with mass and stiffness eccentricities to compare all of the cases together. Moreover, conventional design method was applied with two cases ($Q/W = 0.1$ and as in [11]). All results showed that proposed method gives more uniformity in base shears to isolators because maximum shear forces were obtained in conventional method. Similarly, uniformity showed itself in displacement distribution also, as mentioned. Thus, asymmetries in the system can be obtained by mass and stiffness eccentricity and proposed method gives more effective base isolation systems for all of the cases.

CHAPTER 5

CONCLUSIONS

There are many studies which discuss the torsional behavior of seismically isolated structures for different level of eccentricities. They are mainly focused on isolator displacements on these systems. Eccentricities of the structures were applied in terms of mass and structural for different types of structures.

In this study, isolator behaviors with different isolator distributions in both symmetrical and asymmetrical systems were examined. Effectiveness of the base isolation system was tried to increase under torsional amplifications. Structure was selected as torsionally unrestrained system in fixed-base case. Moreover, the building was modelled with conventional and a new design methods using lead-rubber bearings. Then, providing different mass and stiffness eccentricities, behaviors of the isolators were examined. In conventional method, after seismic isolation, system stayed at torsionally unrestrained case again. However, to overcome this issue, new design method was developed and applied to the systems. Analyses were done in real type structure. Comparing the results of two design methods, conventional and proposed, in symmetrical and asymmetrical systems, statements below can be made:

- If a fixed-base structure has a torsionally unrestrained system, isolating it from base with the conventional method does not prevent the unrestrained case. In other words, designing isolators according to the axial loads on them at the

beginning is not a proper method and the first mode stays in torsion again, even it is seismically isolated.

- To make system strong in torsion and obtain it torsionally restrained after isolation, instead of conventional method, a new method developed in this study can be used. Especially codes suggest that systems should be torsionally restrained. Thus, by the help of this new method, outer isolators are strengthened up to a point that translational modes are dominant over the torsional mode.

- Looking the parameters of the formulation of new design method, each parameter shows a linear relation with the stiffness ratio of inner and outer isolators. After multilinear regression analysis, efficiency of the formulation proved with the results. In the proposed method, formula gives an estimated stiffness ratio at the beginning. Then, some arrangements such as increasing the stiffnesses of outer isolators or decreasing the stiffnesses of inner isolators can be done on isolators at the next iterations to get torsionally restrained structure at the target period for translational fundamental mode.

- In conventional method, when designing a torsionally unrestrained structure with lead-rubber bearings, assumed period can not be reached with translational modes. First mode of the system comes torsional at the target period. Translational modes which take the seismic loadings from spectrum, result in a period smaller than the target period. Thus, undesired shear forces can be obtained. Moreover, this phenomenon decreases the effectiveness of seismic base isolation for these kind of structures because base shear distribution to isolators shows less uniformity in conventional method (Tables 80 and 87).

- Torsionally unrestrained structures show brittle behavior because they are weak in torsion. This behavior is not a desired case, especially in codes.

Furthermore, looking the base reactions, systems designed with the proposed method show negligibly higher torques for all seismic inputs, as expected. That proves the necessity of torsional strengthening of systems.

- When two design methods were carried out in their own process, proposed method gave higher displecements at common specific isolators in all cases. This is resulted from gathering the translational modes in the target period in proposed method. Because torsional mode is at first in conventional method, translational modes are smaller than the targeted one. Hence, displacements are lower in conventional method because of the spectral displacement curve.

- In asymmetric systems by mass eccentricities, in accordance with the previous studies about torsional response of base isolation systems, isolators closer to the mass center show higher displacements when compared with the isolators farther from. However, this is valid only for the system torsionally restrained (designed with proposed method). On the other hand, as stated in previous studies, this study also showed that isolators closer to mass center can have greater or smaller displacements from farther ones in torsionally unrestrained systems.

- Looking the results, in addition to the torsional amplifications, as isolated period over fixed-base period ratio (T_I/T_F) increases, displacements of the isolation system increase, as well. Increasing mass eccentricity cases cause this relation. As mass eccentricity increases, isolated period of base isolation system increases, as well. Thus, displacements of base isolation system increase.

- When comparing the total displacements of corner isolators (1, 2, 3 and 4) in asymmetric systems for all seismic inputs, it can be seen that displacement differences are higher in the system designed with conventional method. As

stated in previous studies, due to torsional amplifications, displacement differences between the corner isolators increase. That decreases the effectiveness of the base isolation system. Besides, at each mass and stiffness eccentricity level, proposed method gives more effective base isolation system. Thus, to reach a system that has lower total displacement differences between the isolators, proposed method should be used. By the help of increasing torsional rigidity of structure, isolators show uniformity in displacements, which makes more effective base isolation system.

In conclusion, if a structure is torsionally unrestrained and base isolation with lead-rubber bearings is applied to system, to get a more effective base isolation system, lower base shears or floor accelerations and increase torsional rigidity, instead of conventional design method, the author of this study believes that the system should be designed with the method developed in this study.

Recommendations for Future Work

Comparison of two design method, conventional and proposed, can be applied for the systems having superstructural eccentricities only, instead of mass eccentricities. Although previous studies showed that the superstructural eccentricities do not affect the isolator behavior significantly, that behavior can be examined for the systems designed for these methods.

Conventional and proposed method can be compared for new torsionally unrestrained systems having much more column or axes. Effectiveness of the proposed method can be proved for those systems with more outer isolators to provide torsionally restrained system.

Moreover, buildings that are torsionally restrained at fixed-base case can be studied for both design method. Formulation in proposed method can not be used because system is torsionally restrained already. However, stiffnesses of outer isolators can be increased and inner isolators can be decreased as in proposed method. Then, the effectiveness of systems designed with conventional and proposed method can be compared for different eccentricity levels.

REFERENCES

[1] Jangid, R. S., *Seismic Response of an Asymmetric Base Isolated Structure*, Computers and Structures, Vol. 60, No. 2, Elsevier Science Ltd., pp. 261-267, Great Britain, 1996.

[2] Tena-Colunga, A., Gomez-Soberon, L., *Torsional Response of Base-Isolated Structures due to Asymmetries in the Superstructure*, Engineering Structures 24, Elsevier Ltd., pp. 1587-1599, 2002.

[3] Tena-Colunga, A., Escamilla-Cruz, J. L., *Torsional Amplifications in Asymmetric Base-Isolated Structures*, Engineering Structures 29, Elsevier Ltd., pp. 237-247, 2007.

[4] Kilar, V., Koren, D., *Seismic Behaviour of Asymmetric Base Isolated Structures with Various Distributions of Isolators*, Engineering Structures 31, Elsevier Ltd., pp. 910-921, 2009.

[5] Wolff, E. D., Ipek, C., Constantinou, M. C., Morillas, L., *Torsional Response of Seismically Isolated Structures*, Engineering Structures 59, Elsevier Ltd., pp. 462-468, San Diego, CA, 2013.

[6] ASCE, "Standard ASCE/SEI 7-10", *Minimum Design Loads for Buildings and Other Structures*, American Society of Civil Engineers, Reston, Virginia, 2010.

[7] Zayas V. A., Low S. S., Mahin S. A., *The FPS earthquake resisting system experimental report*, Report No. UCB/EERC-87-01. Earthquake Engineering Research Center, University of California, Berkeley, 1987.

[8] Wolff E. D., Constantinou M. C., *Experimental study of seismic isolation systems with emphasis on secondary system response and verification of accuracy of dynamic response history analysis methods*, Report No. MCEER-04-0001. Multidisciplinary Center for Earthquake Engineering Research, Buffalo, NY, 2004.

[9] Deformations of Conventional vs Isolated Structures, http://www.moriliving.com/en/estate/residence/arkforest/services, last visited on 18.06.2016.

[10] Effects of Increasing Period and Damping on the Demands of Acceleration and Displacement, http://file.scirp.org/Html/1-2740066_52406.htm, last visited on 18.06.2016.

[11] Naeim, F., Kelly, J. M., *Design of Seismic Isolated Structures*, John Wiley & Sons, Inc, Canada, 1999.

[12] Fire Command and Control Facility, Los Angeles, California, http://the-accelerometer.blogspot.com.tr/2015_06_28_archive.html, last visited on 19.06.2016.

[13] Los Angeles City Hall, https://en.wikipedia.org/wiki/Los_Angeles_City_Hall, last visited on 19.06.2016.

[14] *Conference of Providing Earthquake Safety of Structures by Seismic Isolations*, İmaj Ofset Reklam Sanayi Tic. Ltd. Şti., İstanbul, 2005.

[15] Skinner, R. I., Robinson, W. H., McVerry, G. H., *An Introduction to Seismic Isolation*, John Wiley & Sons, Ltd., Baffins Lane, Chishester, West Sussex PO19 IUD, England, 1993.

[16] An Example of a High-Damping Natural Rubber Bearing, http://www.mageba.com.tr/tr/794/Altyap/Sismik-koruma/Yapi-izolasyonu/LASTO-HDRB/Detail.htm, last visited on 20.06.2016.

[17] An Example of a Lead-Rubber Bearing, http://www.taiwanpillar.com.tw/en/about.php?mode=3&id=14, last visited on 20.06.2016.

[18] Özkaya, C., *Seismic Isolation Systems and Design Fundamentals Seminar*, Chamber of Civil Engineers, Ankara, 2015.

[19] An Example of a Friction Pendulum System, http://file.scirp.org/Html/3-1880089_32273.htm, last visited on 21.06.2016.

[20] Kelly, J. M., "Base Isolation: Linear Theory and Design", *Earthquake Spectra*, Vol. 6, No. 2, pp. 223-244, 1990.

[21] Kelly, J. M., "Lecture Notes", *Seismic Base Isolation: Extension of Theory to Buildings*, University of California at Berkeley, California.

[22] Akyüz, U., "Lecture Notes", *Seismic Base Isolation*, Middle East Technical University, Ankara, 2015.

[23] International Conference of Building Officials, "Earthquake Regulations for Seismic-Isolated Structures", *Uniform Building Code*, Whittier, CA, 1997.

[24] *Turkish Earthquake Code*, Turkish Standards Institute, 2007.

[25] Ersoy, U., Özcebe, G., Tankut, T., *Reinforced Concrete*, METU Press, Ankara, 1984.

[26] T.C. İstanbul Büyükşehir Belediyesi, “Eyüp Güzeltepe Sosyal Konut Projesi”, *Architectural Project*, Yüksel Proje.

[27] T.C. İstanbul Büyükşehir Belediyesi, “Eyüp Güzeltepe Sosyal Konut Projesi”, *Reinforced-Concrete Application Project*, Yüksel Proje.

[28] Sucuoğlu, H., Akkar, S., *Basic Earthquake Engineering: From Seismology to Analysis and Design*, Ankara, 2014.

[29] Erdik, M., Şeşetyan, K., Demircioğlu, M. B., Durukal, E., *Earthquake Hazard Assessment*, Bogazici University Kandilli Observatory and Earthquake Research Institute, Istanbul, 2006.

APPENDICES

APPENDIX A

BILINEAR MODELS OF THE LEAD-RUBBER BEARINGS DEFINED IN SAP2000 FOR EACH SYSTEM

In this part, biliniear models of the lead-rubber bearings are shown. Lateral bilinear force versus displacement graphs defined in SAP2000 for each system are illustrated. Units are in kN and meter.

Conventional Method according to Kelly [11]

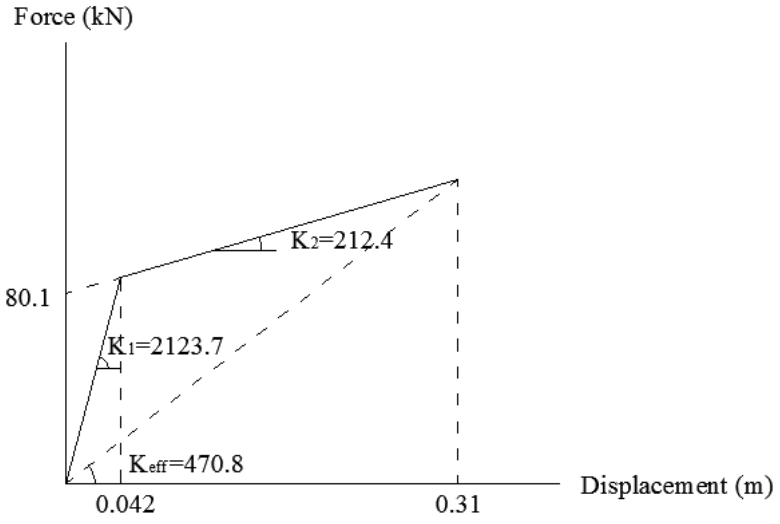


Figure 44. Lateral bilinear model of SC1

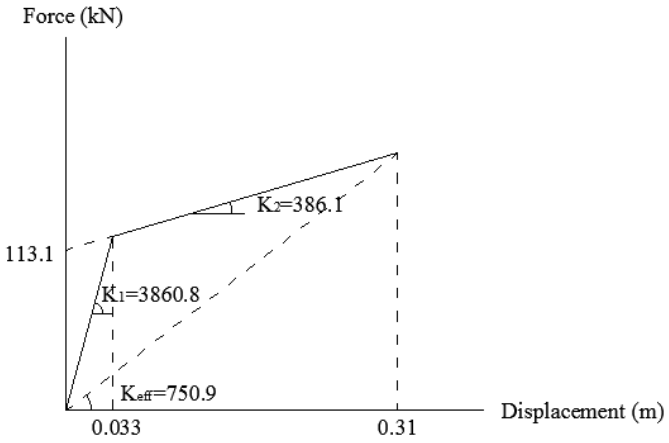


Figure 45. Lateral bilinear model of SC2

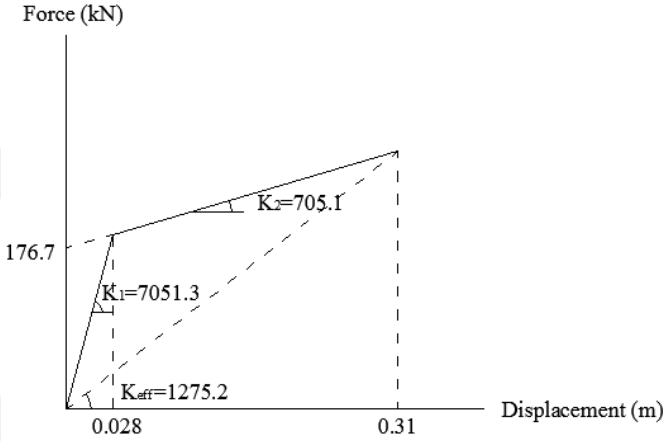


Figure 46. Lateral bilinear model of SC3

Conventional Method (Q/W=0.1)

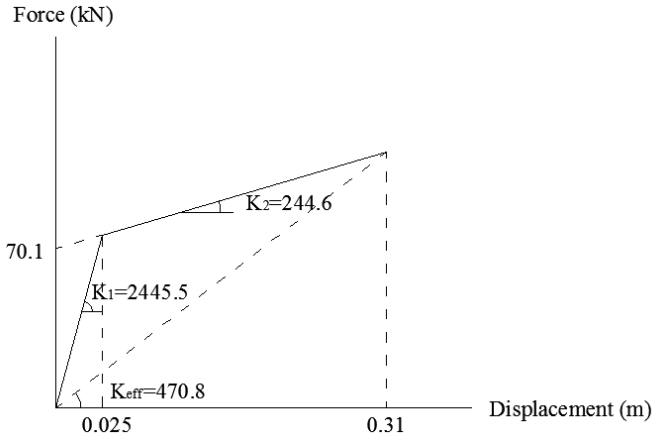


Figure 47. Lateral bilinear model of SC1

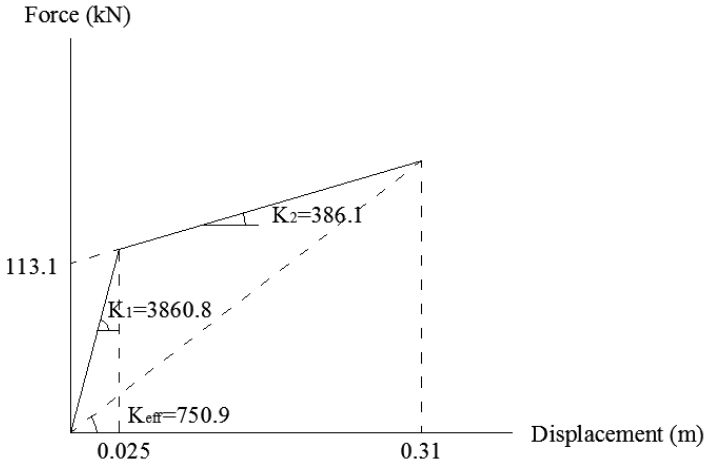


Figure 48. Lateral bilinear model of SC2

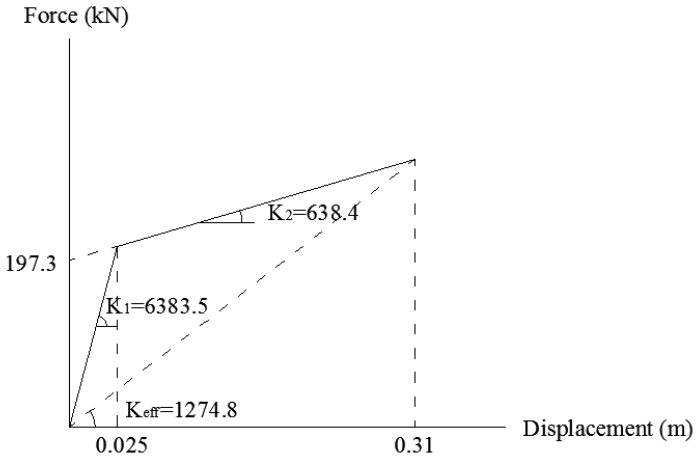


Figure 49. Lateral bilinear model of SC3

Proposed Method

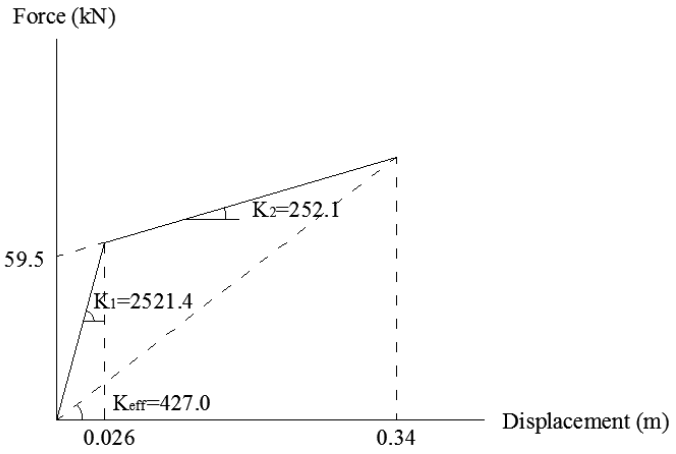


Figure 50. Lateral bilinear model of STI

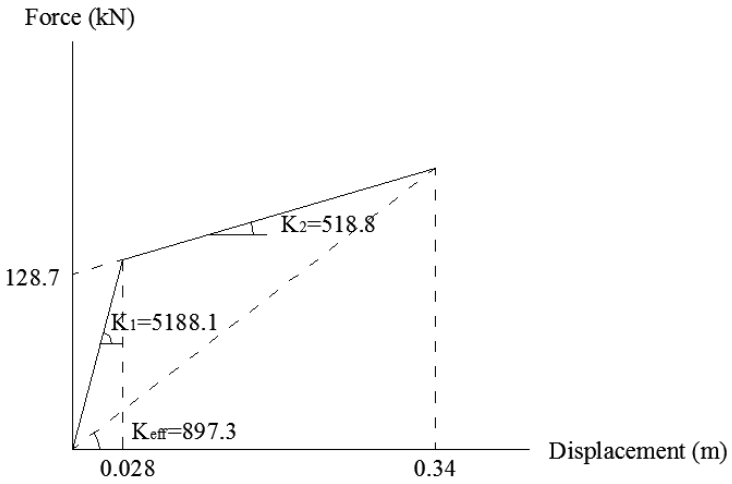


Figure 51. Lateral bilinear model of STO

APPENDIX B

DESIGN CALCULATION DETAILS OF ISOLATORS

Design calculations of SC1

Calculations at the final stage and design checks are shown through Tables 95 to 99. Shear modulus of SC1 was selected 0.4 GPa.

Table 95. Design calculations of SC1 in symmetric case

HORIZONTAL PARAMETERS				
Effective Stiffness			Max Displacement	
K_{eff} (kN/m)		471	D_{TM} (m)	0.31
Total Rubber Thickness, t_r (m)				0.31
Total Rubber Thickness to be Used, t_r (m)				0.4
W_M kN.m	Q kN	K_2 (Kp) kN/m	K_1 kN/m	D_y m
81.053	65.3653	260.144	2601.44	0.02792
Final	73.7156	233.208	2332.08	0.03512
Yield Strength of Lead, f_{py} (MPa)				10
Lead Core Area, A_p (cm^2)				73.7156
Lead Core Diameter, d_p (cm)				9.68801
Lead Core Diameter to be Used, d_p (cm)				10.1
Lead Core Area to be Used, A_p (cm^2)				80.1185
W_M* kN.m	Q* kN	K_2* (Kp*) kN/m	K_1* kN/m	D_y* m
85.9135	80.1185	212.372	2123.72	0.04192
New K_{eff}* (kN/m)				470.818
New β_{eff}* (%)				30.2207

Table 96. Design calculations of SC1 in symmetric case

BEARING DIMENSIONS FROM A_0, A_1, A_2			
Determination of A_0 Based on Allow. Stress for Vertical Load			
$P_{DL+LL} / A_0 = \sigma_c$ (MPa) <=	7.8	A_0 (m^2)	0.09307
Determination of A1 from Shear Strain due to Vertical Load			
$\Upsilon_c = 6S\xi_c = 6S(P_{DL+LL}/EcA1) <= \xi b/3$		A_1 (m^2)	0.05445
		A_1* (m^2)	0.08376
Determination of A_2 from Elastic Modulus & Shear Failure			
$K_p = K_e*[1+12*(A_p/A_0)]$		K_e (kN/m)	114.71
		K_e* (kN/m)	104.461
$K_e*t_r/G = A_{sf}$ (m2)	0.11471	Diameter, d (m)	0.38217
$K_e*t_r/G = A_{sf}$* (m2)	0.10446	Diameter, d (m)	0.3647
$A_2 = B*(B-D_{TM})$ or $A_2 = d^2*(\beta-\sin\beta)/4$		A_2 (m^2)	0.01097
		A_2*(m^2)	0.00712
		A_2**(m^2)	0.06131
Bearing Area from A_0, A_1, A_2		A (m^2)	0.09307
Bearing Diameter, d (cm)		34.42374544	
Bearing Diameter to be Used, d (cm)		52	
Bearing Area to be Used, A (cm^2)		2123.716634	

Table 97. Design calculations of SC1 in symmetric case

ISOLATOR ELEMENT DETAILS	
Single Layer Thickness of a Circular Pad, t (cm)	0.65
Single Layer Thickness to be Used, t (cm)	1
New Shape Factor, S	13
Reselected Compression Modulus, E_C* (MPa)	405.6
Number of Single Rubber Layer	40
Single Steel Plate Thickness, t_s (mm) > 2 mm	2.16272
Single Steel Plate Thickness to be Used, t_s (mm)	2.6
Cover Steel Plate Thicknesses, tc (mm)	30
Effective Height of the Lead Core, H_p (cm)	50.14
H_p / d_p Ratio	4.96436
Lead Core Dimension Situation $1.25 <= H_p/d_p <= 5.0$	OK
Total Height of the Isolator, H (cm)	56.14

Table 98. Design calculations of SC1 in symmetric case

SELECTION OF SHAPE FACTOR			
$K_V/K_H > 400$	$6S^2 > 400$	$S > 8.165$ (S>10)	
S to be Used, S	20	Bearing Type	Circular
Compression Modulus, E_C (MPa)			960

Table 99. Design checks of SC1 in symmetric case

SHEAR STRAIN AND STABILITY CONDITIONS		
SHEAR STRAIN CONDITION		
$\Upsilon_c = 6S\xi_c = 6S(P_{DL+LL}/E_cA) <= \xi b/3$	Υ_c	0.65736
	Status	OK
STABILITY CONDITION - STATIC		
Stress due to Axial Load on the Pad, σ_c (MPa)		3.41825
Critical Stress Against Buckling, σ_{crit} (MPa)		7.50847
Stability Status		OK
STABILITY CONDITION - DYNAMIC		
Shear Strain due to Compression, Υ_c		1.2703
Shear Strain due to Earthquake Load, Υ_{eq}		0.775
Rotation Angle due to Earthquake, θ		0.00553
Shear Strain due to Rotation, Υ_{sr}		0.18703
Total Strain, Υ_{total}		2.23232
Stability Status		OK

Thus, SC1 is a lead-rubber bearing with bearing diameter of 52 cm, lead core diameter of 10.1 cm and a total height of 56.14 cm. Moreover, SC1 has a vertical effective stiffness of 215345 kN/m.

Design calculations of SC2

Calculations at the final stage and design checks are shown through Table 100 to 104. Shear modulus of SC2 was selected as 0.7 GPa.

Table 100. Design calculations of SC2 in symmetric case

HORIZONTAL PARAMETERS				
Effective Stiffness			Max Displacement	
K_{eff} (kN/m)		751	D_{TM} (m)	0.31
Total Rubber Thickness, t_r (m)				0.31
Total Rubber Thickness to be Used, t_r (m)				0.4
W_M kN.m	Q kN	K_2 (K_p) kN/m	K_1 kN/m	D_y m
122.435	98.7382	432.49	4324.9	0.02537
Final	109.558	397.586	3975.86	0.03062
Yield Strength of Lead, f_{py} (MPa)				10
Lead Core Area, A_p (cm2)				109.558
Lead Core Diameter, d_p (cm)				11.8108
Lead Core Diameter to be Used, d_p (cm)				12
Lead Core Area to be Used, A_p (cm^2)				113.097
W_M* kN.m	Q* kN	K_2* (K_p*) kN/m	K_1* kN/m	D_y* m
125.516	113.097	386.082	3860.82	0.03255
New K_{eff}* (kN/m)				750.912
New β_{eff}* (%)				27.6826

Table 101. Design calculations of SC2 in symmetric case

ISOLATOR ELEMENT DETAILS	
Single Layer Thickness of a Circular Pad, t (cm)	0.6625
Single Layer Thickness to be Used, t (cm)	1
New Shape Factor, S	13.25
Reselected Compression Modulus, E_C* (MPa)	737.363
Number of Single Rubber Layer	40
Single Steel Plate Thickness, t_s (mm) > 2 mm	3.76002
Single Steel Plate Thickness to be Used, t_s (mm)	4
Cover Steel Plate Thicknesses, t_c (mm)	30
Effective Height of the Lead Core, H_p (cm)	55.6
H_p / d_p Ratio	4.63333
Lead Core Dimension Situation 1.25 <= H_p/d_p <= 5.0	OK
Total Height of the Isolator, H (cm)	61.6

Table 102. Design calculations of SC2 in symmetric case

BEARING DIMENSIONS FROM A_0, A_1, A_2			
Determination of A0 Based on Allow. Stress for Vertical Load			
$P_{DL+LL} / A_0 = \sigma_c$ (MPa) <=	7.8	A_0 (m^2)	0.17482
Determination of A1 from Shear Strain due to Vertical Load			
$\Upsilon_c = 6S\xi c = 6S(P_{DL+LL}/E_cA_1) <= \xi b/3$		A_1 (m^2)	0.05844
		A_1* (m^2)	0.08821
Determination of A_2 from Elastic Modulus & Shear Failure			
$K_p = K_e*[1+12*(A_p/A_0)]$		K_e (kN/m)	223.825
		K_e* (kN/m)	217.349
$K_e*t_r/G = A_{sf}$ (m^2)	0.1279	Diameter, d (m)	0.40354
$K_e*t_r/G = A_{sf}$* (m^2)	0.1242	Diameter, d (m)	0.39766
$A_2 = B*(B-D_{TM})$ or $A_2 = d^2*(\beta-\sin\beta)/4$		A_2 (m^2)	0.01653
		A_2*(m^2)	0.01491
		A_2**(m^2)	0.06624
Bearing Area from A_0, A_1, A_2		A (m^2)	0.17482
Bearing Diameter, d (cm)		47.17910107	
Bearing Diameter to be Used, d (cm)		53	
Bearing Area to be Used, A (cm^2)		2206.183441	

Table 103. Design checks of SC2 in symmetric case

SHEAR STRAIN AND STABILITY CONDITIONS		
SHEAR STRAIN CONDITION		
$\Upsilon_c = 6S\xi c = 6S(P_{DL+LL}/E_cA) <= \xi b/3$	Υ_c	0.66639
	Status	OK
STABILITY CONDITION - STATIC		
Stress due to Axial Load on the Pad, σ_c (MPa)		6.18076
Critical Stress Against Buckling, σ_{crit} (MPa)		13.6501
Stability Status		OK
STABILITY CONDITION - DYNAMIC		
Shear Strain due to Compression, Υ_c		1.14581
Shear Strain due to Earthquake Load, Υ_{eq}		0.775
Rotation Angle due to Earthquake, θ		0.00553
Shear Strain due to Rotation, Υ_{sr}		0.19429
Total Strain, Υ_{total}		2.1151
Stability Status		OK

Table 104. Design calculations of SC2 in symmetric case

SELECTION OF SHAPE FACTOR			
$K_V/K_H > 400$	$6S^2 > 400$	$S > 8.165$ (S>10)	
S to be Used, S	20	Bearing Type	Circular
Compression Modulus, E_C (MPa)			1680

Hence, SC2 is a lead-rubber bearing with bearing diameter of 53 cm, lead core diameter of 12 cm and a total height of 61.6 cm. Moreover, SC2 has a vertical effective stiffness of 406689 kN/m.

Design calculations of SC3

Calculations at the final stage and design checks are shown through Table 105 to 109. Shear modulus of SC3 was selected as 0.8 GPa.

Table 105. Design calculations of SC3 in symmetric case

HORIZONTAL PARAMETERS				
Effective Stiffness			Max Displacement	
K_{eff} (kN/m)		1275	D_{TM} (m)	0.31
Total Rubber Thickness, t_r (m)				0.31
Total Rubber Thickness to be Used, t_r (m)				0.4
W_M kN.m	Q kN	K_2 (K_p) kN/m	K_1 kN/m	D_y m
184.767	149.006	794.336	7943.36	0.02084
Final	161.379	754.424	7544.24	0.02377
Yield Strength of Lead, f_{py} (MPa)				10
Lead Core Area, A_p (cm^2)				161.379
Lead Core Diameter, d_p (cm)				14.3344
Lead Core Diameter to be Used, d_p (cm)				15
Lead Core Area to be Used, A_p (cm^2)				176.715
W_M* kN.m	Q* kN	K_2* (K_p*) kN/m	K_1* kN/m	D_y* m
199.443	176.715	705.13	7051.3	0.02785
New K_{eff}* (kN/m)				1275.18
New β_{eff}* (%)				25.9027

Table 106. Design calculations of SC3 in symmetric case

BEARING DIMENSIONS FROM A_0, A_1, A_2			
Determination of A0 Based on Allow. Stress for Vertical Load			
$P_{DL+LL} / A_0 = \sigma_c$ (MPa) <=	7.8	A_0 (m^2)	0.34964
Determination of A1 from Shear Strain due to Vertical Load			
$\Upsilon_c = 6S\xi c = 6S(P_{DL+LL}/E_cA_1)$ <= $\xi b/3$		A_1 (m^2)	0.10227
		A_1* (m^2)	0.12211
Determination of A_2 from Elastic Modulus & Shear Failure			
$K_p = K_e*[1+12*(A_p/A_0)]$		K_e (kN/m)	469.606
		K_e* (kN/m)	438.922
$K_e*t_r/G = A_{sf}$ (m^2)	0.2348	Diameter, d (m)	0.54677
$K_e*t_r/G = A_{sf}$* (m^2)	0.21946	Diameter, d (m)	0.52861
$A_2 = B*(B-D_{TM})$ or $A_2 = d^2*(\beta-\sin\beta)/4$		A_2 (m^2)	0.07488
		A_2*(m^2)	0.06554
		A_2**(m^2)	0.15253
Bearing Area from A_0, A_1, A_2		A (m^2)	0.34964
Bearing Diameter, d (cm)		66.7213246	
Bearing Diameter to be Used, d (cm)		67	
Bearing Area to be Used, A (cm^2)		3525.652355	

Table 107. Design calculations of SC3 in symmetric case

ISOLATOR ELEMENT DETAILS	
Single Layer Thickness of a Circular Pad, t (cm)	0.8375
Single Layer Thickness to be Used, t (cm)	1
New Shape Factor, S	16.75
Reselected Compression Modulus, E_C* (MPa)	1346.7
Number of Single Rubber Layer	40
Single Steel Plate Thickness, t_s (mm) > 2 mm	3.26559
Single Steel Plate Thickness to be Used, t_s (mm)	3.5
Cover Steel Plate Thicknesses, t_c (mm)	30
Effective Height of the Lead Core, H_p (cm)	53.65
H_p / d_p Ratio	3.57667
Lead Core Dimension Situation 1.25 <= H_p/d_p <= 5.0	OK
Total Height of the Isolator, H (cm)	59.65

Table 108. Design calculations of SC3 in symmetric case

SELECTION OF SHAPE FACTOR			
$K_V/K_H > 400$	$6S^2 > 400$	$S > 8.165$ (S>10)	
S to be Used, S	20	Bearing Type	Circular
Compression Modulus, E_C (MPa)			1920

Table 109. Design checks of SC3 in symmetric case

SHEAR STRAIN AND STABILITY CONDITIONS		
SHEAR STRAIN CONDITION		
$\Upsilon_c = 6S\xi_c = 6S(P_{DL+LL}/E_cA) <= \xi b/3$	Υ_c	0.57726
	Status	OK
STABILITY CONDITION - STATIC		
Stress due to Axial Load on the Pad, σ_c (MPa)		7.73525
Critical Stress Against Buckling, σ_{crit} (MPa)		24.9301
Stability Status		OK
STABILITY CONDITION - DYNAMIC		
Shear Strain due to Compression, Υ_c		0.74753
Shear Strain due to Earthquake Load, Υ_{eq}		0.775
Rotation Angle due to Earthquake, θ		0.00553
Shear Strain due to Rotation, Υ_{sr}		0.31049
Total Strain, Υ_{total}		1.83302
Stability Status		OK

Therefore, SC3 is a lead-rubber bearing with bearing diameter of 67 cm, lead core diameter of 15 cm and a total height of 59.65 cm. Moreover, SC3 has a vertical effective stiffness of 1186999 kN/m.

Design calculations of STI

Calculations at the final stage and design checks are shown through Table 110 to 114. Shear modulus of STI was selected 0.4 GPa.

Table 110. Design calculations of STI in symmetric case

HORIZONTAL PARAMETERS				
Effective Stiffness			Max Displacement	
K_{eff} (kN/m)		400	D_{TM} (m)	0.34
Total Rubber Thickness, t_r (m)				0.34
Total Rubber Thickness to be Used, t_r (m)				0.35
W_M kN.m	Q kN	K_2 (K_p) kN/m	K_1 kN/m	D_y m
72.6336	53.4071	242.92	2429.2	0.02443
Final	58.2578	228.654	2286.54	0.02831
Yield Strength of Lead, f_{py} (MPa)				10
Lead Core Area, A_p (cm^2)				58.2578
Lead Core Diameter, d_p (cm)				8.61255
Lead Core Diameter to be Used, d_p (cm)				8.7
Lead Core Area to be Used, A_p (cm^2)				59.4468
W_M* kN.m	Q* kN	K_2* (K_p*) kN/m	K_1* kN/m	D_y* m
74.6183	59.4468	252.135	2521.35	0.0262
New K_{eff}* (kN/m)				426.979
New β_{eff}* (%)				24.0603

Table 111. Design calculations of STI in symmetric case

ISOLATOR ELEMENT DETAILS	
Single Layer Thickness of a Circular Pad, t (cm)	0.6625
Single Layer Thickness to be Used, t (cm)	1
New Shape Factor, S	13.25
Reselected Compression Modulus, E_C* (MPa)	421.35
Number of Single Rubber Layer	35
Single Steel Plate Thickness, t_s (mm) > 2 mm	2.33732
Single Steel Plate Thickness to be Used, t_s (mm)	2.5
Cover Steel Plate Thicknesses, t_c (mm)	30
Effective Height of the Lead Core, H_p (cm)	43.5
H_p / d_p Ratio	5
Lead Core Dimension Situation 1.25 <= H_p/d_p <= 5.0	OK
Total Height of the Isolator, H (cm)	49.5

Table 112. Design calculations of STI in symmetric case

BEARING DIMENSIONS FROM A_0, A_1, A_2			
Determination of A_0 Based on Allow. Stress for Vertical Load			
$P_{DL+LL} / A_0 = \sigma c$ (MPa) <=	7.8	A_0 (m^2)	0.11445
Determination of A_1 from Shear Strain due to Vertical Load			
$\Upsilon c = 6S\xi c = 6S(P_{DL+LL}/EcA_1) <= \xi b/3$		A_1 (m^2)	0.06695
		A_1* (m^2)	0.10106
Determination of A_2 from Elastic Modulus & Shear Failure			
$K_p = K_e*[1+12*(A_p/A_0)]$		K_e (kN/m)	140.858
		K_e* (kN/m)	155.323
$K_e*t_r/G = A_{sf}$ (m^2)	0.12325	Diameter, d (m)	0.39614
$K_e*t_r/G = A_{sf}$* (m^2)	0.13591	Diameter, d (m)	0.41598
$A_2 = B*(B-D_{TM})$ or $A^2 = d\text{^}2*(\beta-\sin\beta)/4$		A_2 (m^2)	0.00772
		A_2*(m^2)	0.01238
		A_2**(m^2)	0.05368
Bearing Area from A_0, A_1, A_2		A (m^2)	0.11445
Bearing Diameter, d (cm)		38.17358588	
Bearing Diameter to be Used, d (cm)		53	
Bearing Area to be Used, A (cm^2)		2206.183441	

Table 113. Design checks of STI in symmetric case

SHEAR STRAIN AND STABILITY CONDITIONS		
SHEAR STRAIN CONDITION		
$\Upsilon c = 6S\xi c = 6S(P_{DL+LL}/E_cA) <= \xi b/3$	Υ_c	0.76347
	Status	OK
STABILITY CONDITION - STATIC		
Stress due to Axial Load on the Pad, σ_c (MPa)		4.0464
Critical Stress Against Buckling, σ_{crit} (MPa)		8.91433
Stability Status		OK
STABILITY CONDITION - DYNAMIC		
Shear Strain due to Compression, Υ_c		1.43466
Shear Strain due to Earthquake Load, Υ_{eq}		0.97143
Rotation Angle due to Earthquake, θ		0.00607
Shear Strain due to Rotation, Υ_{sr}		0.24353
Total Strain, Υ_{total}		2.64962
Stability Status		OK

Table 114. Design calculations of STI in symmetric case

SELECTION OF SHAPE FACTOR			
$K_V/K_H > 400$	6S^2 > 400	S > 8.165 (S>10)	
S to be Used, S	20	Bearing Type	Circular
Compression Modulus, E_C (MPa)			960

Thus, STI is a lead-rubber bearing with bearing diameter of 53 cm, lead core diameter of 8.7 cm and a total height of 49.5 cm. Moreover, STI has a vertical effective stiffness of 265593 kN/m.

Design calculations of STO

Calculations at the final stage and design checks are shown through Table 115 and 119. Shear modulus of STO was selected 0.5 GPa.

Table 115. Design calculations of STO in symmetric case

HORIZONTAL PARAMETERS				
Effective Stiffness			Max Displacement	
K_{eff} (kN/m)		870	D_{TM} (m)	0.34
Total Rubber Thickness, t_r (m)				0.34
Total Rubber Thickness to be Used, t_r (m)				0.35
W_M kN.m	Q kN	K_2 (K_p) kN/m	K_1 kN/m	D_y m
157.978	116.16	528.352	5283.52	0.02443
Final	126.711	497.322	4973.22	0.02831
Yield Strength of Lead, f_{py} (MPa)				10
Lead Core Area, A_p (cm^2)				126.711
Lead Core Diameter, d_p (cm)				12.7017
Lead Core Diameter to be Used, d_p (cm)				12.8
Lead Core Area to be Used, A_p (cm^2)				128.68
W_M* kN.m	Q* kN	K_2* (K_p*) kN/m	K_1* kN/m	D_y* m
160.819	128.68	518.812	5188.12	0.02756
New K_{eff}* (kN/m)				897.281
New β_{eff}* (%)				24.6758

Table 116. Design calculations of STO in symmetric case

BEARING DIMENSIONS FROM A_0, A_1, A_2			
Determination of A0 Based on Allow. Stress for Vertical Load			
$P_{DL+LL} / A_0 = \sigma_c$ (MPa) <=	7.8	A_0 (m^2)	0.3358
Determination of A_1 from Shear Strain due to Vertical Load			
$\Upsilon c = 6S\xi c = 6S(P_{DL+LL}/E_cA_1) <= \xi b/3$		A_1 (m^2)	0.15716
		A_1* (m^2)	0.18489
Determination of A_2 from Elastic Modulus & Shear Failure			
$K_p = K_e*[1+12*(A_p/A_0)]$		K_e (kN/m)	340.669
		K_e* (kN/m)	355.39
$K_e*t_r/G = A_{sf}$ (m^2)	0.23847	Diameter, d (m)	0.55102
$K_e*t_r/G = A_{sf}$* (m^2)	0.24877	Diameter, d (m)	0.5628
$A_2 = B*(B-D_{TM})$ or $A_2 = d\text{^}2*(\beta-\sin\beta)/4$		A_2 (m^2)	0.0638
		A_2*(m^2)	0.0698
		A_2**(m^2)	0.142
Bearing Area from A_0, A_1, A_2		A (m^2)	0.3358
Bearing Diameter, d (cm)		65.38797567	
Bearing Diameter to be Used, d (cm)		68	
Bearing Area to be Used, A (cm^2)		3631.681108	

Table 117. Design calculations of STO in symmetric case

ISOLATOR ELEMENT DETAILS	
Single Layer Thickness of a Circular Pad, t (cm)	0.85
Single Layer Thickness to be Used, t (cm)	1
New Shape Factor, S	17
Reselected Compression Modulus, E_C* (MPa)	867
Number of Single Rubber Layer	35
Single Steel Plate Thickness, t_s (mm) > 2 mm	3.36906
Single Steel Plate Thickness to be Used, t_s (mm)	3.5
Cover Steel Plate Thicknesses, t_c (mm)	30
Effective Height of the Lead Core, H_p (cm)	46.9
H_p / d_p Ratio	3.66406
Lead Core Dimension Situation $1.25 <= H_p/d_p <= 5.0$	OK
Total Height of the Isolator, H (cm)	52.9

Table 118. Design calculations of STO in symmetric case

SELECTION OF SHAPE FACTOR			
$K_V/K_H > 400$	6S^2 > 400	S > 8.165 (S>10)	
S to be Used, S	20	Bearing Type	Circular
Compression Modulus, E_C (MPa)			1200

Table 119. Design checks of STO in symmetric case

SHEAR STRAIN AND STABILITY CONDITIONS		
SHEAR STRAIN CONDITION		
$\Upsilon c = 6S\xi c = 6S(P_{DL+LL}/E_cA) <= \xi b/3$	Υ_c	0.8485
	Status	OK
STABILITY CONDITION - STATIC		
Stress due to Axial Load on the Pad, σ_c (MPa)		7.21228
Critical Stress Against Buckling, σ_{crit} (MPa)		18.3428
Stability Status		OK
STABILITY CONDITION - DYNAMIC		
Shear Strain due to Compression, Υ_c		1.10274
Shear Strain due to Earthquake Load, Υ_{eq}		0.97143
Rotation Angle due to Earthquake, θ		0.00607
Shear Strain due to Rotation, Υ_{sr}		0.40089
Total Strain, Υ_{total}		2.47505
Stability Status		OK

Therefore, STO is a lead-rubber bearing with bearing diameter of 68 cm, lead core diameter of 12.8 cm and a total height of 52.9 cm. Moreover, STO has a vertical effective stiffness of 899619 kN/m.

APPENDIX C

CHECKS OF ISOLATORS UNDER GROUND MOTION HISTORIES

In this part, isolators designed with response spectrum analyses were checked under time historiy analyses. Forces coming from the seismic load combinations are shown in Table 81. According to that forces, safeties of isolators are tabled below.

Design check of SC1

Table 120. Design checks of SC1

SHEAR STRAIN AND STABILITY CONDITIONS		
SHEAR STRAIN CONDITION		
$\Upsilon_c = 6S\xi_c = 6S(P_{DL+LL}/E_cA) <= \xi_b/3$	Υ_c	0.65736
	Status	OK
STABILITY CONDITION - STATIC		
Stress due to Axial Load on the Pad, σ_c (MPa)		3.41825
Critical Stress Against Buckling, σ_{crit} (MPa)		7.50847
Stability Status		OK
STABILITY CONDITION - DYNAMIC		
Shear Strain due to Compression, Υ_c		1.74999
Shear Strain due to Earthquake Load, Υ_{eq}		0.775
Rotation Angle due to Earthquake, θ		0.00553
Shear Strain due to Rotation, Υ_{sr}		0.18703
Total Strain, Υ_{total}		2.71202
Stability Status		OK

Design check of SC2

Table 121. Design checks of SC2

SHEAR STRAIN AND STABILITY CONDITIONS		
SHEAR STRAIN CONDITION		
$\Upsilon_c = 6S\xi_c = 6S(P_{DL+LL}/E_cA) <= \xi_b/3$	Υ_c	0.66639
	Status	OK
STABILITY CONDITION - STATIC		
Stress due to Axial Load on the Pad, σ_c (MPa)		6.18076
Critical Stress Against Buckling, σ_{crit} (MPa)		13.6501
Stability Status		OK
STABILITY CONDITION - DYNAMIC		
Shear Strain due to Compression, Υ_c		1.55811
Shear Strain due to Earthquake Load, Υ_{eq}		0.775
Rotation Angle due to Earthquake, θ		0.00553
Shear Strain due to Rotation, Υ_{sr}		0.19429
Total Strain, Υ_{total}		2.52739
Stability Status		OK

Design check of SC3

Table 122. Design checks of SC3

SHEAR STRAIN AND STABILITY CONDITIONS		
SHEAR STRAIN CONDITION		
$\Upsilon_c = 6S\xi_c = 6S(P_{DL+LL}/E_cA) <= \xi_b/3$	Υ_c	0.57726
	Status	OK
STABILITY CONDITION - STATIC		
Stress due to Axial Load on the Pad, σ_c (MPa)		7.73525
Critical Stress Against Buckling, σ_{crit} (MPa)		24.9301
Stability Status		OK
STABILITY CONDITION - DYNAMIC		
Shear Strain due to Compression, Υ_c		0.93649
Shear Strain due to Earthquake Load, Υ_{eq}		0.775
Rotation Angle due to Earthquake, θ		0.00553
Shear Strain due to Rotation, Υ_{sr}		0.31049
Total Strain, Υ_{total}		2.02198
Stability Status		OK

Design check of STI

Table 123. Design checks of STI

SHEAR STRAIN AND STABILITY CONDITIONS		
SHEAR STRAIN CONDITION		
$\Upsilon_c = 6S\xi_c = 6S(P_{DL+LL}/E_cA) <= \xi_b/3$	Υ_c	0.76347
	Status	OK
STABILITY CONDITION - STATIC		
Stress due to Axial Load on the Pad, σ_c (MPa)		4.0464
Critical Stress Against Buckling, σ_{crit} (MPa)		8.91433
Stability Status		OK
STABILITY CONDITION - DYNAMIC		
Shear Strain due to Compression, Υ_c		1.70313
Shear Strain due to Earthquake Load, Υ_{eq}		0.97143
Rotation Angle due to Earthquake, θ		0.00607
Shear Strain due to Rotation, Υ_{sr}		0.24353
Total Strain, Υ_{total}		2.91809
Stability Status		OK

Design check of STO

Table 124. Design checks of STO

SHEAR STRAIN AND STABILITY CONDITIONS		
SHEAR STRAIN CONDITION		
$\Upsilon_c = 6S\xi_c = 6S(P_{DL+LL}/E_cA) <= \xi_b/3$	Υ_c	0.8485
	Status	OK
STABILITY CONDITION - STATIC		
Stress due to Axial Load on the Pad, σ_c (MPa)		7.21228
Critical Stress Against Buckling, σ_{crit} (MPa)		18.3428
Stability Status		OK
STABILITY CONDITION - DYNAMIC		
Shear Strain due to Compression, Υ_c		1.26163
Shear Strain due to Earthquake Load, Υ_{eq}		0.97143
Rotation Angle due to Earthquake, θ		0.00607
Shear Strain due to Rotation, Υ_{sr}		0.40089
Total Strain, Υ_{total}		2.63395
Stability Status		OK